Introduction to Numerical Hydrodynamics and Radiative Transfer

II. Hydrodynamics

Bernd Freytag

Uppsala University

2015-02-23

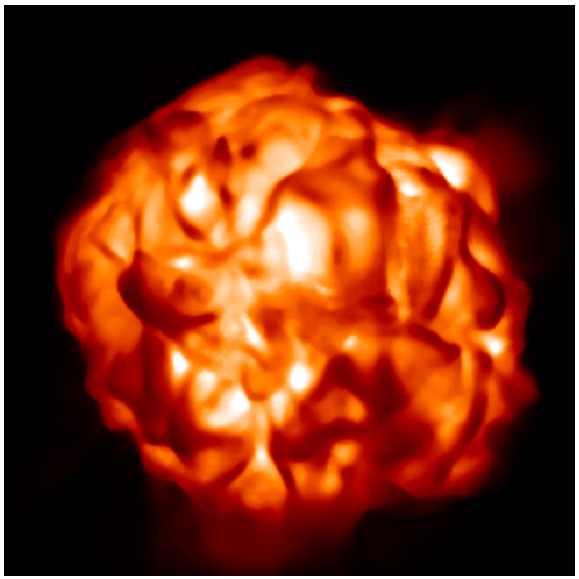
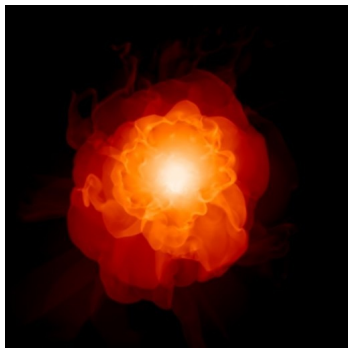
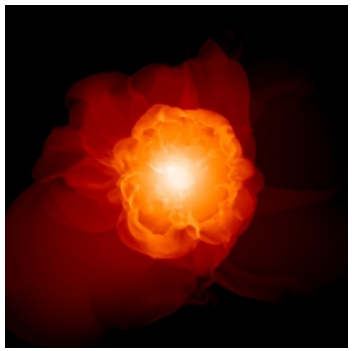
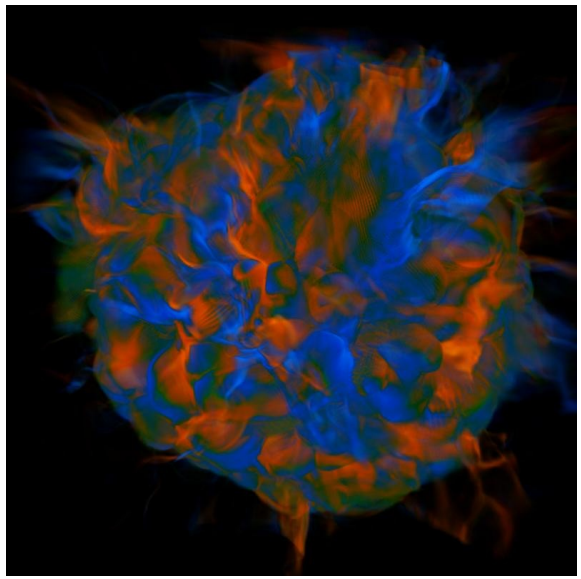

Outline of the course

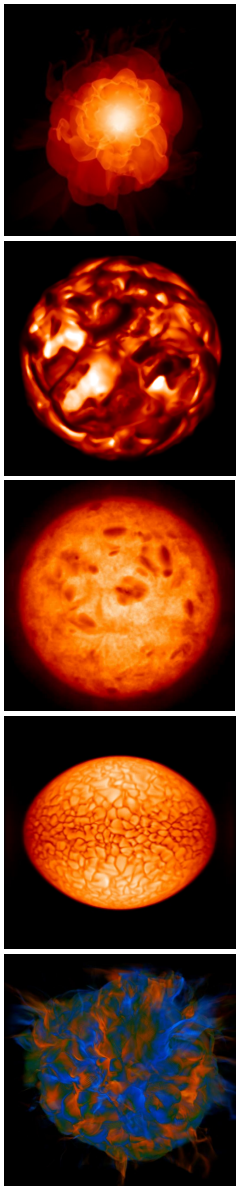

Table of contents

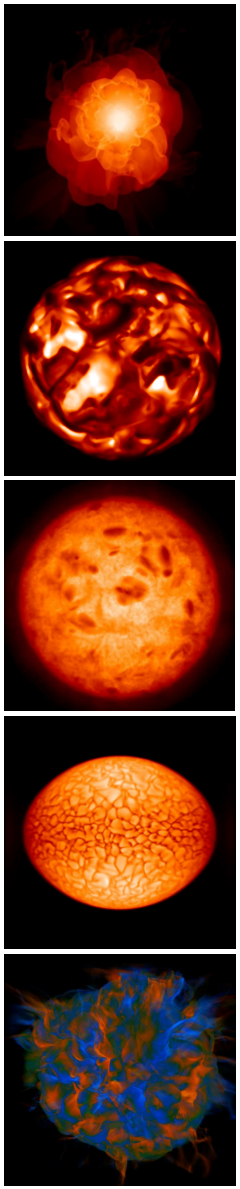

The Euler Equations in differential form (vectors)

The Euler Equations in differential conservation form in vector notation are

$$\begin{aligned} \frac{\partial \rho}{\partial t} &+ \boldsymbol{\nabla}\cdot(\rho\,\boldsymbol{v}) &&= 0 \\ \frac{\partial \rho \boldsymbol{v}}{\partial t} &+ \boldsymbol{\nabla}\cdot\left(\rho\,\boldsymbol{v}:\boldsymbol{v} + P\,\bar{\bar{\mathrm{I}}}\right) &&= \boldsymbol{0} \\ \frac{\partial \rho e_{\mathrm{ik}}}{\partial t} &+ \boldsymbol{\nabla}\cdot([\rho\,e_{\mathrm{ik}} + P]\,\boldsymbol{v}) &&= 0 \end{aligned} \tag{1}$$

They describe the inviscid flow of
density ρ, momentum $\rho\boldsymbol{v}$, and total energy ρe_{ik}, with

ρ	mass density
$\boldsymbol{v}$	velocity vector
e_{ik}	total (internal + kinetic) energy per mass unit
P	pressure
$\bar{\bar{\mathrm{I}}}$	unity tensor .

The Euler Equations in differential form (components)

The Euler Equations in differential conservation form, split into components, are

$$
\begin{aligned}
&\frac{\partial}{\partial t}\,\rho && + \frac{\partial}{\partial x}\,(\rho v_x) && + \frac{\partial}{\partial y}\,(\rho v_y) && + \frac{\partial}{\partial z}\,(\rho v_z) && = 0 \\
&\frac{\partial}{\partial t}\begin{pmatrix}\rho v_x\\ \rho v_y\\ \rho v_z\end{pmatrix} && + \frac{\partial}{\partial x}\begin{pmatrix}\rho v_x\ v_x + P\\ \rho v_y\ v_x\\ \rho v_z\ v_x\end{pmatrix} && + \frac{\partial}{\partial y}\begin{pmatrix}\rho v_x\ v_y\\ \rho v_y\ v_y + P\\ \rho v_z\ v_y\end{pmatrix} && + \frac{\partial}{\partial z}\begin{pmatrix}\rho v_x\ v_z\\ \rho v_y\ v_z\\ \rho v_z\ v_z + P\end{pmatrix} && = \begin{pmatrix}0\\0\\0\end{pmatrix} \qquad (2)\\
&\frac{\partial}{\partial t}\,\rho e_{\mathrm{ik}} && + \frac{\partial}{\partial x}\,([\rho e_{\mathrm{ik}} + P]\ v_x) && + \frac{\partial}{\partial y}\,([\rho e_{\mathrm{ik}} + P]\ v_y) && + \frac{\partial}{\partial z}\,([\rho e_{\mathrm{ik}} + P]\ v_z) && = 0\ .
\end{aligned}
$$

It is a non-linear system of first-order partial differential equations (PDEs).

The solution of the Euler Equations

The task is now:
Find a solution

$$(\rho, \rho \boldsymbol{v}, \rho e_{\mathrm{ik}})\,(\boldsymbol{x}, t) \tag{3}$$

for Eq. (2) for given initial conditions

$$(\rho, \rho \boldsymbol{v}, \rho e_{\mathrm{ik}})\,(\boldsymbol{x}, t_0) \quad , \tag{4}$$

boundary conditions (for example)

$$(\rho, \rho \boldsymbol{v}, \rho e_{\mathrm{ik}})\,(\boldsymbol{x}_{\mathrm{boundaries}}, t) \quad , \tag{5}$$

and material function (equation of state)

$$P = P\,(\rho, e_{\mathrm{i}}) \tag{6}$$

with

$$e_{\mathrm{i}} = e_{\mathrm{ik}} - \tfrac{1}{2}\boldsymbol{v}\cdot\boldsymbol{v} \quad ! \tag{7}$$

The prototype numerical solution of the Euler Equations

The hydrodynamics equations (1) or (2) can be put into the form

$$\frac{\partial}{\partial t}\left(\rho, \rho \boldsymbol{v}, \rho e_{\mathrm{ik}}\right) = f\left(\rho, \rho \boldsymbol{v}, \rho e_{\mathrm{ik}}\right) \tag{8}$$

where the function f contains the terms with the spatial derivatives. It can be approximated by

$$\Delta\left(\rho, \rho \boldsymbol{v}, \rho e_{\mathrm{ik}}\right) \approx \Delta t \;\; f\left(\rho, \rho \boldsymbol{v}, \rho e_{\mathrm{ik}}\right) \tag{9}$$

Idea:

1. Consider the state quantities $\left(\rho, \rho \boldsymbol{v}, \rho e_{\mathrm{ik}}\right)$ on a discrete grid.
2. Take an initial state $\left(\rho, \rho \boldsymbol{v}, \rho e_{\mathrm{ik}}\right)\left(\boldsymbol{x}, t_0\right)$.
3. Compute $\boldsymbol{v}$, e_{i}, and P.
4. Compute the spatial derivatives to get the right-hand side of Eq. (8).
5. Get a small change of $\left(\rho, \rho \boldsymbol{v}, \rho e_{\mathrm{ik}}\right)$ via Eq. (9).
6. Update $\left(\rho, \rho \boldsymbol{v}, \rho e_{\mathrm{ik}}\right)$.
7. Restart at 3.

There 1000 ways how this can be done and 10000 ways how it can go wrong. . .

Possible basic quantities

What do we need to describe a – simple – fluid locally?

- Macroscopic bulk velocity $\boldsymbol{v}$ (or momentum $\rho\boldsymbol{v}$)
- Two thermodynamic quantities, e.g.
  - temperature T and pressure P
  - entropy s and pressure P
  - mass density ρ and internal energy e_{i}

All quantities depend on space $\boldsymbol{x}$ and time t coordinates. We assume

- LTE: two thermodynamic quantities are sufficient to describe the local microscopic state of the fluid completely:
  ionization/dissociation, molecule formation, occupation numbers, microscopic velocity distribution
- We do not need to look at the atomic level: we have a continuous fluid.

Choice of basic quantities

We choose the conserved variables

- density ρ,
- momentum $\rho \boldsymbol{v}$,
- total energy ρe_{ik}

as basic quantities, because they have

- no source terms (we ignore gravity here),
- simpler transport properties

rather than the primitive variables, e.g.,

- density ρ,
- velocity $\boldsymbol{v}$,
- pressure P

or

- density ρ,
- velocity $\boldsymbol{v}$,
- temperature T.

Fluxes through surface

Fluxes with velocity v
through surface element dA
with normal vector $\hat{\boldsymbol{n}}$:

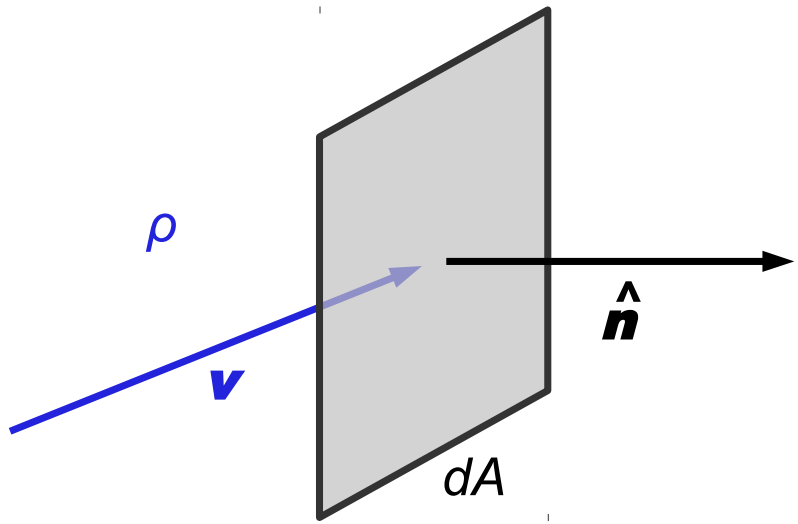

Mass transport $\rightarrow$ change of mass per time:

$$\rho\, \boldsymbol{v} \cdot \hat{\boldsymbol{n}}\, dA \tag{10}$$

Momentum transport and acceleration by pressure force along surface normal $\rightarrow$ change of momentum per time

$$[\rho\, \boldsymbol{v} : \boldsymbol{v}\, \hat{\boldsymbol{n}} + P\, \hat{\boldsymbol{n}}]\; dA \tag{11}$$

Energy transport and work done by pressure $\rightarrow$ change of total energy per time

$$[\rho e_{\mathrm{ik}} + P]\, \boldsymbol{v} \cdot \hat{\boldsymbol{n}}\, dA \tag{12}$$

Shear forces (friction) are ignored.
There are no torsional forces (only relevant in solids).

Changes of the conserved quantities

Without source terms, the only change between time t_1 and t_0 to the amount of a conserved variable inside a volume V comes from the flux through its surface ∂V. Integrating Eqs. (10) to (12) over that surface and time thus gives

$$\int_V \rho\left(\boldsymbol{x}, t_1\right) dV - \int_V \rho\left(\boldsymbol{x}, t_0\right) dV = -\int_{t_0}^{t_1} \oint_{\partial V} \rho\, \boldsymbol{v}\cdot\hat{\boldsymbol{n}}\, dA\, dt \tag{13}$$

$$\int_V \rho\boldsymbol{v}\left(\boldsymbol{x}, t_1\right) dV - \int_V \rho\boldsymbol{v}\left(\boldsymbol{x}, t_0\right) dV = -\int_{t_0}^{t_1} \oint_{\partial V} \left[\rho\, \boldsymbol{v}:\boldsymbol{v} + P\bar{\bar{\mathrm{I}}}\right] \hat{\boldsymbol{n}}\, dA\, dt \tag{14}$$

$$\int_V \rho e_{\mathrm{ik}}\left(\boldsymbol{x}, t_1\right) dV - \int_V \rho e_{\mathrm{ik}}\left(\boldsymbol{x}, t_0\right) dV = -\int_{t_0}^{t_1} \oint_{\partial V} \left[\rho e_{\mathrm{ik}} + P\right] \boldsymbol{v}\cdot\hat{\boldsymbol{n}}\, dA\, dt \tag{15}$$

The unity tensor $\bar{\bar{\mathrm{I}}}$ has been squeezed in,

$$P\hat{\boldsymbol{n}} = P\bar{\bar{\mathrm{I}}}\,\hat{\boldsymbol{n}}\ . \tag{16}$$

Euler Equations in integral form

After a slight rearrangement we get the Euler Equations in integral form:

$$\begin{aligned}
\int_V \left[\rho\left(\boldsymbol{x}, t_1\right) - \rho\left(\boldsymbol{x}, t_0\right)\right] dV &+ \int_{t_0}^{t_1} \oint_{\partial V} \rho\, \boldsymbol{v}\cdot\hat{\boldsymbol{n}}\, dA\, dt &= 0 \\
\int_V \left[\rho\boldsymbol{v}\left(\boldsymbol{x}, t_1\right) - \rho\boldsymbol{v}\left(\boldsymbol{x}, t_0\right)\right] dV &+ \int_{t_0}^{t_1} \oint_{\partial V} \left[\rho\, \boldsymbol{v}:\boldsymbol{v} + P\,\bar{\bar{\mathrm{I}}}\right] \hat{\boldsymbol{n}}\, dA\, dt &= \mathbf{0} \qquad (17) \\
\int_V \left[\rho e_{\mathrm{ik}}\left(\boldsymbol{x}, t_1\right) - \rho e_{\mathrm{ik}}\left(\boldsymbol{x}, t_0\right)\right] dV &+ \int_{t_0}^{t_1} \oint_{\partial V} \left[\rho e_{\mathrm{ik}} + P\right] \boldsymbol{v}\cdot\hat{\boldsymbol{n}}\, dA\, dt &= 0
\end{aligned}$$

There is a close correspondence to the Euler Equations in differential form (1). Note however, that in the integral form there are no derivatives.

Euler Equations: from integral to differential form I

To transform the mass transport equation into differential form the first line of Eq. (17) is divided by $(t_1 - t_0)$,

$$\int_V \frac{\rho(\boldsymbol{x}, t_1) - \rho(\boldsymbol{x}, t_0)}{t_1 - t_0}\, dV + \frac{1}{t_1 - t_0} \int_{t_0}^{t_1} \oint_{\partial V} \rho\, \boldsymbol{v} \cdot \hat{\boldsymbol{n}}\, dA\, dt = 0 \ . \tag{18}$$

Taking the limes $t_1 \to t_0$ and assuming that the derivative $\frac{\partial \rho}{\partial t}$ exists for all $\boldsymbol{x}$ we get

$$\int_V \frac{\partial \rho}{\partial t}\, dV + \oint_{\partial V} \rho\, \boldsymbol{v} \cdot \hat{\boldsymbol{n}}\, dA = 0 \ . \tag{19}$$

Now, the Gauß theorem is applied (assuming that the divergence $\boldsymbol{\nabla} \cdot \rho \boldsymbol{v}$ does exist) to transform the surface integral into a volume integral. We get

$$\int_V \frac{\partial \rho}{\partial t}\, dV + \int_V \boldsymbol{\nabla} \cdot \rho \boldsymbol{v}\, dV = 0 \ . \tag{20}$$

Euler Equations: from integral to differential form II

Merging the two integrals gives

$$\int_V \left(\frac{\partial \rho}{\partial t} + \boldsymbol{\nabla} \cdot \rho \boldsymbol{v} \right) \, dV = 0 \ . \tag{21}$$

Because this is true for all (even small) volumes we conclude that the integrand has to be zero and get the differential form of the mass transport equation,

$$\frac{\partial \rho}{\partial t} + \boldsymbol{\nabla} \cdot \rho \boldsymbol{v} = 0 \ . \tag{22}$$

This works the same for the energy equation and requires only a generalization of the Gauß theorem to be applicable to the momentum equation.

Hydrodynamics equations including viscosity

The viscous hydrodynamics equations are

$$\begin{aligned} \frac{\partial \rho}{\partial t} &+ \boldsymbol{\nabla}\cdot(\rho\,\boldsymbol{v}) &&= 0 \\ \frac{\partial \rho \boldsymbol{v}}{\partial t} &+ \boldsymbol{\nabla}\cdot\left(\rho\,\boldsymbol{v}:\boldsymbol{v} - \bar{\bar{\mathsf{T}}}\right) &&= \mathbf{0} \\ \frac{\partial \rho e_{\mathrm{ik}}}{\partial t} &+ \boldsymbol{\nabla}\cdot\left(\left[\rho\, e_{\mathrm{ik}} - \bar{\bar{\mathsf{T}}}\right]\boldsymbol{v}\right) &&= 0 \end{aligned} \tag{23}$$

with the stress tensor $\bar{\bar{\mathsf{T}}}$ (including a term for the gas pressure)

$$\bar{\bar{\mathsf{T}}} = -P\bar{\bar{\mathsf{I}}} + \mu\left\{\left[\boldsymbol{\nabla}:\boldsymbol{v} + (\boldsymbol{\nabla}:\boldsymbol{v})^{\mathrm{T}}\right] - \frac{2}{3}\boldsymbol{\nabla}\cdot\boldsymbol{v}\,\bar{\bar{\mathsf{I}}}\right\} \tag{24}$$

depending on the dynamic viscosity μ.
Note: via $\bar{\bar{\mathsf{T}}}$ Eq. (23) contains second derivatives.

Hydrodynamics equations including gravity

The Euler Equations with gravity are

$$\begin{aligned} \frac{\partial \rho}{\partial t} &+ \boldsymbol{\nabla}\cdot(\rho\,\boldsymbol{v}) &&= 0 \\ \frac{\partial \rho \boldsymbol{v}}{\partial t} &+ \boldsymbol{\nabla}\cdot\left(\rho\,\boldsymbol{v}:\boldsymbol{v} + P\bar{\bar{\mathrm{I}}}\right) &&= -\rho\boldsymbol{\nabla}\Phi \\ \frac{\partial \rho e_{\mathrm{ikg}}}{\partial t} &+ \boldsymbol{\nabla}\cdot([\rho\, e_{\mathrm{ikg}} + P]\,\boldsymbol{v}) &&= 0 \end{aligned} \tag{25}$$

with the gravitational potential Φ. The total energy e_{ikg} now contains a contribution due to the potential,

$$e_{\mathrm{ikg}} = e_{\mathrm{i}} + \tfrac{1}{2}\boldsymbol{v}\cdot\boldsymbol{v} + \Phi \quad . \tag{26}$$

Note: the momentum equation now contains a true source term.

Hydrodynamics equations including magnetic fields

The equations of ideal magneto-hydrodynamics (MHD) are

$$\begin{aligned}
\frac{\partial \rho}{\partial t} &+ \boldsymbol{\nabla}\cdot(\rho\,\boldsymbol{v}) &&= 0 \\
\frac{\partial \rho \boldsymbol{v}}{\partial t} &+ \boldsymbol{\nabla}\cdot\left(\rho\,\boldsymbol{v}:\boldsymbol{v} + P\bar{\bar{\mathsf{I}}} - \bar{\bar{\mathsf{T}}}_{\mathrm{mag}}\right) &&= \boldsymbol{0} \\
\frac{\partial \boldsymbol{B}}{\partial t} &+ \boldsymbol{\nabla}\cdot(\boldsymbol{v}:\boldsymbol{B} - \boldsymbol{B}:\boldsymbol{v}) &&= \boldsymbol{0} \\
\frac{\partial \rho e_{\mathrm{ikb}}}{\partial t} &+ \boldsymbol{\nabla}\cdot\left(\left[\rho\, e_{\mathrm{ikb}} + P - \bar{\bar{\mathsf{T}}}_{\mathrm{mag}}\right]\boldsymbol{v}\right) &&= 0
\end{aligned} \tag{27}$$

with the magnetic field $\boldsymbol{B}$ (with $\boldsymbol{\nabla}\cdot\boldsymbol{B} = 0$) and the Maxwell stress tensor $\bar{\bar{\mathsf{T}}}_{\mathrm{mag}}$

$$\bar{\bar{\mathsf{T}}}_{\mathrm{mag}} = -\tfrac{1}{2}\boldsymbol{B}\cdot\boldsymbol{B}\,\bar{\bar{\mathsf{I}}} + \boldsymbol{B}:\boldsymbol{B}\ . \tag{28}$$

The total energy e_{ikb} now contains a contribution from the magnetic field,

$$e_{\mathrm{ikb}} = e_{\mathrm{i}} + \tfrac{1}{2}\boldsymbol{v}\cdot\boldsymbol{v} + \tfrac{1}{2}\boldsymbol{B}\cdot\boldsymbol{B}/\rho\ . \tag{29}$$

Hydrodynamics equations including radiation

The hydrodynamics equations including radiative terms are

$$\begin{aligned}
\frac{\partial \rho}{\partial t} &+ \nabla\cdot(\rho\,\boldsymbol{v}) &&= 0 \\
\frac{\partial \rho \boldsymbol{v}}{\partial t} &+ \nabla\cdot\left(\rho\,\boldsymbol{v}:\boldsymbol{v} + P\bar{\bar{\mathrm{I}}} + \bar{\bar{\mathrm{P}}}_{\mathrm{rad}}\right) &&= \boldsymbol{0} \\
\frac{\partial \rho e_{\mathrm{ik}}}{\partial t} &+ \nabla\cdot\left(\left[\rho\,e_{\mathrm{ik}} + P\right]\boldsymbol{v} + \boldsymbol{F}_{\mathrm{rad}}\right) &&= 0
\end{aligned} \tag{30}$$

where the radiative energy flux $\boldsymbol{F}_{\mathrm{rad}}$ and the radiation pressure $\bar{\bar{\mathrm{P}}}_{\mathrm{rad}}$ are computed from the intensity $I_\nu\left(\boldsymbol{x}, \hat{\boldsymbol{n}}, \nu\right)$ as (c_{l}: speed of light, ν: frequency)

$$\boldsymbol{F}_{\mathrm{rad}}\left(\boldsymbol{x}\right) = \int_0^\infty \oint_\Omega \hat{\boldsymbol{n}}\, I_\nu\left(\boldsymbol{x}, \hat{\boldsymbol{n}}, \nu\right) d\omega\, d\nu \tag{31}$$

$$\bar{\bar{\mathrm{P}}}_{\mathrm{rad}}\left(\boldsymbol{x}\right) = \frac{1}{c_{\mathrm{l}}} \int_0^\infty \oint_\Omega \hat{\boldsymbol{n}}:\hat{\boldsymbol{n}}\, I_\nu\left(\boldsymbol{x}, \hat{\boldsymbol{n}}, \nu\right) d\omega\, d\nu \ . \tag{32}$$

Types of differential equations

- Number of distinct derivatives
  - Only 1: ordinary DE (integration of particle trajectories, Runge-Kutta ODE solvers)
  - More than 1: partial DE $\Longleftarrow\Longleftarrow\Longleftarrow$
- Order of the derivatives
  - Only 1st order (possibly (quasi-)hyperbolic? transport?) $\Longleftarrow\Longleftarrow\Longleftarrow$
  - Higher order (possibly parabolic? dissipation?)
- Number of equations
  - Only 1: scalar DE
  - More than 1: system of DEs $\Longleftarrow\Longleftarrow\Longleftarrow$
- (Non-)linearity
  - Linear (decomposition into eigenfunctions, Fourier analysis)
  - Non-linear (complicated) $\Longleftarrow\Longleftarrow\Longleftarrow$
- Initial and boundary conditions
  - Initial conditions (advance in time) $\Longleftarrow\Longleftarrow\Longleftarrow$
  - Only boundary conditions (iterative relaxation methods)

Standard 3D Euler Equations $\Longleftarrow\Longleftarrow\Longleftarrow$

Regimes of flows, often characterized by dimensionless numbers

- Non-relativistic/relativistic ($\beta = v/c_{\mathrm{light}}$)
- Small/large Mach number ($Ma = v/c_{\mathrm{sound}}$)
  - Zero-Mach-number (hydrostatic conditions)
  - Small-Mach-number
    - Non-linear, nearly incompressible: stellar interiors
    - Linear small-amplitude: waves
  - Transsonic (Mach number ≈ 1): cool stellar atmospheres
  - Highly supersonic: jets
- Small/large Reynolds number (Re)
  - Low-Reynolds-number (very viscous)
  - High-Reynolds-number (often turbulent): stellar atmospheres
- Influence of rotation (Co, Ro)
- Not/weakly/strongly stratified
- No/weak/strong coupling to radiation
- No/weak/strong coupling to magnetic fields ($\beta_{\mathrm{plasma}} = P_{\mathrm{gas}}/P_{\mathrm{mag}}$)

Each combination might favor or even require a different numerical approach.

Conditions in stellar atmospheres

Flows in stellar atmospheres:

- Outer “boundary” of star: energy from the interior is radiated into space
- Dominant stratification: “essentially 1D” (but: planetary atmospheres)
- Transition region between optically thick and thin regime
- Low viscosity (large Reynolds numbers)
- Flow speeds typically near sonic (Mach numbers not far below 1)
- Magnetic fields can play a role – in some cases

Approximations:

- Ignore viscous effects from Eq. (23).
- Keep terms due to gravity as in Eq. (25).
- Keep the influence of radiation as in Eq. (30).
- Ignore (or keep) magnetic fields in Eq. (27).

Stationary case: plane-parallel atmosphere: assumptions

Assumption: gravity in z direction (downward):

$$\Phi = gz \ . \tag{33}$$

Assumption: quasi-stationarity (no trends, but fluctuations allowed)
Averaging over t, x, and y gives for the averaged quantities

$$\frac{\partial}{\partial t} = 0, \quad \frac{\partial}{\partial x} = 0, \quad \frac{\partial}{\partial y} = 0 \ . \tag{34}$$

Stationary case: results

The quasi-stationary combination of Eq. (25) and Eq. (30) gives (see Eq. (2)):
Mass transport:
mass loss or infall

$$\langle \rho v_z(z) \rangle = \text{const} \tag{35}$$

Horizontal momentum:
possibly horizontal laminar flow

$$\langle \rho v_x v_z(z) \rangle = \text{const}, \quad \langle \rho v_y v_z(z) \rangle = \text{const} \tag{36}$$

Vertical momentum:
turbulent, gas, radiation pressure + gravity $\rightarrow$ pressure stratification

$$\frac{\partial}{\partial z}\left(\langle \rho v_z v_z \rangle + \langle P \rangle + \langle P_{\text{rad},z} \rangle\right) = -\langle \rho \rangle g \tag{37}$$

Energy flux:
convective and radiative energy transport $\rightarrow$ temperature stratification

$$\langle [\rho e_{\text{ikg}} + P] v_z \rangle + \langle F_{\text{rad},z} \rangle = \text{const} = F_* \tag{38}$$

Static case

Further assumption:

$$v_x = v_y = v_z = 0 \tag{39}$$

Result:
No mass loss:

$$\langle \rho v_z (z) \rangle = 0 \tag{40}$$

Hydrostatic pressure stratification:

$$\frac{\partial}{\partial z} \left(\langle P \rangle + \langle P_{\mathrm{rad},z} \rangle \right) = -\langle \rho \rangle g \tag{41}$$

Stratification in radiative equilibrium:

$$\langle F_{\mathrm{rad},z} \rangle = \mathrm{const} = F_* \tag{42}$$

Coupling of radiation transport and hydrodynamics

Radiation transport $\rightarrow$ hydrodynamics:

- affects energy and momentum
- non-local coupling
- possibly short radiative time-scale $\rightarrow$ stiff terms

Hydrodynamics $\rightarrow$ radiation transport:

- transport through complex 3D structures
- spatial fluctuations of ρ and e_{i} $\rightarrow$ fluctuations of opacities and source function
- Doppler shifts of wavelengths of lines

1D Euler Equations in conservation form

The Euler Equations (2) restricted to one spatial dimension,

$$\frac{\partial}{\partial t}\begin{pmatrix}\rho\\ \rho v\\ \rho e_{\mathrm{ik}}\end{pmatrix}+\frac{\partial}{\partial x}\begin{pmatrix}\rho\, v\\ \rho v\, v+P\\ [\rho e_{\mathrm{ik}}+P]\;\; v\end{pmatrix}=\begin{pmatrix}0\\ 0\\ 0\end{pmatrix} \tag{43}$$

have the form (conservation form)

$$\frac{\partial}{\partial t}\boldsymbol{q}+\frac{\partial}{\partial x}\boldsymbol{F}(\boldsymbol{q})=\mathbf{0} \tag{44}$$

for the quantity vector $\boldsymbol{q}$ with flux vector $\boldsymbol{F}$,

$$\boldsymbol{q}=\begin{pmatrix}\rho\\ \rho v\\ \rho e_{\mathrm{ik}}\end{pmatrix}\quad,\quad\boldsymbol{F}=\begin{pmatrix}\rho\, v\\ \rho v\, v+P\\ [\rho e_{\mathrm{ik}}+P]\;\; v\end{pmatrix}\quad. \tag{45}$$

Quasi-linear system

In Eq. (44) we can compute the spatial derivative and get

$$\frac{\partial}{\partial t}\boldsymbol{q} + \bar{\bar{\mathrm{A}}}\,\frac{\partial}{\partial x}\boldsymbol{q} = \mathbf{0} \tag{46}$$

with the Jacobian

$$\bar{\bar{\mathrm{A}}} = \frac{\partial \boldsymbol{F}}{\partial \boldsymbol{q}} \quad . \tag{47}$$

A system of partial differential equations in the form of Eq. (46) is called quasi-linear if

$$\bar{\bar{\mathrm{A}}} = \bar{\bar{\mathrm{A}}}\left(\boldsymbol{q}, x, t\right) \quad . \tag{48}$$

It is linear if $\bar{\bar{\mathrm{A}}}$ is constant.

Hyperbolic system

A linear system (46) of PDEs is called hyperbolic if $\bar{\bar{A}}$ is diagonalizable, i.e., there exists a matrix $\bar{\bar{Q}}$ with

$$\bar{\bar{\Lambda}} = \bar{\bar{Q}}^{-1} \bar{\bar{A}} \bar{\bar{Q}} \tag{49}$$

and $\bar{\bar{\Lambda}}$ is in diagonal form with real numbers on the diagonal: the eigenvalues of $\bar{\bar{A}}$. With the definition

$$\boldsymbol{q}' := \bar{\bar{Q}}^{-1} \boldsymbol{q} \tag{50}$$

Eq. (46) gets the characteristic form

$$\frac{\partial}{\partial t} \boldsymbol{q}' + \bar{\bar{\Lambda}} \frac{\partial}{\partial x} \boldsymbol{q}' = \mathbf{0} \ . \tag{51}$$

This is now a set of independent equations, each of the simple form

$$\frac{\partial}{\partial t} q_i' + \lambda_i \frac{\partial}{\partial x} q_i' = 0 \ . \tag{52}$$

A quasi-linear system with $\bar{\bar{A}}(\boldsymbol{q}, x, t)$ can be hyperbolic at point $(\boldsymbol{q}, x, t)$.

Eigenvalues for the Euler Equations

For the 1D Euler Equations (43) we get the eigenvalues

$$\begin{pmatrix} v \\ v+c \\ v-c \end{pmatrix} , \tag{53}$$

corresponding to the flow with velocity v and two acoustic waves travelling with sound speed $\pm c$ relative to the flow.

Table of contents

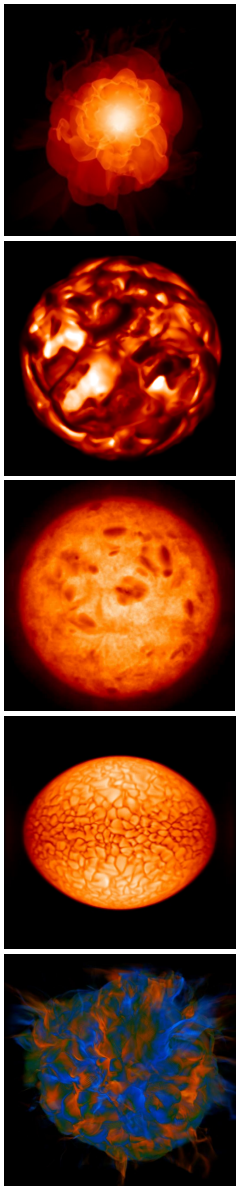

Linear advection as special case: density and momentum

In a 1D flow described by Eq. (43) assuming $\frac{\partial P}{\partial x} = 0$ and $\frac{\partial v}{\partial x} = 0$ at $t = t_0$ gives for the mass

$$0 = \frac{\partial \rho}{\partial t} + \frac{\partial \rho\, v}{\partial x} \tag{54}$$

$$= \frac{\partial \rho}{\partial t} + v\frac{\partial \rho}{\partial x} \ , \tag{55}$$

for the momentum

$$0 = \frac{\partial \rho v}{\partial t} + \frac{\partial \rho v\, v}{\partial x} \tag{56}$$

$$= v\left(\frac{\partial \rho}{\partial t} + v\frac{\partial \rho}{\partial x}\right) + \rho\,\frac{\partial v}{\partial t} \tag{57}$$

$$= \rho\,\frac{\partial v}{\partial t} \ . \tag{58}$$

Linear advection as special case: total energy

For the total energy we get

$$
\begin{aligned}
0 &= \frac{\partial \rho e_{\mathrm{ik}}}{\partial t} + \frac{\partial \rho e_{\mathrm{ik}}\, v}{\partial x} && (59)\\
&= \frac{\partial}{\partial t}\left(\rho e_{\mathrm{i}} + \frac{1}{2}\rho v^2\right) + \frac{\partial}{\partial x}\left(\rho e_{\mathrm{i}}\, v + \frac{1}{2}\rho v^2\, v\right) && (60)\\
&= \frac{1}{2}v^2\left(\frac{\partial \rho}{\partial t} + v\frac{\partial \rho}{\partial x}\right) + \left(\frac{\partial \rho e_{\mathrm{i}}}{\partial t} + \frac{\partial \rho e_{\mathrm{i}}\, v}{\partial x}\right) && (61)\\
&= \frac{\partial \rho e_{\mathrm{i}}}{\partial t} + v\frac{\partial \rho e_{\mathrm{i}}}{\partial x}\ . && (62)
\end{aligned}
$$

Linear advection as special case

Finally, we get for the pressure $P(\rho e_\mathrm{i}, \rho)$

$$\frac{\partial P}{\partial t} = \left.\frac{\partial P}{\partial \rho e_\mathrm{i}}\right|_\rho \frac{\partial \rho e_\mathrm{i}}{\partial t} + \left.\frac{\partial P}{\partial \rho}\right|_{\rho e_\mathrm{i}} \frac{\partial \rho}{\partial t} \tag{63}$$

$$= \left.\frac{\partial P}{\partial \rho e_\mathrm{i}}\right|_\rho \left(-v\frac{\partial \rho e_\mathrm{i}}{\partial x}\right) + \left.\frac{\partial P}{\partial \rho}\right|_{\rho e_\mathrm{i}} \left(-v\frac{\partial \rho}{\partial x}\right) \tag{64}$$

$$= -v\frac{\partial P}{\partial x} = 0 \ . \tag{65}$$

Thus, v and P are constant in space and time.
The passive advection of ρ and ρe_i is described by the linear advection equation

$$\frac{\partial \rho}{\partial t} + v\frac{\partial \rho}{\partial x} = 0 \tag{66}$$

with $v = \mathrm{const}$.

Analytic solution of the linear advection equation

For the initial condition

$$\rho(x, t_0) = \rho_0(x) \tag{67}$$

the advection equation (66) has the general solution

$$\tilde{\rho}(x, t) = \rho_0(x - v[t - t_0]) \quad . \tag{68}$$

Proof by checking: it fulfills the initial condition and

$$\frac{\partial \tilde{\rho}}{\partial t} + v \frac{\partial \tilde{\rho}}{\partial x} = \frac{\mathrm{d}\rho_0}{\mathrm{d}x}(-v) + v \frac{\mathrm{d}\rho_0}{\mathrm{d}x} 1 = 0 \quad . \tag{69}$$

Solution along characteristic curves

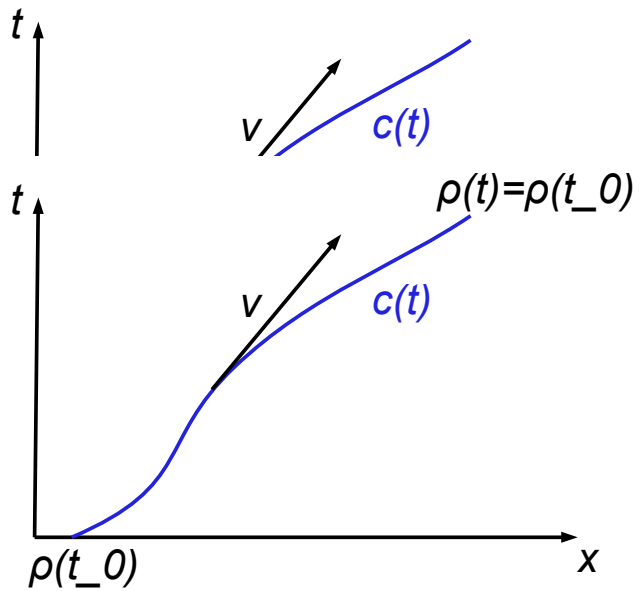

For a quasi-linear PDE

$$\frac{\partial \rho}{\partial t} + v(\rho, x, t)\ \frac{\partial \rho}{\partial x} = 0 \tag{70}$$

a curve $c(t)$ with

$$\frac{\mathrm{d}c}{\mathrm{d}t} = v \tag{71}$$

or sometimes the corresponding map $\mathbb{R} \to \mathbb{R}^2$: $t \to (c(t), t)$ is called characteristic curve or characteristic. For the linear advection equation (66), these curves have the general form

$$c(t) = v\,t + x_0 \ . \tag{72}$$

Along $c(t)$ we get for a solution $\tilde{\rho}(x, t)$ of Eq. (66)

$$\frac{\mathrm{d}}{\mathrm{d}t}\tilde{\rho}(c(t), t) = \frac{\partial \tilde{\rho}}{\partial t} + \frac{\partial \tilde{\rho}}{\partial x}\frac{\mathrm{d}c}{\mathrm{d}t} = \frac{\partial \tilde{\rho}}{\partial t} + v\frac{\partial \tilde{\rho}}{\partial x} = 0 \ . \tag{73}$$

I.e., the solution $\tilde{\rho}$ is constant along the characteristic $c(t)$.

Simple ODE: discretization

The simple ordinary differential equation (ODE)

$$\frac{\mathrm{d}y}{\mathrm{d}t} = -a\,y \tag{74}$$

with initial value

$$y\,(t_0) = y_0 \tag{75}$$

is of first order and linear with constant coefficient a. It has the obvious solution

$$y\,(t) = y_0\,\mathrm{e}^{-a(t-t_0)} \quad . \tag{76}$$

For discrete time steps

$$t^n = \Delta t\,n + t_0 \tag{77}$$

the straight-forward replacement $\mathrm{d}t \to \Delta t$ gives the most simple discretization (explicit Euler scheme: approximation of y by a piecewise linear curve)

$$y^{n+1} = y^n - a\,y^n\,\Delta t \quad . \tag{78}$$

Simple ODE: examples

First-order integration of ODE with different time steps:

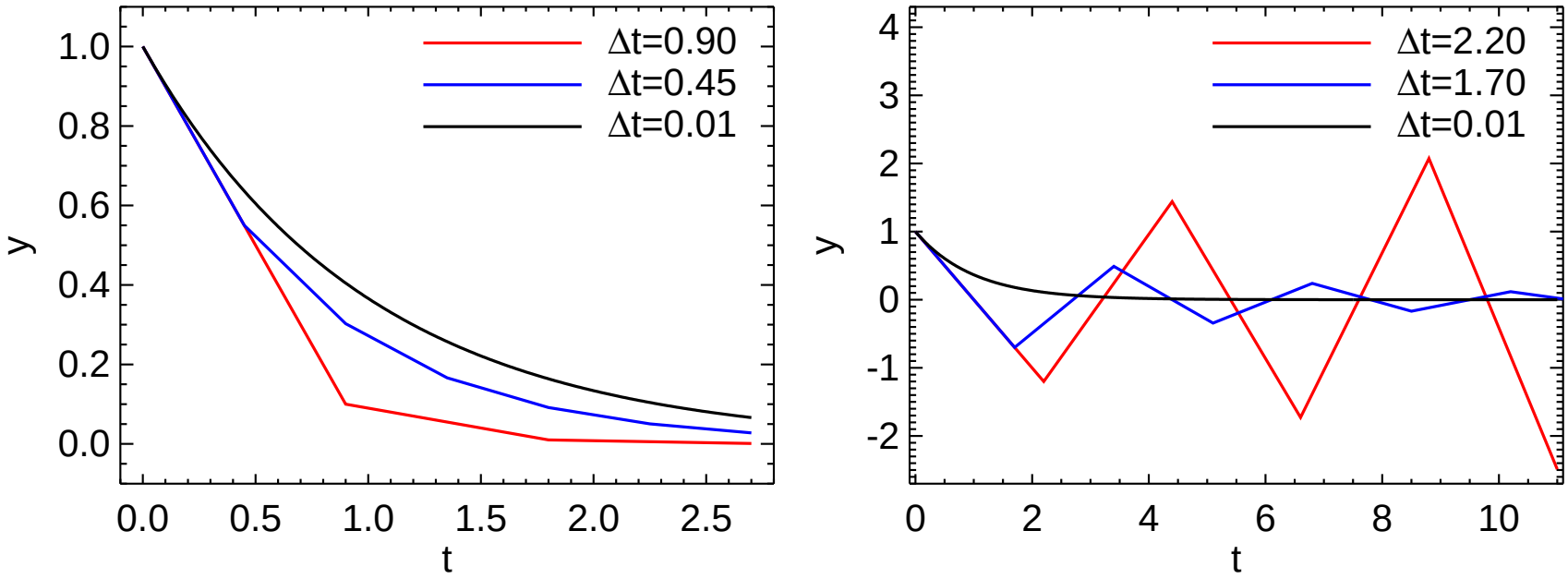

The figure shows examples for Eq. (78) for $a = 1$. The

$$\text{criterion for stability:} \qquad \Delta t < 2/a \tag{79}$$

$$\text{criterion for positivity:} \qquad \Delta t < 1/a \tag{80}$$

have a simple interpretation: too large time steps lead to conflicts with the actual curvature of the solution.

Simple ODE: remarks

To get accurate results with the Euler scheme (78) the time step Δt has to be very small.
In actual applications one should use a scheme that

- is of higher order (e.g., a 4th-order Runge-Kutta scheme) to allow much larger time steps and to improve the efficiency and accuracy of the scheme,
- has a build-in adjustment of the time step to guarantee stability even for variable coefficients,
- and/or is specially adapted for the type of ODE under consideration.

However, the simple scheme in Eq. (78) could – in principle – be used.

Parabolic PDE: heat equation

The heat equation

$$\frac{\partial y}{\partial t} = K \frac{\partial^2 y}{\partial x^2} \tag{81}$$

is a simple parabolic PDE where the conductivity K is a positive constant. With the initial values

$$y(x, t_0) = y_0(x) \tag{82}$$

and boundary values

$$y(x_1, t) = y_1(t) \quad , \quad y(x_2, t) = y_2(t) \tag{83}$$

it models, e.g., heat flux or radiative energy transport in the (optically thick) stellar interior.

Parabolic PDE: discretization

For discrete time steps on a spatial grid

$$t^n = \Delta t\, n + t_0 \tag{84}$$

$$x_i = \Delta x\, i + x_0 \quad , \tag{85}$$

the discretization in time and space

$$\frac{\partial y}{\partial t} \rightarrow \frac{y_i^{n+1} - y_i^n}{\Delta t} \tag{86}$$

$$\frac{\partial^2 y}{\partial x^2} \rightarrow \frac{y_{i+1}^n - 2y_i^n + y_{i-1}^n}{\Delta x^2} \tag{87}$$

gives the explicit Euler scheme

$$y_i^{n+1} = y_i^n + \frac{\Delta t}{\Delta x^2} K \left(y_{i+1}^n - 2y_i^n + y_{i-1}^n \right) \quad . \tag{88}$$

Parabolic PDE: stability

Stability of Euler scheme for heat equation: $\Delta t K/\Delta x^2$=0.2, 0.4, 0.6:

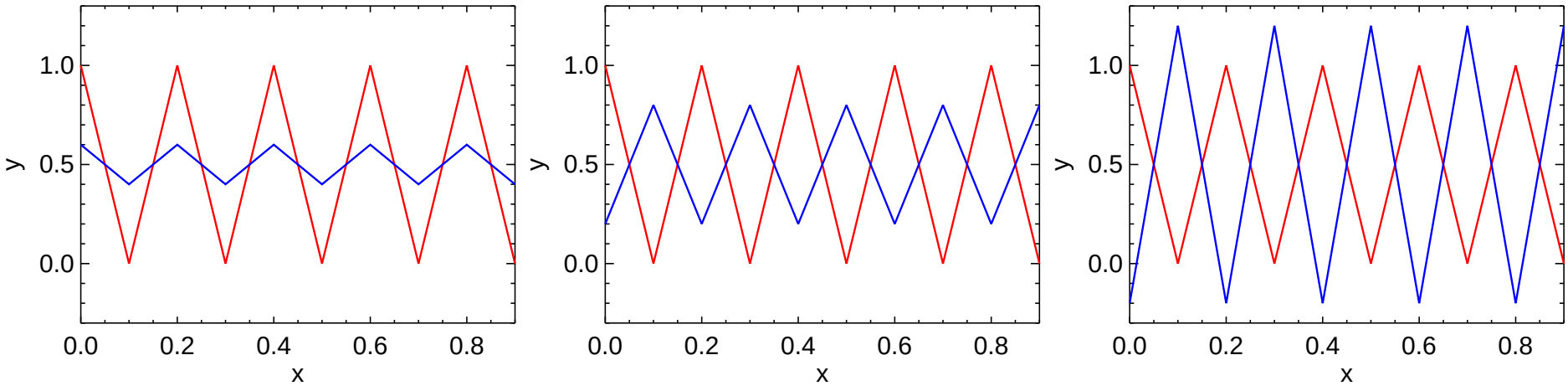

Examples for a simple $(1, 0, 1, 0, \ldots)$ initial condition (red) after a single step. The

$$\text{criterion for stability:} \quad \Delta t/\Delta x^2 < 1/(2K) \tag{89}$$

$$\text{criterion for positivity:} \quad \Delta t/\Delta x^2 < 1/(4K) \tag{90}$$

are comparable to the case of an ODE.

Parabolic PDE: example

Euler scheme for heat equation:

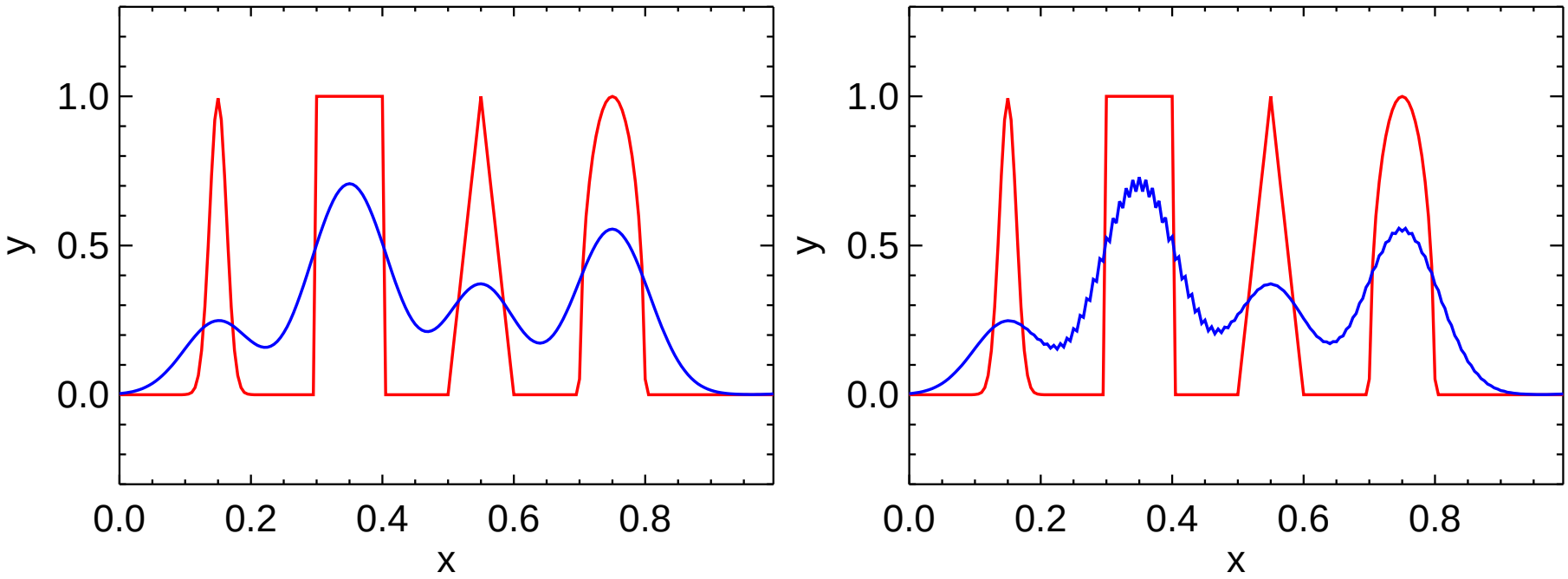

Examples for “spikes” initial condition (red) and periodic boundaries for two time steps $\Delta tK/\Delta x^2$=0.1, 0.5 after 500 or 100 steps, respectively (blue).
The slightly too large time step (0.5) causes the non-decaying spurious oscillations in the right panel.
The simple discretization (88) gives reasonable results.

Linear advection equation: discretization

The prototype of a hyperbolic PDE, the linear advection equation (66), can be discretized for discrete time steps on a spatial grid

$$t^n = \Delta t\, n + t_0 \tag{91}$$

$$x_i = \Delta x\, i + x_0 \tag{92}$$

by replacing

$$\frac{\partial \rho}{\partial t} \rightarrow \frac{\rho_i^{n+1} - \rho_i^n}{\Delta t} \tag{93}$$

$$\frac{\partial \rho}{\partial x} \rightarrow \frac{\rho_{i+1}^n - \rho_{i-1}^n}{2\Delta x} \quad . \tag{94}$$

The result is the explicit Euler scheme ("naive" scheme, FTCS scheme)

$$\rho_i^{n+1} = \rho_i^n - \frac{\Delta t}{2\Delta x}\, v \left(\rho_{i+1}^n - \rho_{i-1}^n\right) \quad . \tag{95}$$

This looks a bit similar to the discretization of the heat equation (88).

Linear advection equation: crash

Euler scheme for advection equation:

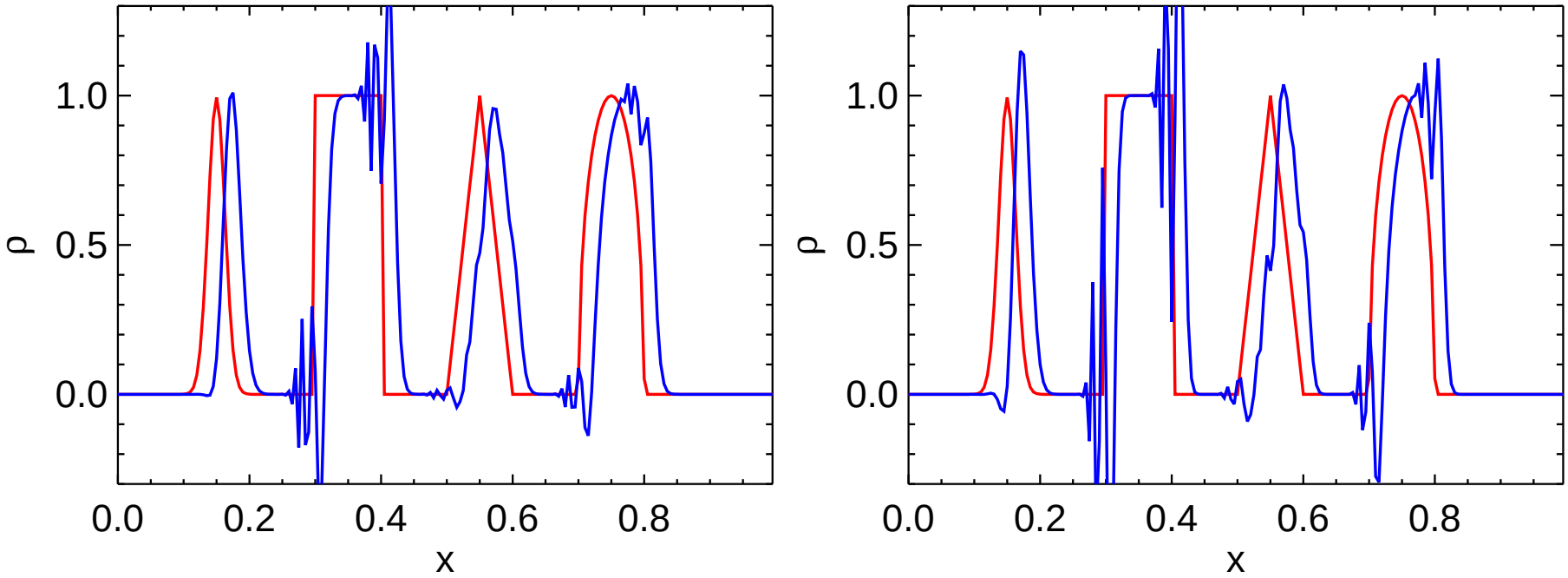

Examples for “spikes” initial condition (red) and periodic boundaries for two time steps $\Delta tv/\Delta x$=0.1, 0.5 after 50 or 10 steps, respectively (blue).

The exponentially growing oscillations render the scheme useless.

Linear advection equation: the lesson

Conclusions regarding the naive explicit Euler scheme (95) for the linear advection equation (66) (that worked well for the ODE and the parabolic PDE):

- The scheme is useless.
- Linear stability analysis: the scheme is unconditionally unstable, i.e., reducing the time step does not help!
- Stability does matter.

Why?

Discretization in space: wishlist

- We want: representation of "real" distribution of ρ (, $\boldsymbol{v}$, e_{i}) by finite set of numbers
- We need: restriction: transformation continuous values $\rightarrow$ discrete representation
- We need: reconstruction: transformation discrete representation$\rightarrow$ continuous values
- We get: hints for the discretization of the spatial and temporal operators

Concepts of "restriction" and "reconstruction" are often used during the construction or analysis of a numerical scheme.
These concepts might not show up in the actual algorithm: different concepts may result in the very same scheme.

Discretization in space by finite differences

Finite difference methods:

- Restriction: sampling
- Reconstruction: interpolation (by polynomials)
- Derivatives become finite differences

"Sampling" means: to go from continuous values of $\rho(x)$ to a discrete set of values ρ_i for a grid with $x_i = \Delta x\, i + x_0$ we set

$$\rho_i = \rho\left(x_i\right) \quad . \tag{96}$$

Discretization in space by finite volumes

Finite volume methods:

- Restriction: integration over control volume
- Reconstruction: reconstruction (by polynomials)
- Derivatives can become finite differences (or can be avoided)

To go from continuous values of $\rho(x)$ to a discrete set of values ρ_i for a grid with $x_i = \Delta x\, i + x_0$ we integrate over the "control volume" associated to each grid point. In one dimension that might be

$$\rho_i = \frac{1}{\Delta x} \int_{x_i - \Delta x/2}^{x_i + \Delta x/2} \rho\,(x)\; dx \quad . \tag{97}$$

Discretization in space by other methods

Finite element methods:

- Representation by a finite set of simple base functions (piecewise polynomials) with compact (“finite”) support
- Usually used on an unstructured grid to model the flow around complex bodies
- More often used in engineering than in astrophysics

Spectral methods:

- Representation by a finite set of harmonical functions (e.g. sine waves)
- Spatial derivatives become multiplications with wave vector
- Good for flows with small non-linear interactions
- Typically used for flows in the stellar interior (with low Mach numbers)

Smoothed Particle Hydrodynamics (SPH):

- Representation by a finite set of “large particles” that move freely
- Grid is replaced by particle positions
- Particle density translates into fluid density

Discretization in space: grids

In one spatial dimension one can choose between

- Eulerian grid: fixed in space
- Lagrangian grid: moving with the flow (makes the linear 1D advection trivial)
- Hybrid grid: moving with another speed
- No “grid”: SPH (grid is replaced by particle positions)

In the following examples the grid points will be fixed (Eulerian) and equidistant.

- In multi-dimensions things become more complicated.
- Some advanced “real world” techniques (hierarchical grids perhaps with adaptive mesh refinement) are build upon methods with simple Eulerian grids.

Integral form and weak solution

- Any solution of the advection equation in differential form (66) has to be sufficiently smooth, so that it has derivatives.
- However, any function – even a discontinuous one – can be propagated along characteristics (Page 35).

Transformation: linear advection equation in integral form (see Page 52 and Page 12):

$$\int_{x_0}^{x_1} \int_{t_0}^{t_1} \left[\frac{\partial \rho}{\partial t} + v \frac{\partial \rho}{\partial x} \right] dt\, dx = 0 \ , \tag{98}$$

$$\int_{x_0}^{x_1} \int_{t_0}^{t_1} \frac{\partial \rho}{\partial t} dt\, dx + v \int_{t_0}^{t_1} \int_{x_0}^{x_1} \frac{\partial \rho}{\partial x} dx\, dt = 0 \ , \tag{99}$$

$$\int_{x_0}^{x_1} \left[\rho(x, t_1) - \rho(x, t_0) \right] dx + v \int_{t_0}^{t_1} \left[\rho(x_1, t) - \rho(x_0, t) \right] dt = 0 \tag{100}$$

Definition: Weak solution of PDE in differential form: solution of PDE in integral form.

In smooth regions: weak solution = solution.

Integral form and flux centering

Flux centering:

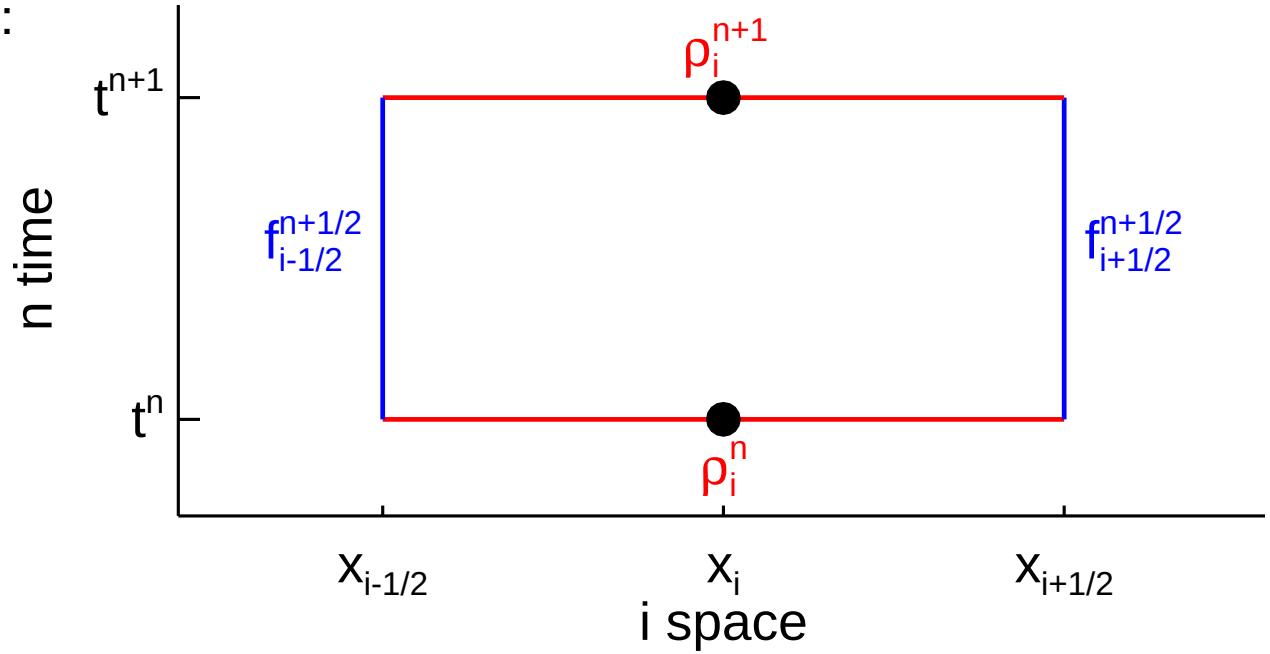

Integral form from Eq. (100) for one cell with width Δx and one time step Δt:

$$\underbrace{\int_{x_{i-\frac{1}{2}}}^{x_{i+\frac{1}{2}}} \rho\left(x, t^{n+1}\right) dx}_{\Delta x\, \rho_i^{n+1}} - \underbrace{\int_{x_{i-\frac{1}{2}}}^{x_{i+\frac{1}{2}}} \rho\left(x, t^{n}\right) dx}_{\Delta x\, \rho_i^{n}} + \underbrace{\int_{t^n}^{t^{n+1}} v\, \rho\left(x_{i+\frac{1}{2}}, t\right) dt}_{\Delta t\, f_{i+\frac{1}{2}}^{n+\frac{1}{2}}} - \underbrace{\int_{t^n}^{t^{n+1}} v\, \rho\left(x_{i-\frac{1}{2}}, t\right) dt}_{\Delta t\, f_{i-\frac{1}{2}}^{n+\frac{1}{2}}} = 0 \quad (101)$$

Centering of quantities, fluxes, and differences

Centering:

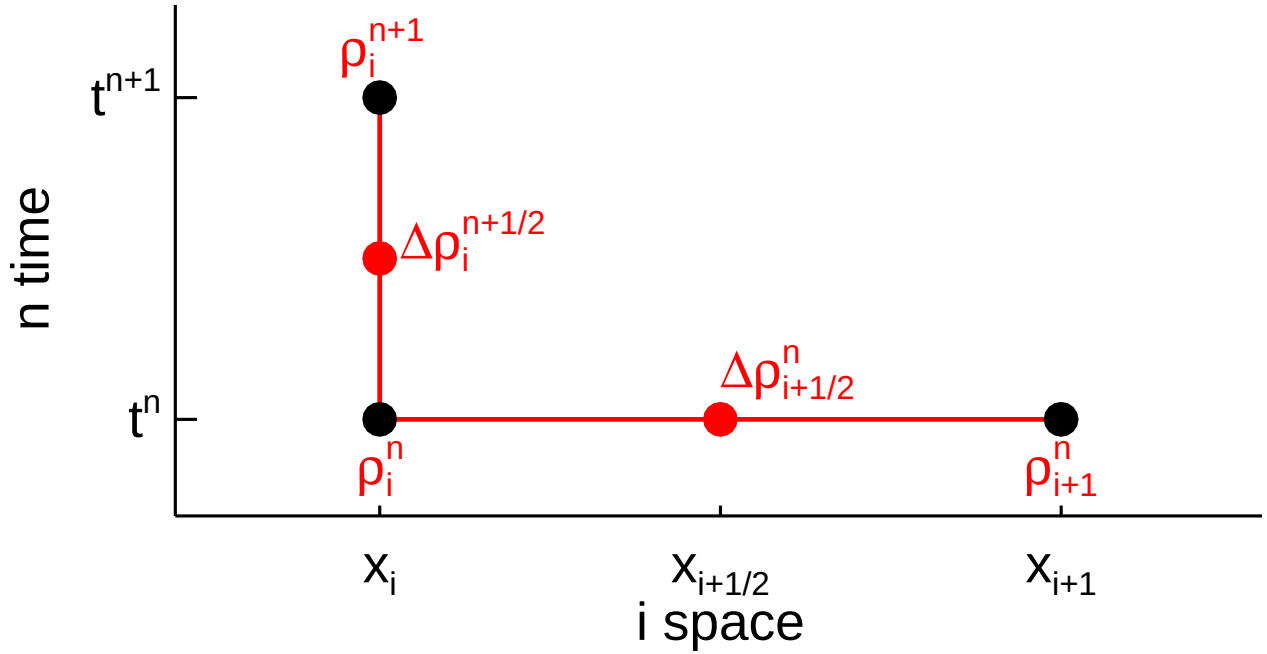

Examples for “natural centering”:

- Quantities at grid points (integer indices): e.g. $\rho_i^n, \rho_{i+1}^n, \ldots$
- Spatial differences of quantities (half-integer i indices): e.g. $\Delta\rho_{i+\frac{1}{2}}^n = \rho_{i+1}^n - \rho_i^n$
- Time differences of quantities (half-integer n indices): e.g. $\Delta\rho_i^{n+\frac{1}{2}} = \rho_i^{n+1} - \rho_i^n$
- Fluxes at half-integer i indices (and – in fact – preferably at half-integer n indices) to get update properly centered: $\Delta\rho_i^{n+\frac{1}{2}} = -\frac{\Delta t}{\Delta x}\left(f_{i+\frac{1}{2}}^n - f_{i-\frac{1}{2}}^n\right)$

Effects of centering of quantities

Centering:

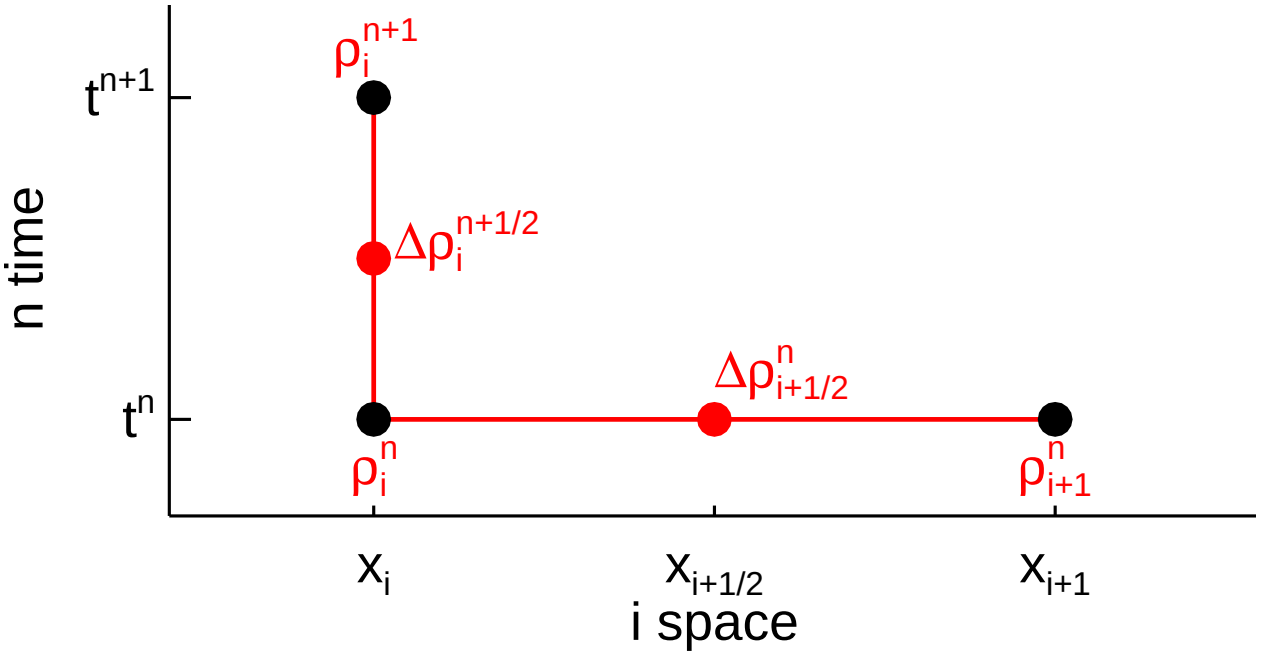

Effects of "natural centering":

- $\frac{\rho_{i+1}^n - \rho_i^n}{x_{i+1} - x_i}$ is $O(\Delta x)$ for $\frac{\partial \rho}{\partial x}(x_i)$ and $\frac{\partial \rho}{\partial x}(x_{i+1})$.
- $\frac{\rho_{i+1}^n - \rho_i^n}{x_{i+1} - x_i}$ is $O(\Delta x^2)$ for $\frac{\partial \rho}{\partial x}\left(x_{i+\frac{1}{2}}\right)$.
- $\frac{\rho_{i+1}^n - \rho_{i-1}^n}{x_{i+1} - x_{i-1}}$ is $O(\Delta x^2)$ for $\frac{\partial \rho}{\partial x}(x_i)$.

Update formula in conservation form

After computing, e.g., from the fluxes in the cells

$$f(\rho_i^n) = v\,\rho_i^n \tag{102}$$

the fluxes at cell boundaries

$$f^n_{i+\frac{1}{2}} \quad , \tag{103}$$

that characterize a method, the update can be done by the formula

$$\rho_i^{n+1} = \rho_i^n - \frac{\Delta t}{\Delta x}\left(f^n_{i+\frac{1}{2}} - f^n_{i-\frac{1}{2}}\right) \quad . \tag{104}$$

This is the conservation form because the summed-up density changes only due to fluxes through the boundaries and is conserved otherwise,

$$\sum_{i=i_0}^{i_1} \rho_i^{n+1} = \sum_{i=i_0}^{i_1} \rho_i^n - \frac{\Delta t}{\Delta x}\sum_{i=i_0}^{i_1}\left(f^n_{i+\frac{1}{2}} - f^n_{i-\frac{1}{2}}\right) \tag{105}$$

$$= \sum_{i=i_0}^{i_1} \rho_i^n - \frac{\Delta t}{\Delta x}\left[f^n_{i_1+\frac{1}{2}} + \sum_{i=i_0}^{i_1-1}\left(f^n_{i+\frac{1}{2}} - f^n_{i+\frac{1}{2}}\right) - f^n_{i_0-\frac{1}{2}}\right] \tag{106}$$

$$= \underbrace{\sum_{i=i_0}^{i_1} \rho_i^n}_{\text{initial total mass}} - \underbrace{\frac{\Delta t}{\Delta x}\left(f^n_{i_1+\frac{1}{2}} - f^n_{i_0-\frac{1}{2}}\right)}_{\text{fluxes through boundaries}} \quad . \tag{107}$$

Stencil diagrams

Stencil diagram:

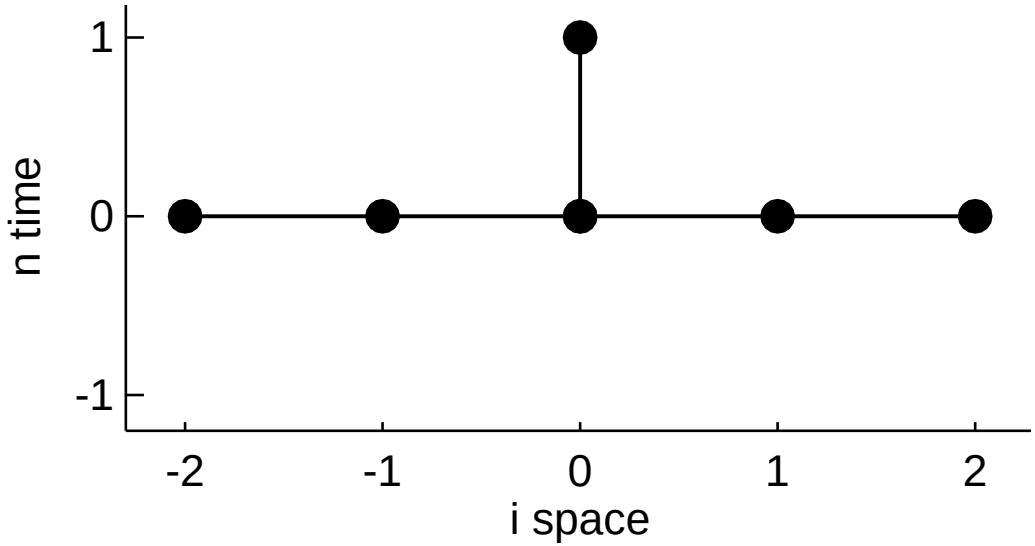

The density ρ_i^{n+1} at grid point i and time step $n+1$ depends on values at the old time step n (direct numerical domain of dependence, stencil)

$$\rho_{i-k}^n, \rho_{i-k+1}^n, \ldots, \rho_{i+l}^n \quad . \tag{108}$$

This is sketched in a so-called stencil diagram above.
Looking the other way, a stencil diagram tells also which points

$$\rho_{i-l}^{n+1}, \rho_{i-l+1}^{n+1}, \ldots, \rho_{i+k}^{n+1} \tag{109}$$

at the new time step $n+1$ are influenced by ρ_i^n (range of influence).

Stencil diagrams: spatial centering

Stencil diagrams with different spatial centering: FTBS, FTCS, FTFS:

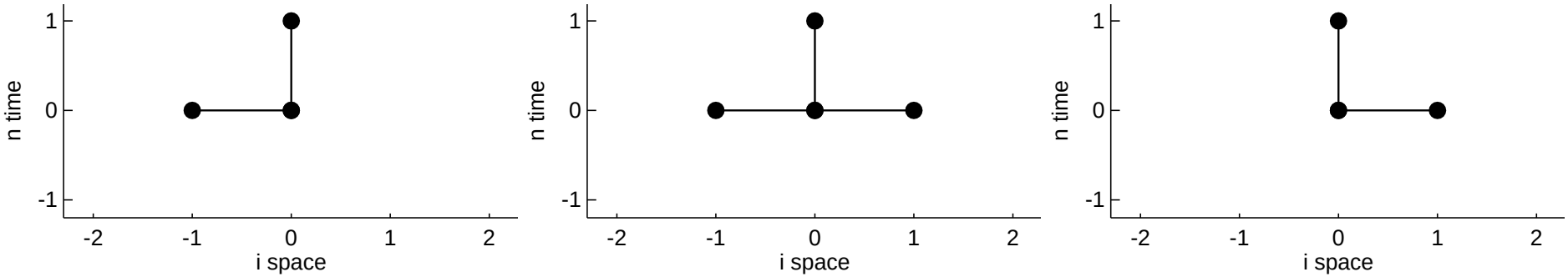

The figure shows stencil diagrams for 3 schemes with FT (forward-time) centering and different spatial centerings:

- BS: backward-space
- CS: center-space
- FS: forward-space

The middle panel corresponds to the FTCS scheme from Eq. (95).

Stencil diagrams: centering in time

Stencil diagrams with different time centering: FTCS, time-centered implicit, BTCS, CTCS (leapfrog):

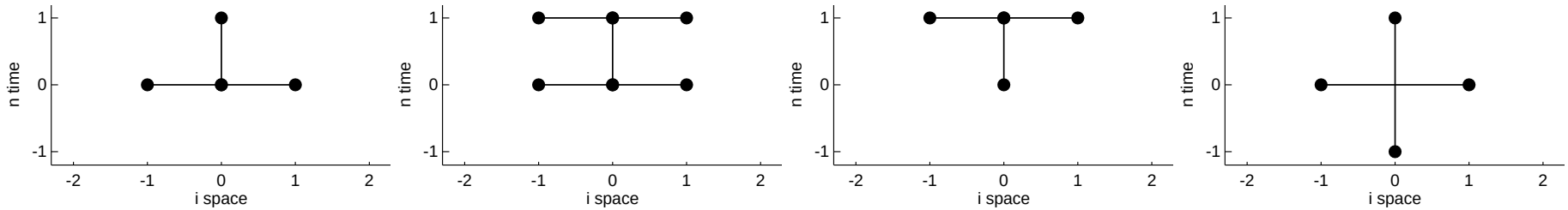

This figure shows stencil diagrams for 4 schemes with CS and different time centering:

- FT: forward-time (explicit)
- time-centered implicit: (implicit)
- BT: backward-time (fully implicit)
- CT, Leapfrog: center-time (explicit, uses 3 time planes)

In implicit schemes each value at the new time level typically depends on all values at the old level: The full domain of dependence is larger than the direct domain of dependence.

CFL condition

Stencil diagrams with too small (left) and sufficiently large (right) stencil:

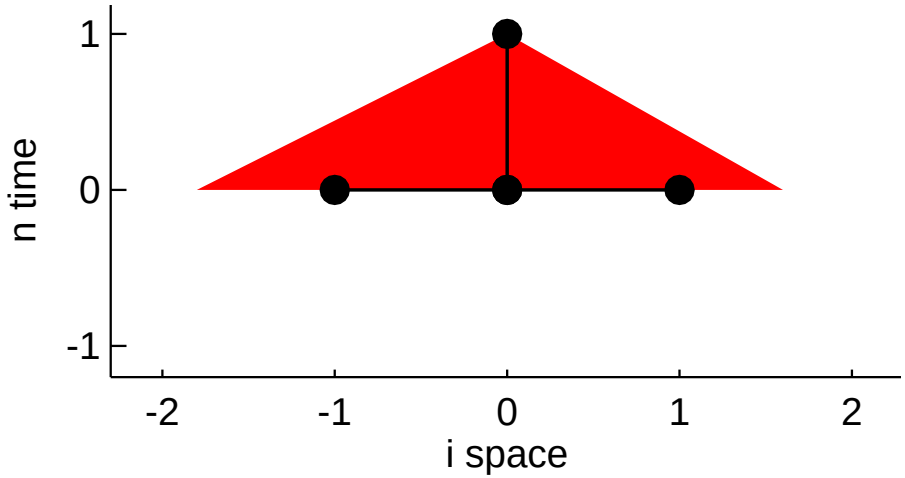

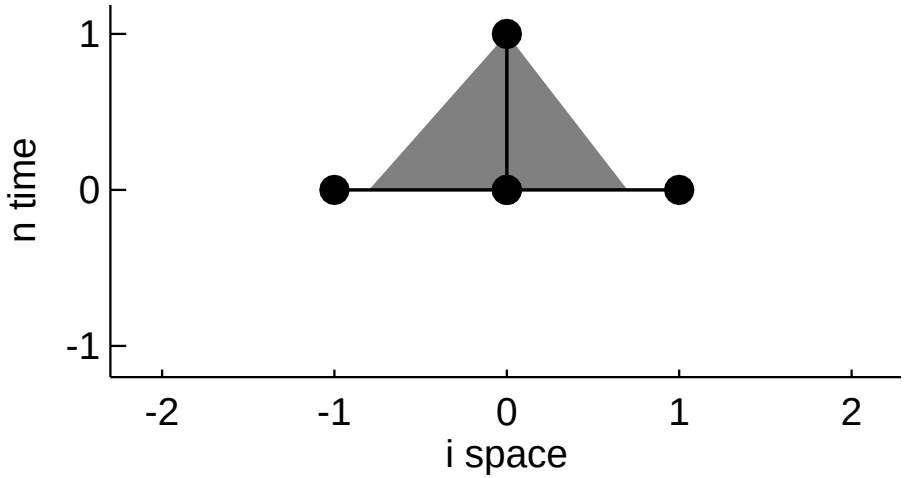

Due to the finite travelling speed of waves hyperbolic PDEs have a finite physical domain of dependence.

Courant-Friedrichs-Levy condition (CFL condition):

- The full numerical domain of dependence must contain the physical domain of dependence.

The CFL condition is necessary for stability (but not sufficient).

Truncation error

A sufficiently smooth function can be expanded in a Taylor series:

$$\rho(x+\Delta x,t)=\sum_{l=0}^{\infty}\frac{1}{l!}\frac{\partial^l\rho}{\partial x^l}\bigg|_{x,t}\Delta x^l=\rho(x,t)+\frac{\partial\rho}{\partial x}\bigg|_{x,t}\Delta x+O\left(\Delta x^2\right)\quad . \tag{110}$$

Solving for $\frac{\partial\rho}{\partial x}$ gives

$$\frac{\partial\rho}{\partial x}=\frac{\rho(x+\Delta x,t)-\rho(x,t)}{\Delta x}+O\left(\Delta x\right)\quad . \tag{111}$$

Repeating this for the time derivative and applying it to an entire PDE (FTFS) gives

$$\underbrace{\frac{\partial\rho}{\partial t}+v\frac{\partial\rho}{\partial x}}_{\text{PDE}}=\underbrace{\frac{\rho_i^{n+1}-\rho_i^n}{\Delta t}+v\frac{\rho_{i+1}^n-\rho_i^n}{\Delta x}}_{\text{numerical scheme}}+\underbrace{O(\Delta t,\Delta x)}_{\text{truncation error}}\quad . \tag{112}$$

The order of the truncation error is $O\left(\Delta t,\Delta x\right)$ in this case (FTFS).
A high order of the truncation error (both in Δt and Δx) hints at good accuracy for smooth functions.

Consistency – stability – convergence

- Consistency: A numerical scheme is consistent if its discrete operator (with finite differences) converges towards the continuous operator (with derivatives) of the PDE for $\Delta t, \Delta x \to 0$ (vanishing truncation error).
- Stability: "Noise" (from initial conditions, round-off errors,...) does not grow.
- Convergence: The solution of the numerical scheme converges towards the real solution of the PDE for $\Delta t, \Delta x \to 0$.

Lax's equivalence theorem: "Given a properly posed initial value problem and a finite-difference approximation to it that satisfies the consistency condition, stability is the necessary and sufficient condition for convergence."

- Consistency: discrete operator $\overset{\Delta t, \Delta x \to 0}{\longrightarrow}$ PDE operator
- Stability: discrete operator does not amplify "noise"
- Convergence: Numerical solution $\overset{\Delta t, \Delta x \to 0}{\longrightarrow}$ real solution

Lax's equivalence theorem: consistency + stability $\Leftrightarrow$ convergence

Derivations of donor-cell scheme

Donor cell scheme (FTBS, stencil on Page 57, example later on Page 68):

$$\rho_i^{n+1} = \rho_i^n - \frac{\Delta t\, v}{\Delta x} \left(\rho_i^n - \rho_{i-1}^n\right) \quad . \tag{113}$$

Strategies to derive it:

1. Discrete differences:
   - Characteristic curves: mass flows from left to right
   - Replacement: CS of naive scheme $\rightarrow$ difference in upwind direction: BS
2. Characteristics + interpolation:
   - Follow characteristic curve from ρ_i^{n+1} back in time
   - Interpolate between ρ_{i-1}^n and ρ_i^n (linearly)
3. Reconstruct–Solve–Average (RSA, Godunov-type method):
   - Finite volumes (reconstruction-evolution, Reconstruct-Propagate-Average)
   - Reconstruct run of ρ within each cell (here: assume constant ρ)
   - Use exact continuous solution for the time evolution
   - Average intermediate continuous result to get single value in each cell

Important concepts

Important properties of a numerical scheme:

- Consistency (otherwise it does not describe the PDE)
- Stability (and therefore convergence of the solution)
- Conservativity (to prevent leakages)

Further desirable properties of a numerical scheme or code:

- Accuracy: high-order convergence in smooth regions (high-order truncation error), good approximation even at finite resolution, minimal artifacts near discontinuities
- Positivity (boundedness): ρ, P, T always positive
- Simplicity: code should be easy to understand, maintain, and extend
- Efficiency: code should be fast (on a variety of machines)

The non-linear system of the hydrodynamic equations will put additional weight on conservativity and positivity.

Parameters of the following examples

Boundary conditions influence the properties of real world hydrodynamic flows.
Linear 1D advection: infinite domain without boundaries.
Actual implementation of boundary conditions in numerical experiments:

- Adding and filling ghost cells
- Number of ghost cells: depends on stencil
- In examples: periodic boundary conditions

Grid settings:

$$i_{\mathrm{total}} = 200 \ , \quad n_{\mathrm{total}} = 500 \ , \quad \frac{\Delta t\, v}{\Delta x} = 0.4 \quad \Rightarrow \quad \text{one revolution} \tag{114}$$

Initial condition: “spikes” (Gaussian, rectangle, triangle, half-ellipse), see Jiang & Shu (1996).

Naive FTCS scheme

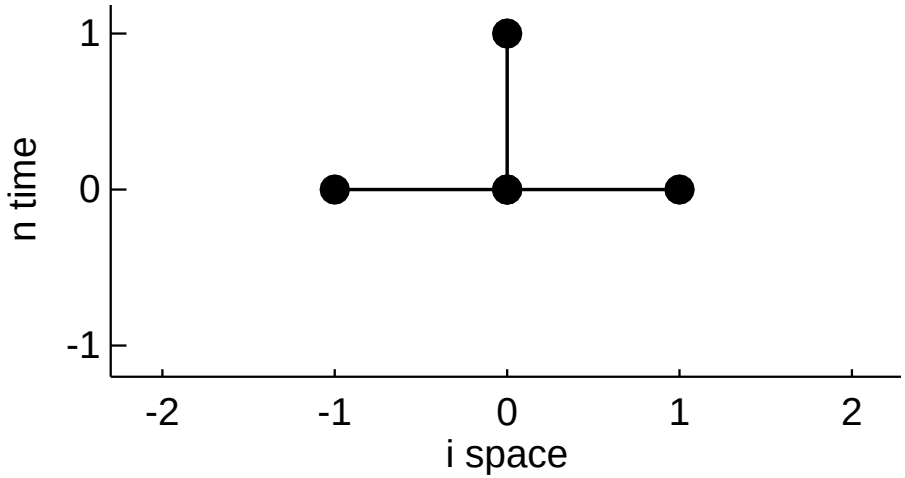

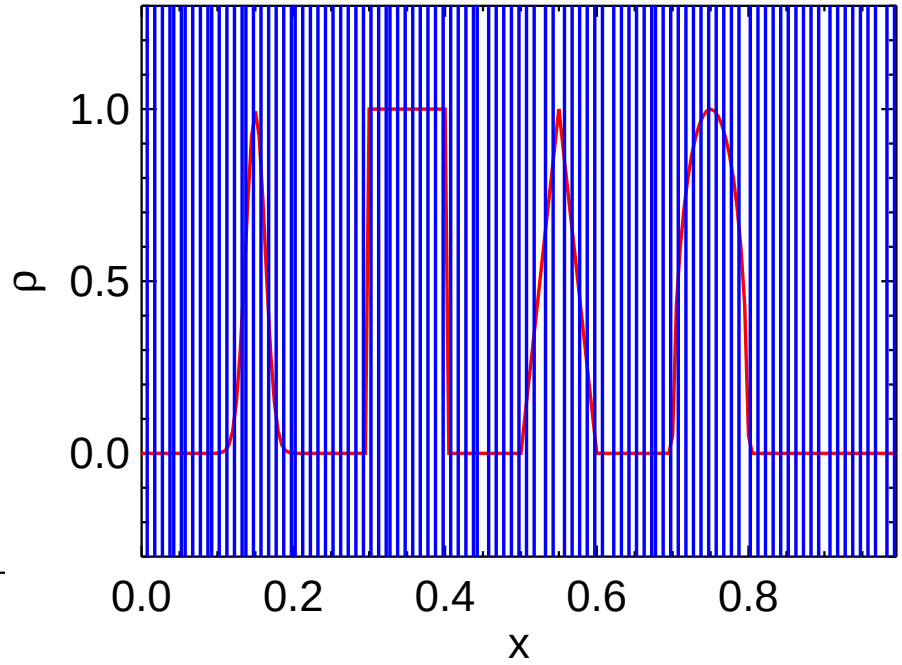

Naive scheme (Euler scheme, FTCS, Page 44) from Eq. (95) with flux at $i + \frac{1}{2}$

$$f^n_{i+\frac{1}{2}} = \frac{1}{2}\left[f(\rho^n_{i+1}) + f(\rho^n_i)\right] \quad . \tag{115}$$

The oscillations already seen on Page 44 grow exponentially. After some time, the numerical result does not have the faintest resemblance to the true solution.

Implicit centered scheme

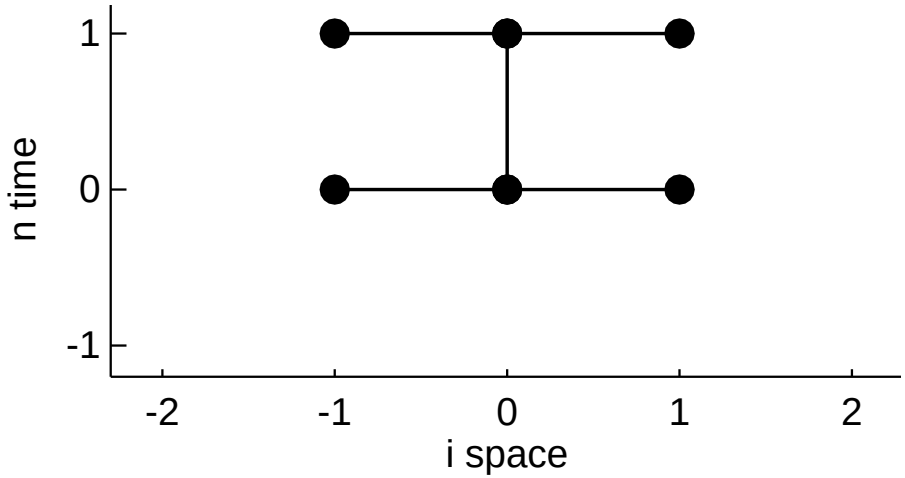

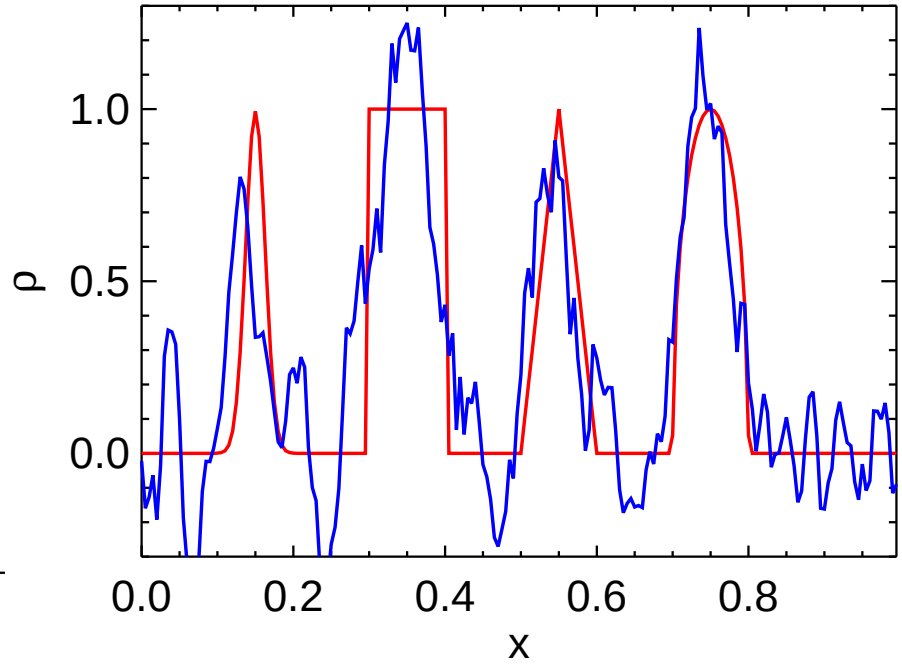

Implicit centered scheme with flux

$$f^n_{i+\frac{1}{2}} = \frac{1}{4}\left[f(\rho^n_{i+1}) + f(\rho^n_i)\right] + \frac{1}{4}\left[f\left(\rho^{n+1}_{i+1}\right) + f\left(\rho^{n+1}_i\right)\right] \quad . \tag{116}$$

The centering of the scheme in space and time seems promising. However, the result is severely distorted compared to the initial condition.

BTCS scheme

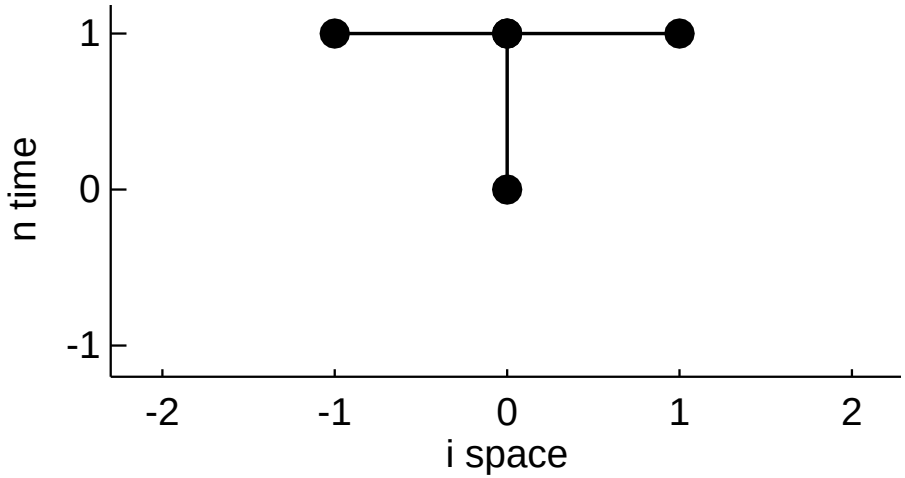

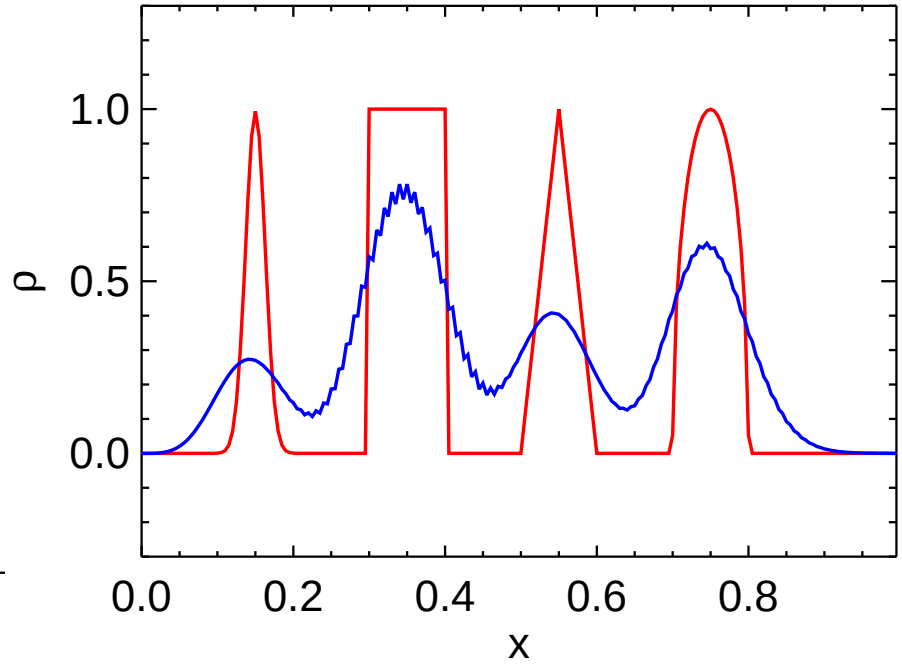

Fully-implicit BTCS scheme with flux

$$f^n_{i+\frac{1}{2}} = \frac{1}{2}\left[f\left(\rho^{n+1}_{i+1}\right) + f\left(\rho^{n+1}_{i}\right)\right] \quad . \tag{117}$$

The fully implicit treatment takes effect: the result looks almost smooth (with some non-decaying small-scale wiggles) but is smeared out heavily.

Donor cell (FTBS) scheme

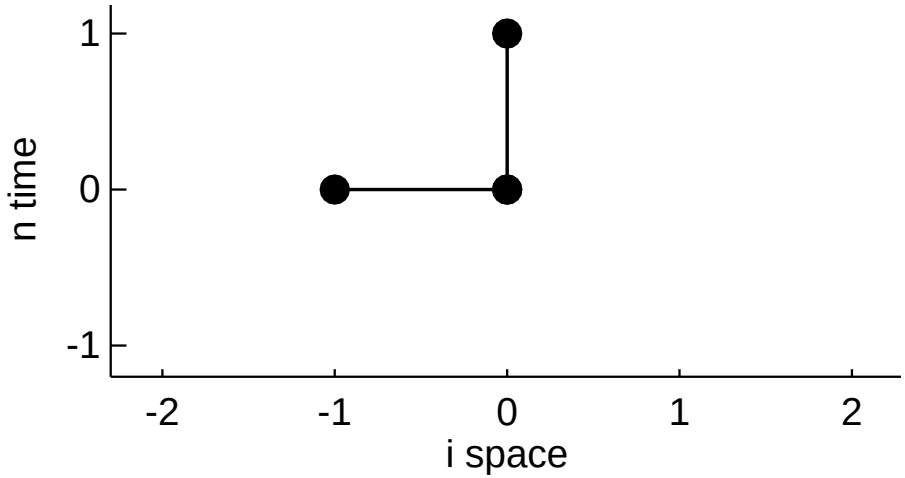

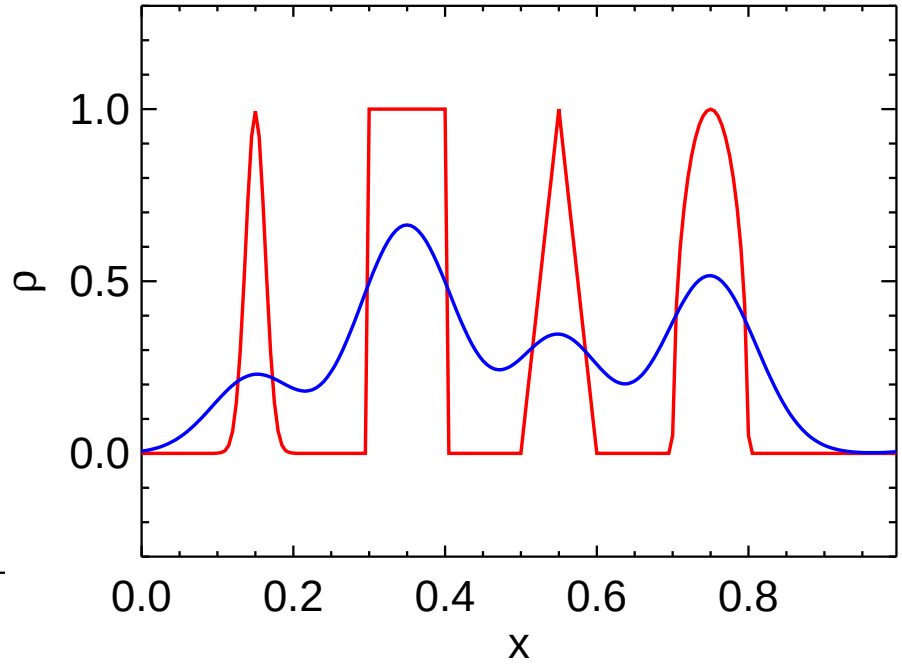

Donor cell scheme (FTBS, 1st order upwind method, derived on Page 62), with flux

$$f^n_{i+\frac{1}{2}} = f(\rho^n_i) \quad . \tag{118}$$

The result is wonderfully smooth but smeared out severely. Upwinding seems promising to achieve stability. However, the accuracy of the scheme has to be improved.

FTFS scheme

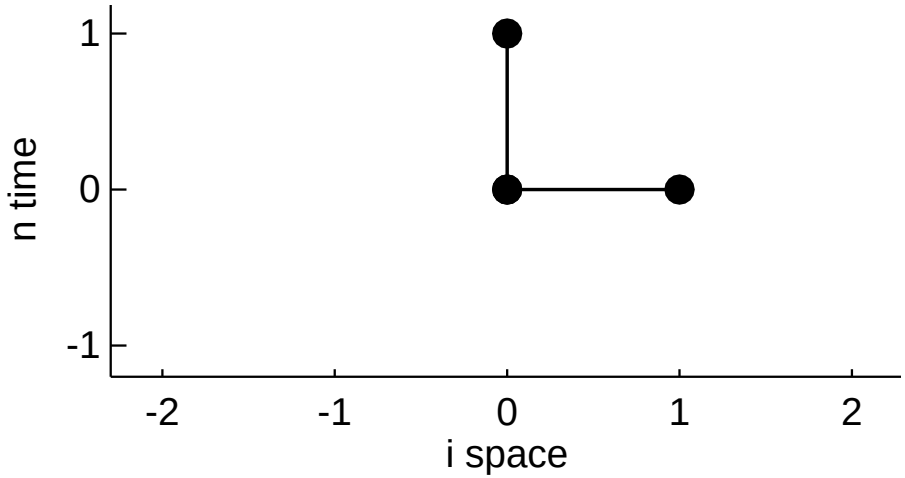

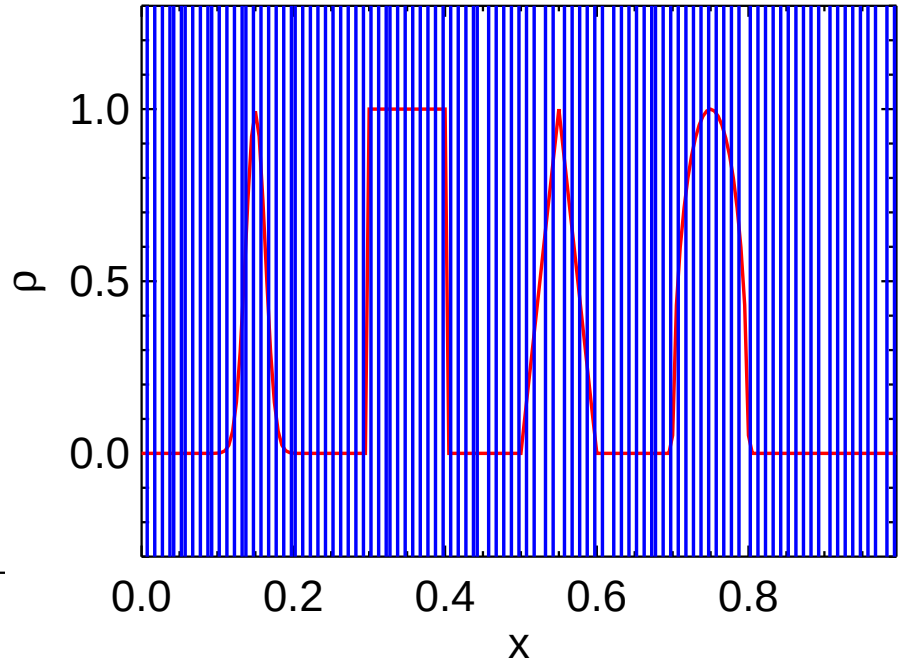

FTFS scheme with flux

$$f^n_{i+\frac{1}{2}} = f(\rho^n_{i+1}) \quad . \tag{119}$$

Small-scale oscillations grow even faster than for the naive scheme and render the FTFS scheme useless (at least for $v > 0$), too.

Lax-Friedrichs scheme

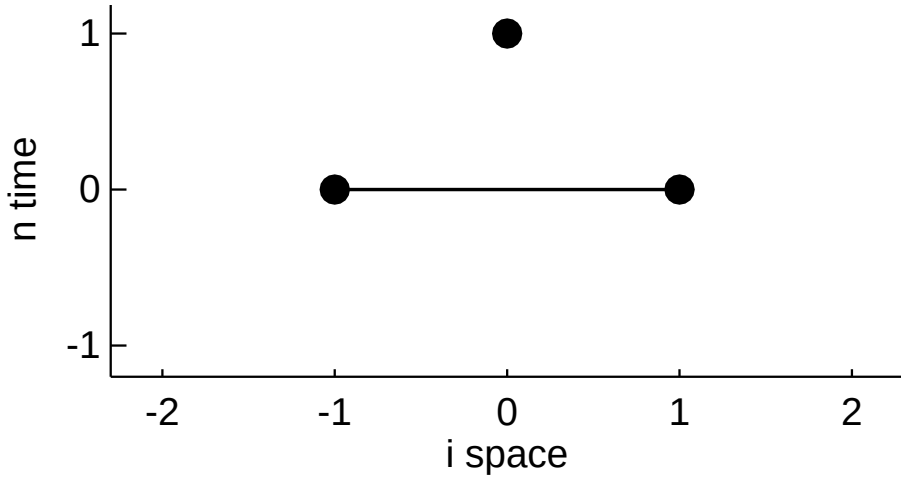

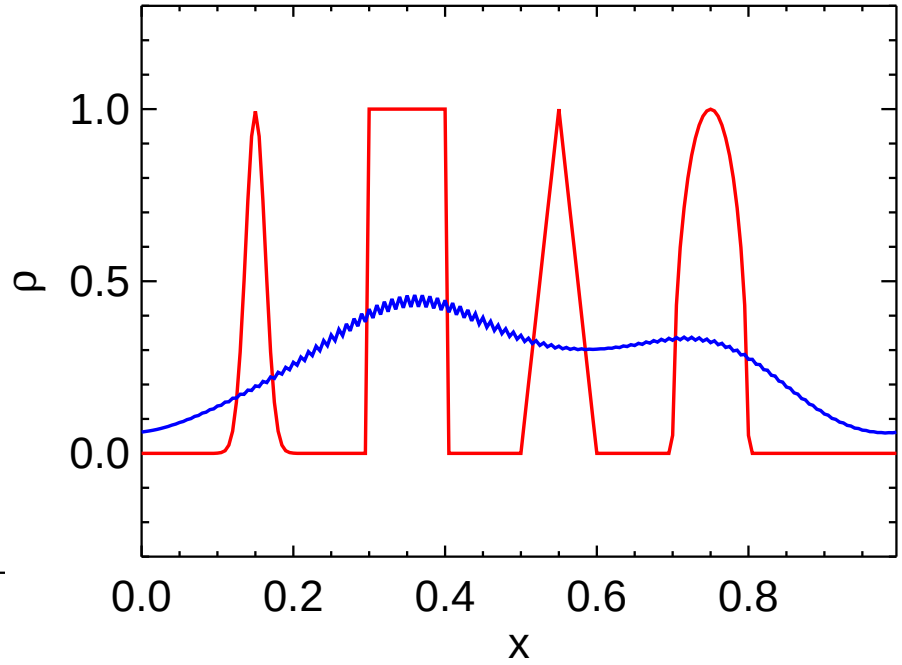

Lax-Friedrichs scheme with flux

$$f^n_{i+\frac{1}{2}} = \frac{1}{2}\left[f(\rho^n_{i+1}) + f(\rho^n_i)\right] - \frac{1}{2}\frac{\Delta x}{\Delta t}\left[\rho^n_{i+1} - \rho^n_i\right] \quad . \tag{120}$$

The smearing is so strong that not even the number of the initial spikes is conserved. And there are some non-decaying small-scale wiggles left (due to odd-even decoupling).

Lax-Wendroff scheme

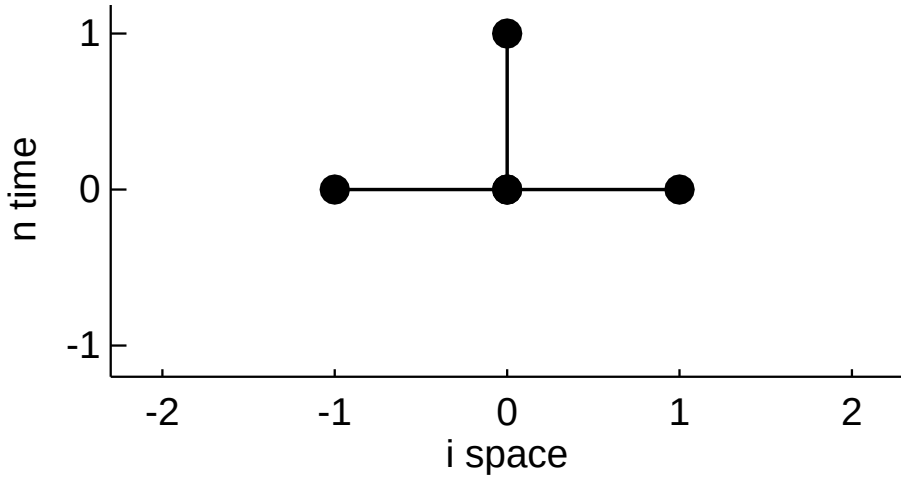

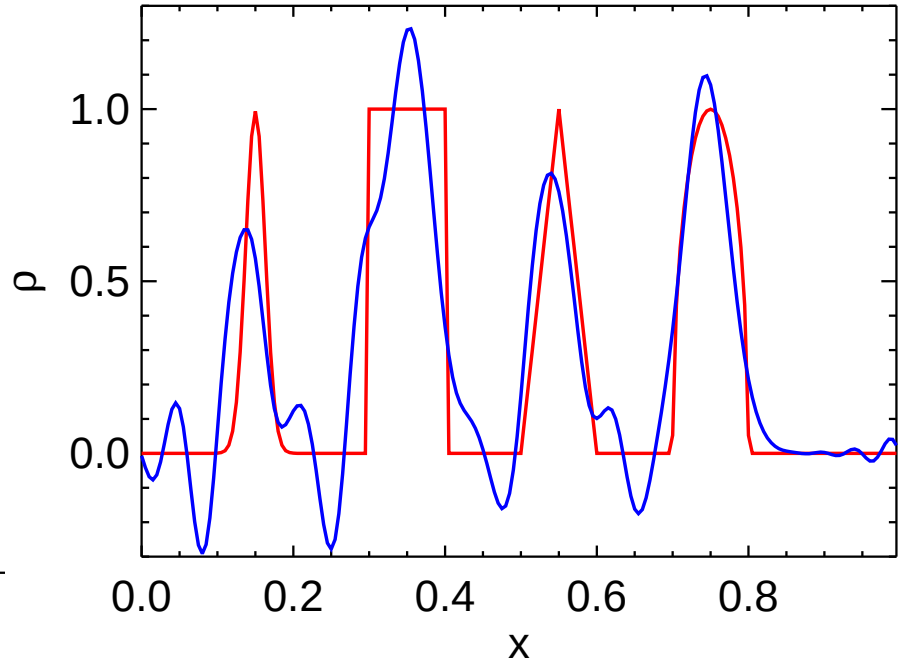

The Lax-Wendroff scheme is $O(\Delta x^2, \Delta t^2)$ with flux

$$f^n_{i+\frac{1}{2}} = \frac{1}{2}\left[f(\rho^n_{i+1}) + f(\rho^n_i)\right] - \frac{1}{2}\frac{v^2\Delta t}{\Delta x}\left[\rho^n_{i+1} - \rho^n_i\right] \quad . \tag{121}$$

The result is smooth with considerable overshoot (that does not much grow with time anymore). This second order scheme might be useful for more regular initial conditions.

Beam-Warming scheme

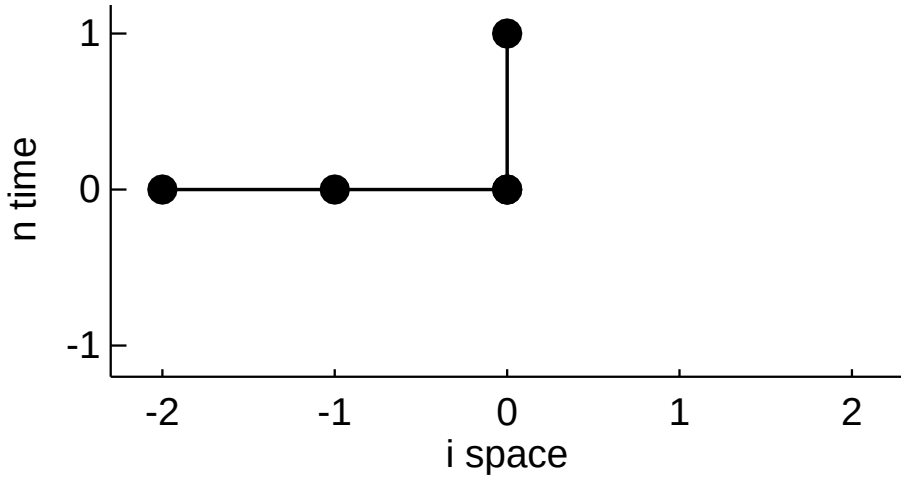

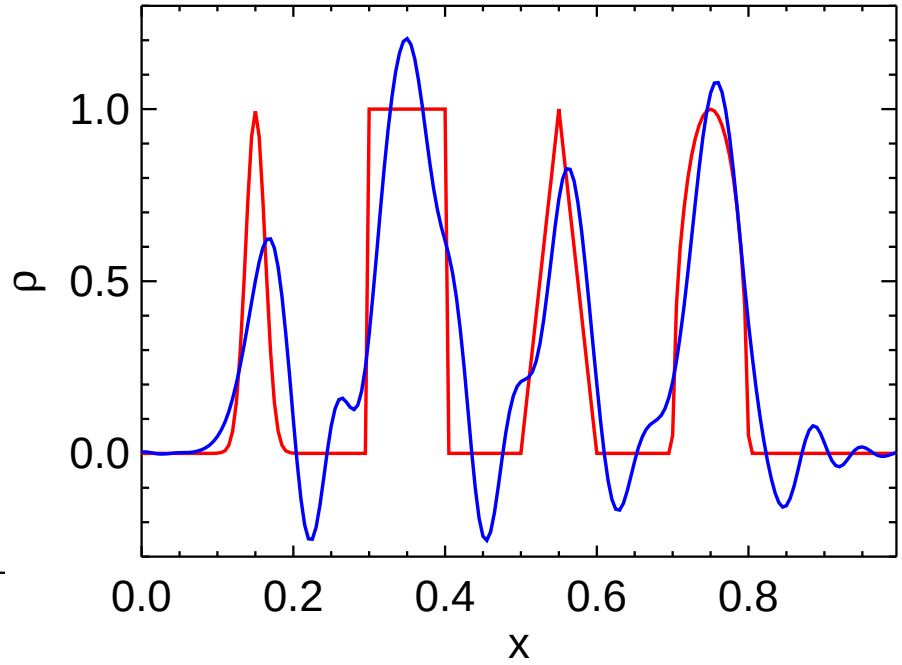

The Beam-Warming scheme is $O(\Delta x^2, \Delta t^2)$ with flux

$$f^n_{i+\frac{1}{2}} = \frac{1}{2}\left[3f(\rho^n_i) - f\left(\rho^n_{i-1}\right)\right] - \frac{1}{2}\frac{v^2\Delta t}{\Delta x}\left[\rho^n_i - \rho^n_{i-1}\right] \quad . \tag{122}$$

The result is smooth with considerable overshoot (that does not much grow with time anymore). This second order scheme might be useful for more regular initial conditions.

Fromm scheme

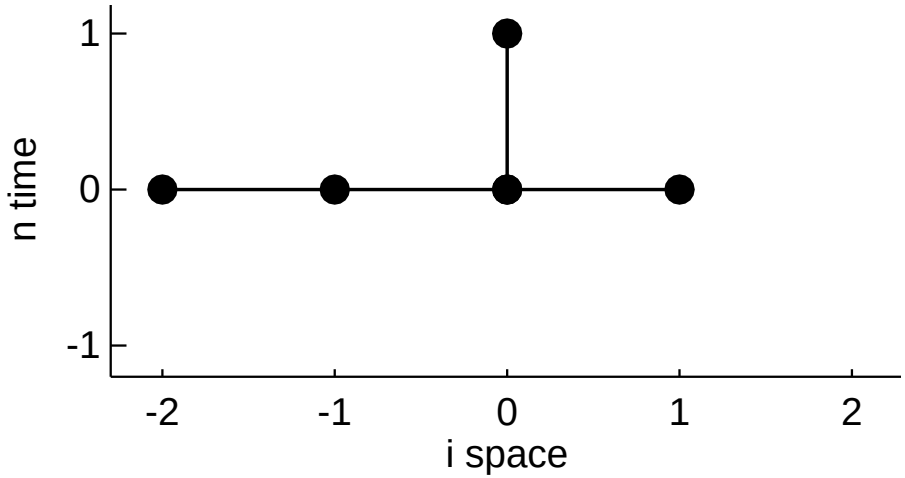

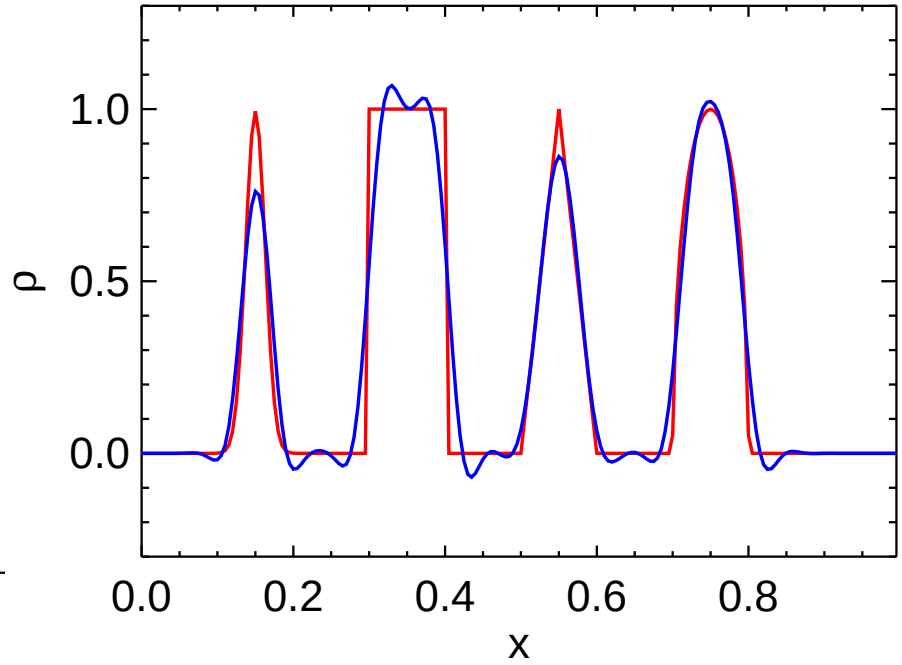

The Fromm scheme is $O(\Delta x^2, \Delta t^2)$ with flux

$$f^n_{i+\frac{1}{2}} = \frac{1}{2}\left(f^n_{\mathrm{Lax-Wendroff},i+\frac{1}{2}} + f^n_{\mathrm{Beam-Warming},i+\frac{1}{2}}\right) \quad . \tag{123}$$

The result is smooth with some amount of overshoot. The initial shape of the spikes is recognizable. So far the best scheme, if the overshoot can be accepted.
See Page 89.

Overshoot

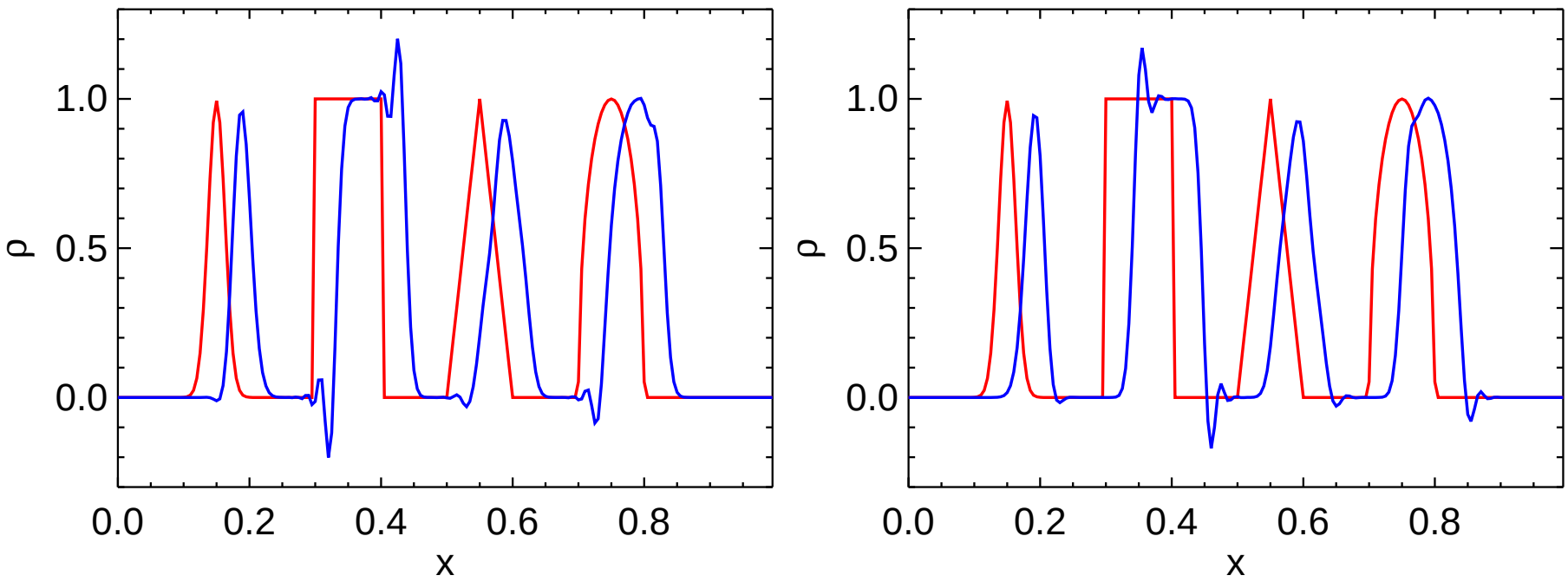

The figure shows the standard example after only n=20 time steps for the Lax-Wendroff (Page 71) and the Beam-Warming scheme (Page 72) displaying overshooting post- and pre-shock oscillations.
This Gibb's phenomenon is closely related to overshoot of parabolic (or higher-order) interpolation schemes.

Artificial viscosity

Inserting the Lax-Friedrichs flux (120) into the conservative update formula (104) results in

$$\rho_i^{n+1} = \underbrace{\rho_i^n - \frac{\Delta t}{2\Delta x}\left[v\rho_{i+1}^n - v\rho_{i-1}^n\right]}_{\text{FTCS scheme}} + \underbrace{\frac{1}{2}\left[\rho_{i+1}^n - 2\rho_i^n + \rho_{i-1}^n\right]}_{\text{artificial viscosity}} . \tag{124}$$

The last term looks like a discrete 2nd derivative and is called artificial viscosity. In general, the flux of any scheme can be written in the form

$$f = \underbrace{f_{\mathrm{FTCS}}}_{\text{FTCS flux}} + \underbrace{\left(f - f_{\mathrm{FTCS}}\right)}_{\text{flux due to artificial viscosity}} . \tag{125}$$

Sometimes, the Lax-Wendroff flux is used as reference,

$$f = \underbrace{f_{\mathrm{Lax-Wendroff}}}_{\text{Lax-Wendroff flux}} + \underbrace{\left(f - f_{\mathrm{Lax-Wendroff}}\right)}_{\text{flux due to artificial viscosity}} . \tag{126}$$

Modified equation for the FTFS scheme I

Keeping one more term in Eq. (110) we get instead of Eq. (112) the equation

$$\underbrace{\underbrace{\frac{\partial \rho}{\partial t} + v\frac{\partial \rho}{\partial x}}_{\text{PDE}} + \underbrace{\frac{1}{2}\frac{\partial^2 \rho}{\partial t^2}\Delta t + \frac{1}{2}v\frac{\partial^2 \rho}{\partial x^2}\Delta x}_{\text{2nd-order terms}}}_{\text{modified equation}} = \underbrace{\frac{\rho_i^{n+1} - \rho_i^n}{\Delta t} + v\frac{\rho_{i+1}^n - \rho_i^n}{\Delta x}}_{\text{numerical scheme}} + \underbrace{O\left(\Delta t^2, \Delta x^2\right)}_{\text{rest error}}. \quad (127)$$

Now, the error is $O\left(\Delta t^2, \Delta x^2\right)$ instead of $O(\Delta t, \Delta x)$.
I.e., the numerical scheme describes the modified equation

$$\frac{\partial \rho}{\partial t} + v\frac{\partial \rho}{\partial x} + \frac{1}{2}\frac{\partial^2 \rho}{\partial t^2}\Delta t + \frac{1}{2}v\frac{\partial^2 \rho}{\partial x^2}\Delta x = 0 \quad (128)$$

better than the original PDE.

Modified equation for the FTFS scheme II

To replace $\frac{\partial^2 \rho}{\partial t^2}$ in the modified equation (128) we write

$$\begin{aligned}
\frac{\partial^2 \rho}{\partial t^2}\Delta t + v\frac{\partial^2 \rho}{\partial x^2}\Delta x &= \frac{\partial}{\partial t}\left(-v\frac{\partial \rho}{\partial x}\right)\Delta t + v\frac{\partial^2 \rho}{\partial x^2}\Delta x + O\left(\Delta t^2, \Delta x^2\right) && (129)\\
&= -v\frac{\partial}{\partial x}\left(\frac{\partial \rho}{\partial t}\right)\Delta t + v\frac{\partial^2 \rho}{\partial x^2}\Delta x + O\left(\Delta t^2, \Delta x^2\right) && (130)\\
&= v^2\frac{\partial^2 \rho}{\partial x^2}\Delta t + v\frac{\partial^2 \rho}{\partial x^2}\Delta x + O\left(\Delta t^2, \Delta x^2\right) && (131)\\
&= v\Delta x\left(\frac{v\Delta t}{\Delta x} + 1\right)\frac{\partial^2 \rho}{\partial x^2} + O\left(\Delta t^2, \Delta x^2\right) && (132)
\end{aligned}$$

and get for the modified equation for the FTFS scheme

$$\frac{\partial \rho}{\partial t} + v\frac{\partial \rho}{\partial x} + \frac{1}{2}v\Delta x\left(\frac{v\Delta t}{\Delta x} + 1\right)\frac{\partial^2 \rho}{\partial x^2} = 0 \ . \qquad (133)$$

The coefficient of the additional diffusion term is positive: it describes anti-diffusion.

Modified equation for the FTBS scheme

A similar procedure gives the modified equation for the FTBS scheme

$$\frac{\partial \rho}{\partial t} + v \frac{\partial \rho}{\partial x} - \frac{1}{2} v \Delta x \left(1 - \frac{v \Delta t}{\Delta x}\right) \frac{\partial^2 \rho}{\partial x^2} = 0 \ . \tag{134}$$

The coefficient of the additional diffusion term is negative if the CFL condition is fulfilled: It describes diffusion, clearly seen on Page 68 (compare the example for the heat equation on Page 42).

Linear stability analysis of original PDE

Lets see what happens to waves in the linear advection equation (66). For the ansatz

$$\rho(x,t) = A(t)\, e^{-\jmath kx} \tag{135}$$

with $\jmath^2 = -1$ we get

$$\frac{\mathrm{d}A}{\mathrm{d}t} + v\,(-\jmath k)\,A = 0 \;\Rightarrow\; \frac{\mathrm{d}A}{\mathrm{d}t} = \jmath vk\,A \;\Rightarrow\; A = A_0\, e^{\jmath vkt}\ , \tag{136}$$

$$\rho = A_0\, e^{\jmath(\omega t - kx)} \tag{137}$$

with

$$\mathrm{abs}(A) = \mathrm{abs}(A_0) = \mathrm{const}\ , \tag{138}$$

$$\omega = vk\ . \tag{139}$$

Dispersion relation (139): no dispersion, all waves move with the same speed v.
Eq. (138): amplitude remains constant – without any diffusion.

Linear stability analysis: use

Linear stability analysis tells about *stability* – of *linear* schemes for *linear* equations.
Linear stability $\Rightarrow$ convergence for consistent schemes (Page 61).

Ansatz: for

$$\rho_i^n = e^{-\jmath ik\Delta x} \tag{140}$$

with $k \leq k_0 = \frac{\pi}{\Delta x}$ we search an amplification factor $A \in \mathbb{C}$ with

$$\rho_i^{n+1} = A\,\rho_i^n = A\,e^{-\jmath ik\Delta x} \quad . \tag{141}$$

Amount abs(A) of $A \Rightarrow$ damping (diffusion) or growth (instability) of waves.
Phase of $A \Rightarrow$ wave speed and dispersion.

Ideally $A = e^{\jmath\omega\Delta t}$ with $\omega = vk$.

Linear stability analysis of naive FTCS scheme

Applying ansatz (140) to the naive FTCS scheme Eq. (95) gives

$$A\, e^{-\jmath ik\Delta x} = e^{-\jmath ik\Delta x} - \frac{\Delta t}{\Delta x}\, v\, \frac{1}{2}\left(e^{-\jmath(i+1)k\Delta x} - e^{-\jmath(i-1)k\Delta x}\right) \quad . \tag{142}$$

Multiplying with $e^{\jmath ik\Delta x}$ and using the Courant number

$$\alpha := \frac{\Delta t}{\Delta x}\, v \tag{143}$$

we get

$$A = 1 - \alpha\, \frac{1}{2}\left(e^{-\jmath k\Delta x} - e^{\jmath k\Delta x}\right) = 1 + \jmath\alpha \sin k\Delta x \quad , \tag{144}$$

$$\mathrm{abs}(A) = \left(1 + \alpha^2 \sin^2 k\Delta x\right)^{\frac{1}{2}} \quad , \tag{145}$$

$$\mathrm{abs}(A) > 1 \quad \text{for } 0 < k\Delta x < \pi \;\; , \;\; \alpha > 0 \;\; . \tag{146}$$

All waves except the ones with smallest wavenumber grow exponentially in time:
The scheme is unconditionally unstable, independent of the time step.

Linear stability analysis of donor cell (FTBS) scheme

Applying ansatz (140) to the donor cell scheme Eq. (113) gives, using Eq. (143),

$$A = 1 - \alpha \left(1 - e^{\jmath k \Delta x}\right) = 1 - \alpha \left(1 - \cos k\Delta x\right) + \jmath \alpha \sin k \Delta x \ , \tag{147}$$

$$\text{abs}(A) = [1 - 2 \underbrace{\left(\alpha - \alpha^2\right)}_{\geq 0 \text{ for } \alpha \in [0,1]} \underbrace{\left(1 - \cos k\Delta x\right)}_{\geq 0}]^{\frac{1}{2}} \ , \tag{148}$$

$$\text{abs}(A) \leq 1 \quad \text{for} \ \ \alpha \in [0, 1] \ . \tag{149}$$

The donor cell scheme is stable if the CFL condition is fulfilled,

$$\frac{\Delta t}{\Delta x} v \in [0, 1] \ . \tag{150}$$

Note: $v \geq 0$ is required (for $v \leq 0$ use FTFS).
Note: $\text{abs}(A) < 1$ is possible: numerical viscosity
Note: $\text{phase}(A) \neq vk\Delta t$: dispersion

Linear stability analysis: remarks

Further issues:

- Severe restriction: linear PDE and linear scheme
- Growth of amplitude means instability – and stability otherwise
- Decline of amplitude indicates numerical viscosity
- Correct solution (constant amplitude) right at the border to instability
- Constant amplitude achievable by time-symmetric schemes (but: wiggles, dispersion)

Conclusions:

- Choice: either instability or wiggles or numerical viscosity
- No linear scheme is really satisfying.

Godunov's idea

Discretization paradigms (see Page 62):

- Finite differences: replace derivatives by differences
- Characteristics: follow characteristics back in time and interpolate at old time-level
- Reconstruct-Solve-Average (RSA): Godunov-type finite-volume scheme

RSA: three steps:

- Reconstruct $\rho(x)$ from ρ_i.
- Solve the exact problem for Δt: shift reconstructed function.
- Average $\rho(x)$ in each cell to get ρ_i.

Note: Exact solution (and reconstruction) can handle shocks $\Rightarrow$ numerical scheme can handle shocks.

Monotonicity

Transport and averaging are easy and well determined. The entire algorithm is determined by the reconstruction scheme.

- Consistency: “reasonable” interpolation
- Accuracy: high-order polynomials
- Conservativity: proper flux formulation
- Stability, positivity: monotonicity preservation

Definition: Total variation:

$$TV = \sum_i \text{abs}(\rho_{i+1} - \rho_i) \tag{151}$$

Definition: TVD property:
A scheme has the TVD property (is “Total Variation Diminishing”) if TV does not increase in time.
$\Rightarrow$ Non-linear stability criterion.

Godunov’s theorem:
Linear monotonicity-preserving methods are first-order accurate, at best.
$\Rightarrow$ Try a non-linear scheme.

Flux of PLM schemes

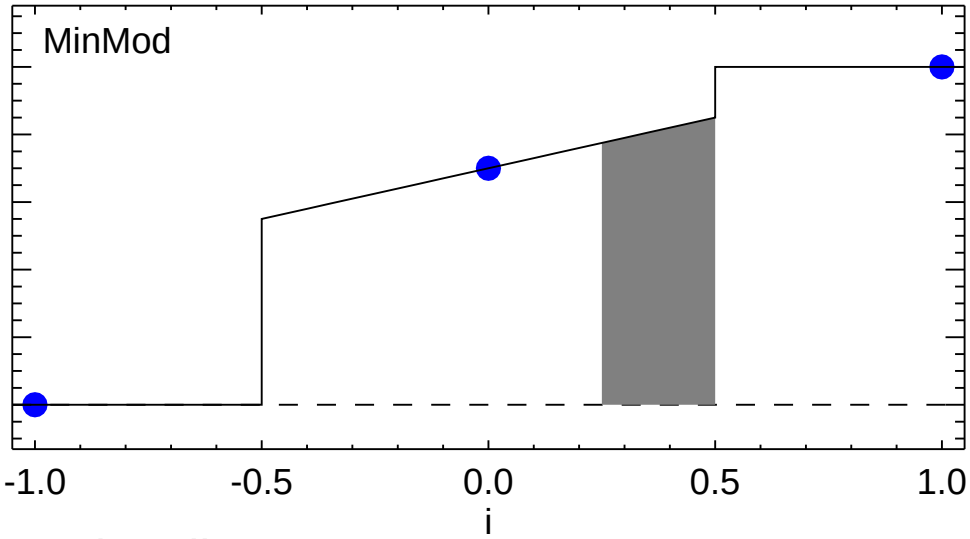

Reconstruction:

- Donor cell scheme: constant ρ within each cell
- Improvement: piecewise linear method (PLM): linear function in each cell

Once we know the cell average ρ_i and the slope $\delta\rho_i$, we get the flux over Δt from

$$f_{i\pm\frac{1}{2}} = v\left\{\rho_i + \frac{1}{2}\,\delta\rho_i\,\mathrm{sign}(v)\left[1 - \mathrm{abs}(v)\,\frac{\Delta t}{\Delta x}\right]\right\} \quad . \tag{152}$$

If the boundary value in the cell is used for the entire cell we get

$$f_{i\pm\frac{1}{2}} = v\left\{\rho_i + \frac{1}{2}\,\delta\rho_i\,\mathrm{sign}(v)\right\} \quad . \tag{153}$$

For $v > 0$ we get from each cell ρ_i the flux $f_{i+\frac{1}{2}}$.
For $v < 0$ we get from each cell ρ_i the flux $f_{i-\frac{1}{2}}$.

Examples: PLM: slopes with linear parameter dependence

Slopes of already encountered (linear) schemes:
Donor cell scheme (slope zero):

$$\delta\rho_i = 0 \tag{154}$$

Lax-Wendroff scheme:

$$\delta\rho_i = \rho_{i+1} - \rho_i \tag{155}$$

Beam-Warming scheme:

$$\delta\rho_i = \rho_i - \rho_{i-1} \tag{156}$$

Fromm scheme:

$$\delta\rho_i = \frac{1}{2}\left(\rho_{i+1} - \rho_{i-1}\right) \tag{157}$$

- The slope $\delta\rho_i$ can be written as function of $\rho_{i+1} - \rho_i$ and $\rho_i - \rho_{i-1}$.
- This function can be considered as a cleverly weighted average.
- For linear schemes, the weights are constants.
- For non-linear schemes, the weights are more complex functions.

PLM: slope-limiter

Alternatively, a slope can be written as

$$\delta\rho_i = \Phi\left(\frac{\rho_i - \rho_{i-1}}{\rho_{i+1} - \rho_i}\right) \delta\rho_i(\text{Lax-Wendroff}) \tag{158}$$

with the help of a (possibly non-linear) slope-limiter or flux-limiter

$$\Phi\left(\frac{\rho_i - \rho_{i-1}}{\rho_{i+1} - \rho_i}\right) = \frac{\delta\rho_i}{\delta\rho_i(\text{Lax-Wendroff})} \tag{159}$$

Note: The slope-limiter for the Lax-Wendroff scheme is 1.
Note: The slope-limiter for the donor cell scheme is 0.

PLM scheme with Minmod slope-limiter

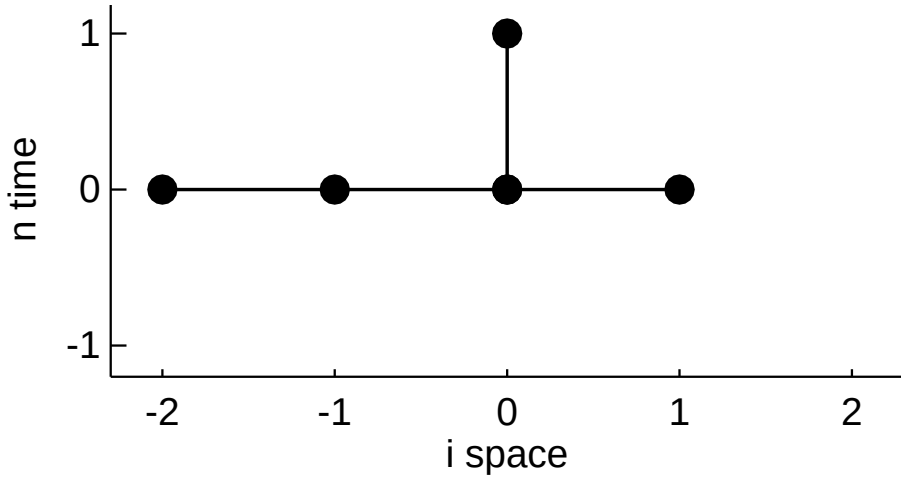

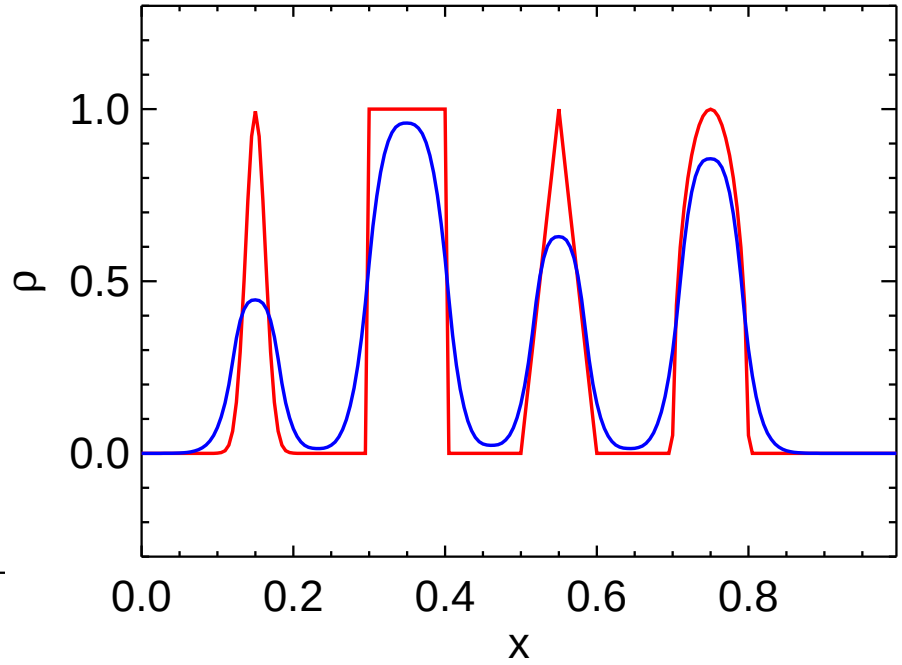

PLM scheme with Minmod slope (minimum allowed 2nd-order slope),

$$\begin{aligned} \delta\rho_i &= \min(\max(\rho_i - \rho_{i-1}, 0), \max(\rho_{i+1} - \rho_i, 0)) + \\ &\quad \max(\min(\rho_i - \rho_{i-1}, 0), \min(\rho_{i+1} - \rho_i, 0)) \quad . \end{aligned} \tag{160}$$

See Page 73.

PLM scheme with vanLeer slope-limiter

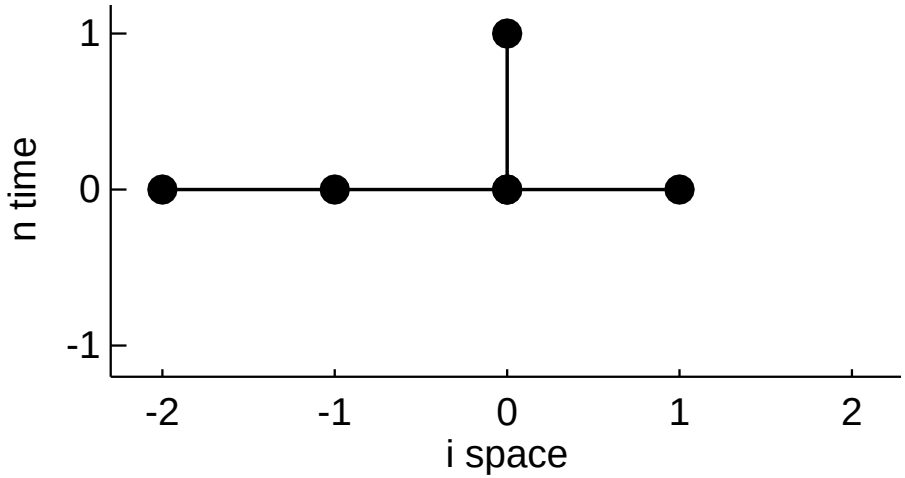

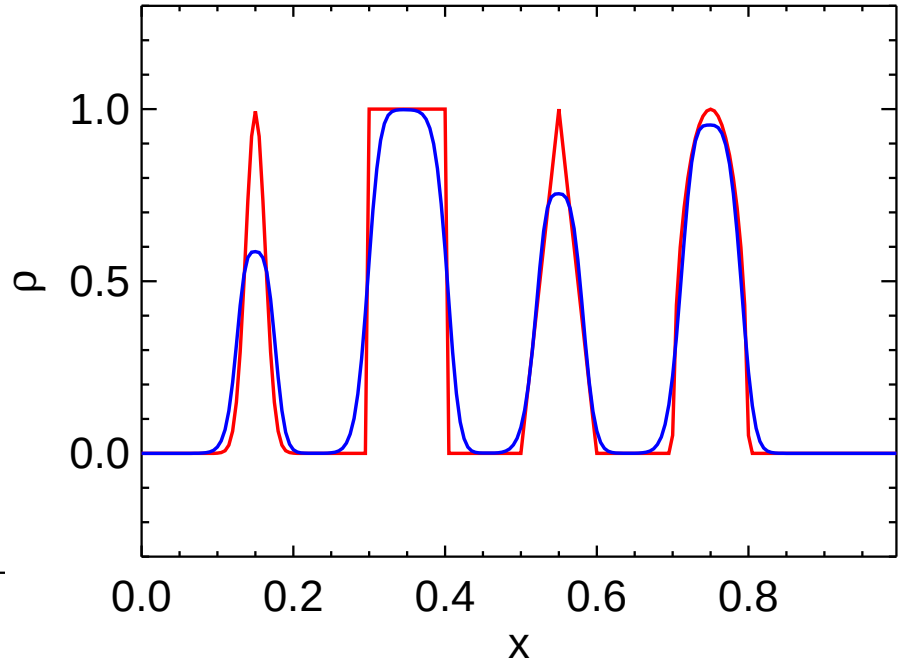

PLM scheme with vanLeer slope (harmonic mean of slopes),

$$\delta\rho_i = \begin{cases} \dfrac{1}{\frac{1}{2}\left(\frac{1}{\rho_i-\rho_{i-1}}+\frac{1}{\rho_{i+1}-\rho_i}\right)} & \text{if } (\rho_i-\rho_{i-1})(\rho_{i+1}-\rho_i) > 0 \\ 0 & \text{elsewhere} \end{cases} . \qquad (161)$$

PLM scheme with Superbee slope-limiter

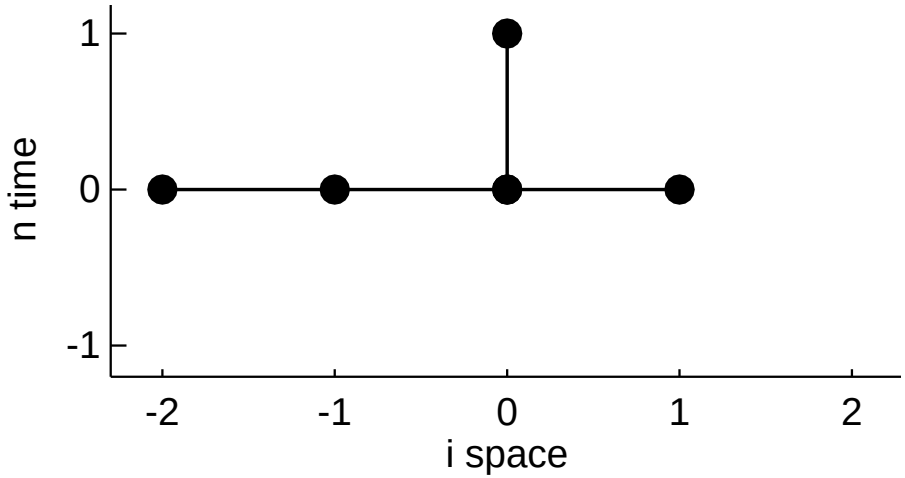

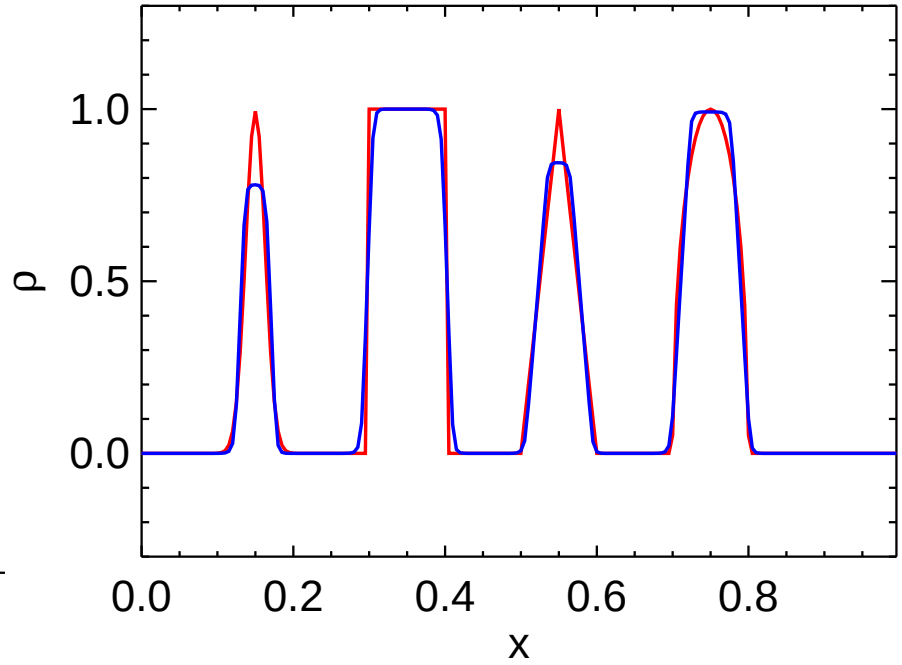

PLM scheme with Superbee slope (maximum allowed 2nd-order slope).

$$\delta\rho_i = [\mathrm{sign}(\rho_i - \rho_{i-1}) + \mathrm{sign}(\rho_{i+1} - \rho_i)] \qquad (162)$$
$$\min\left(\mathrm{abs}(\rho_i - \rho_{i-1})\,, \mathrm{abs}(\rho_{i+1} - \rho_i)\,, \frac{1}{2}\max(\mathrm{abs}(\rho_i - \rho_{i-1})\,, \mathrm{abs}(\rho_{i+1} - \rho_i))\right) \quad .$$

Scheme with Superbee limiter, only boundary value used

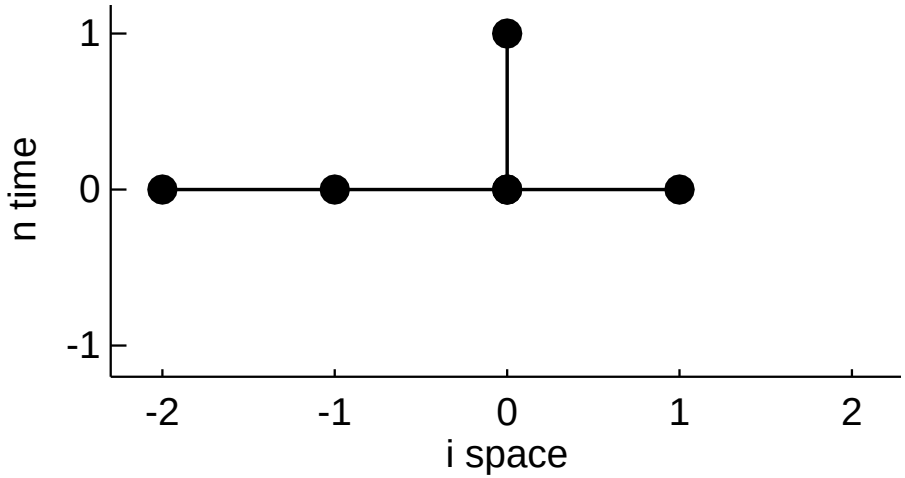

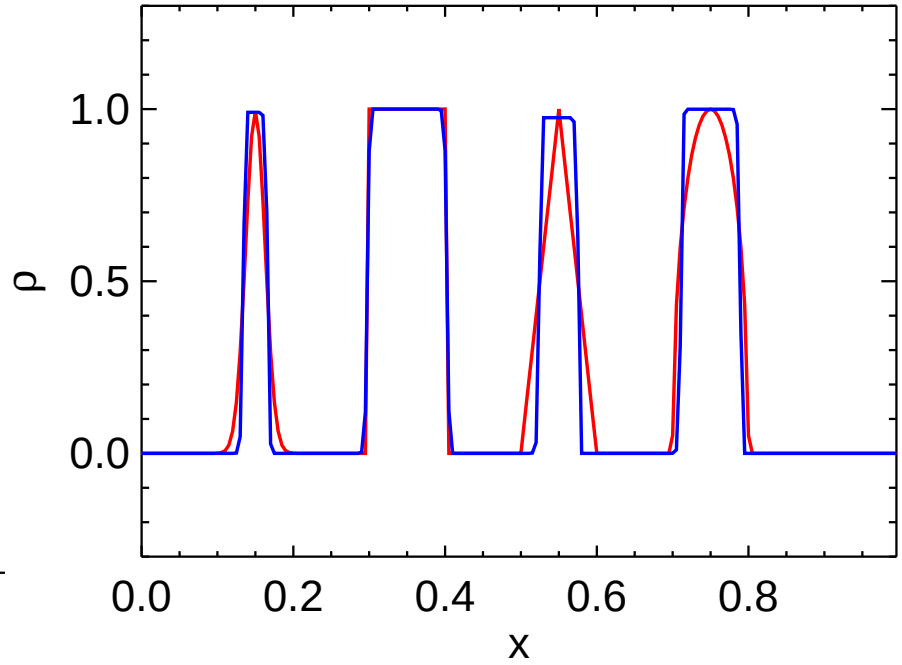

Scheme with Superbee slope where Eq. (153) was used for the flux instead of Eq. (152).
Note the extreme steepening of the slopes: everything is turned into a rectangle.

2nd-order PPM scheme

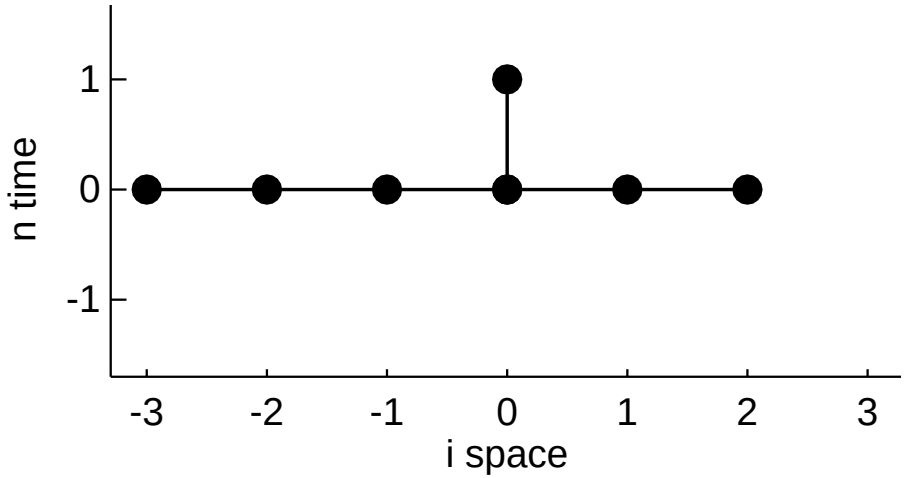

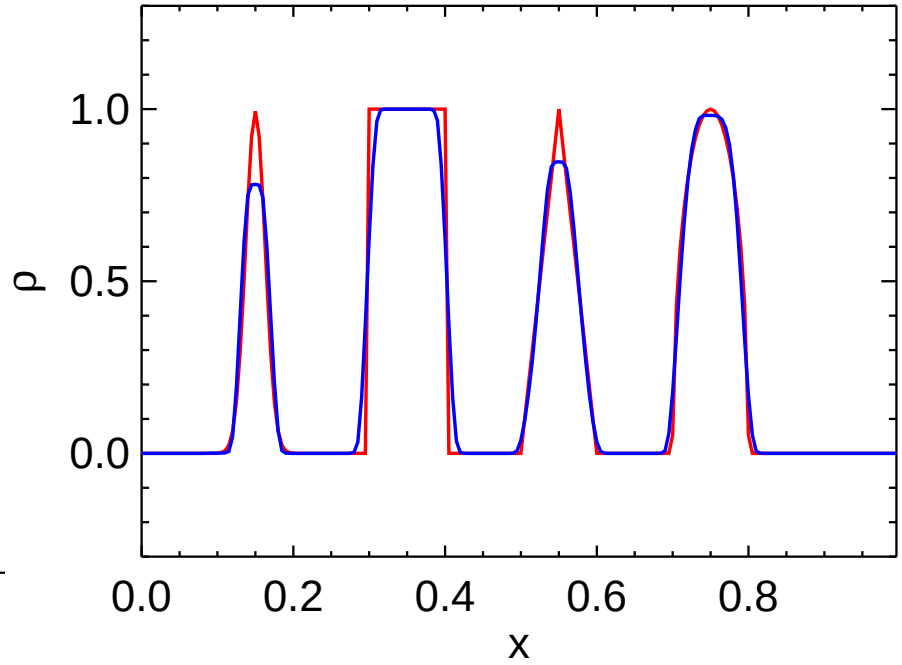

PPM scheme with piecewise parabolic reconstruction. See Colella & Woodward (1984). Idea:

- Represent the quantity in each cell by a parabola.
- Use continuous boundary values if possible.
- Modify the boundary values by introducing jumps if monotonicity requires it.

2nd-order WENO scheme

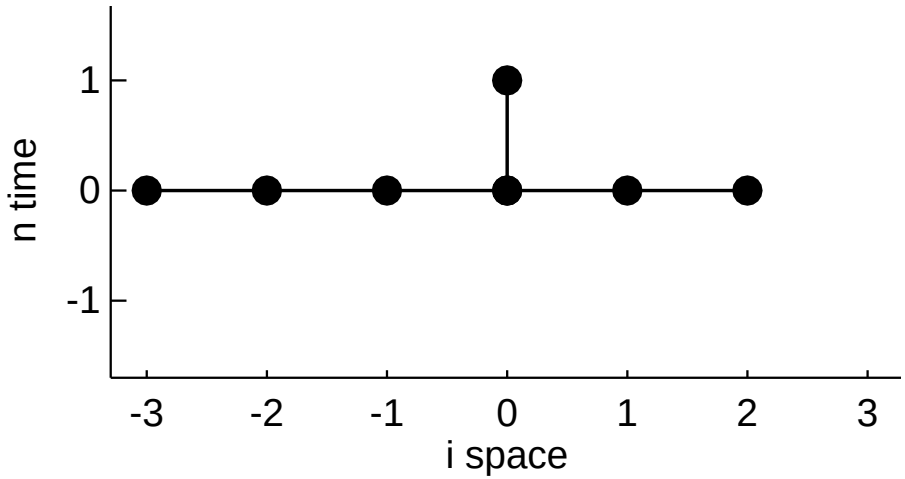

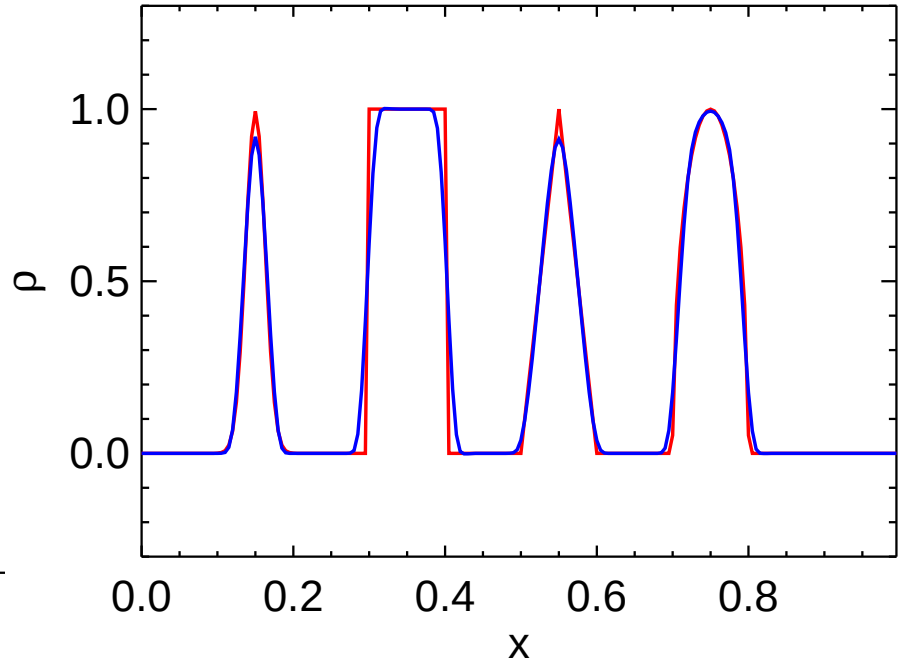

WENO scheme with weighted essentially non-oscillatory reconstruction (with 2nd-order polynomials, without any Runge-Kutta sub-steps). See, e.g., Jiang & Shu (1996). Idea:

- Compute all candidate polynomials that cover the cell (2 straight lines, 3 parabolas, or more higher-order polynomials).
- Give each candidate polynomial a weight according to some smoothness indicator.
- Add the candidates, giving the smoothest one the largest weight.

HBweno scheme: 2nd-order WENO “with Handbrake”

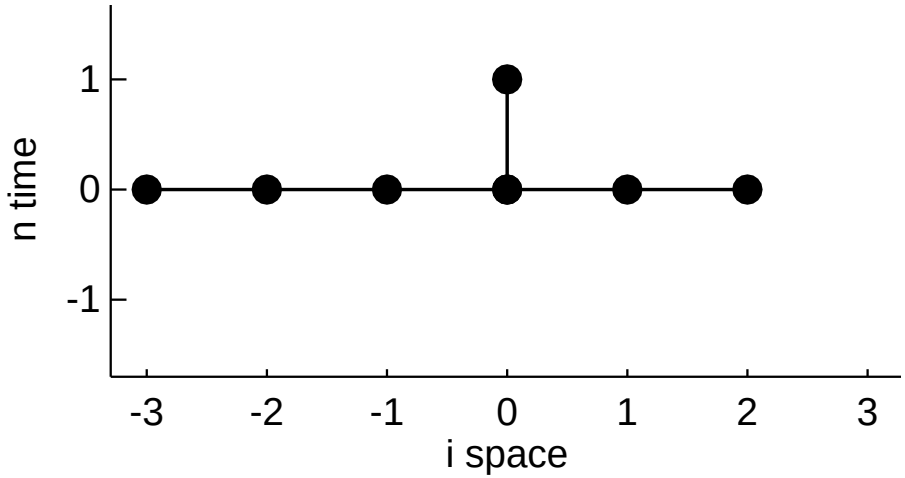

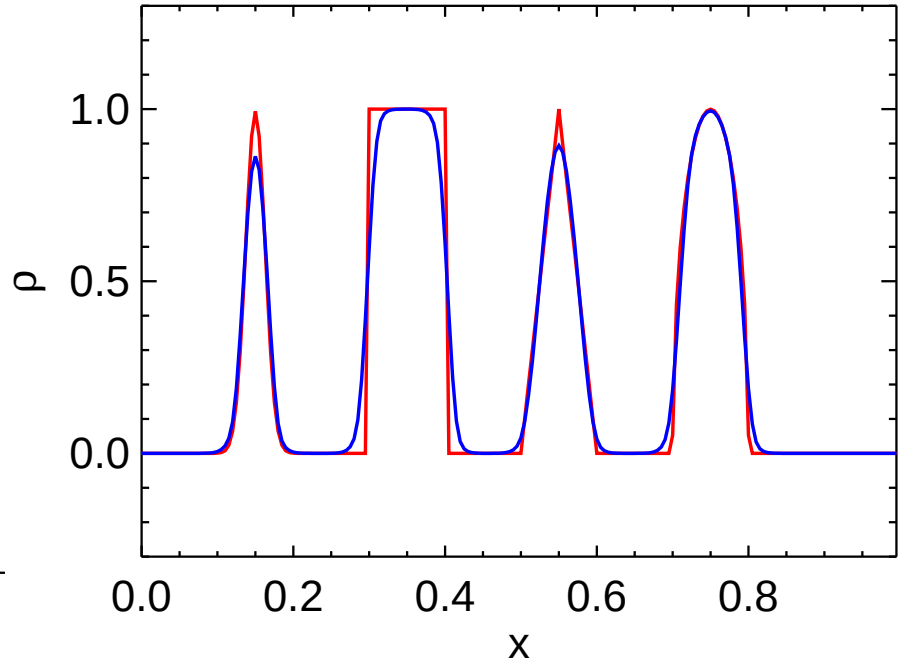

WENO scheme with adaptive additional flattening (with 2nd-order polynomials). See Freytag (CO5BOLD code). Idea:

- Use a WENO scheme as basis.
- Further flatten the reconstruction polynomials if the candidate polynomials all differ significantly.

2nd-order FRmono scheme: “Frankenstein’s method”

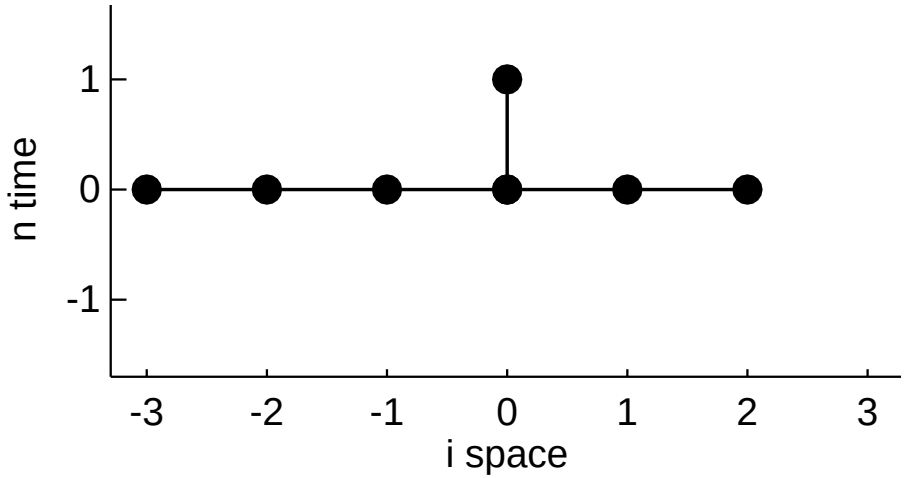

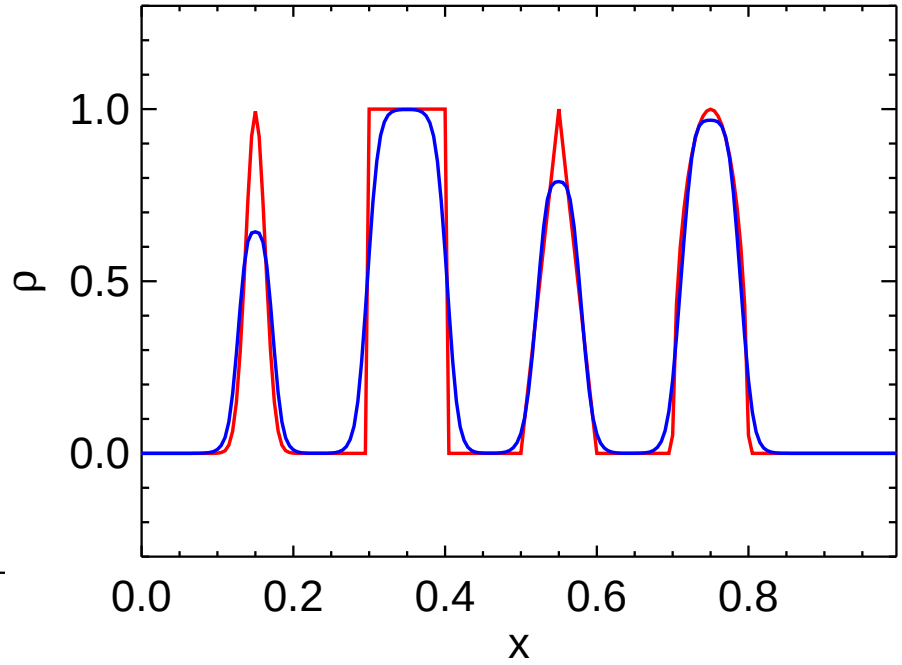

FRmono scheme based on WENO scheme (with 2nd-order polynomials) with PPM-style monotonization. See Freytag (2013). Idea:

- Combine the preference of smooth stencils (WENO) with monotonicity (PPM).

2nd-order FRweno scheme: “Frankenstein’s method”

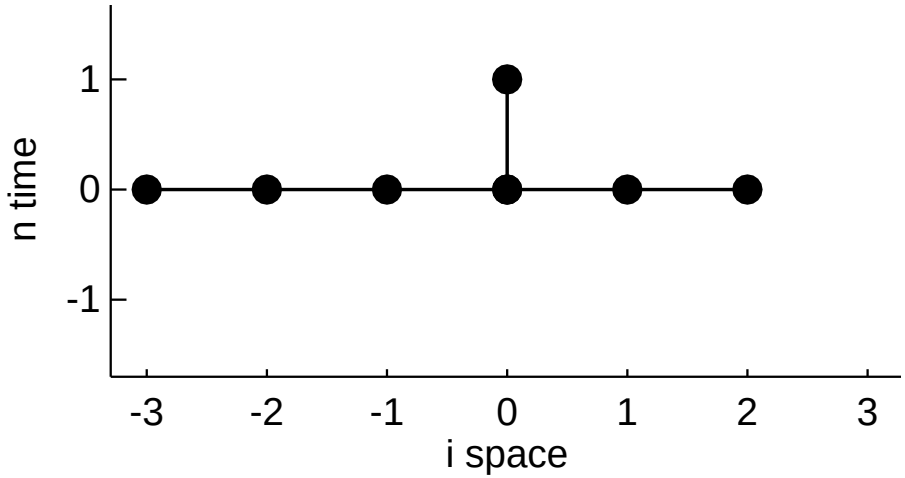

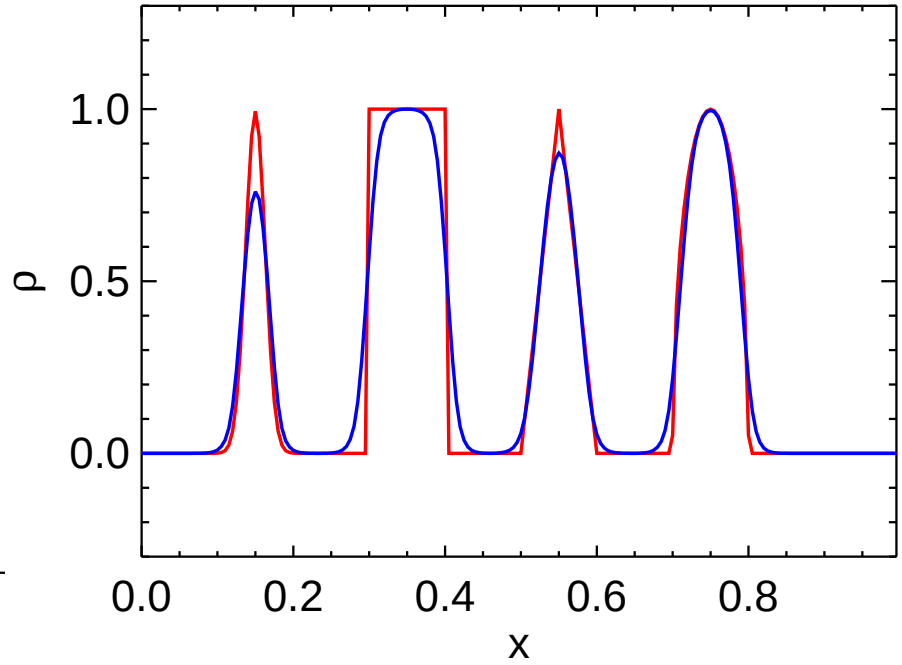

FRweno scheme based on WENO scheme (with 2nd-order polynomials) with not-strict PPM-style monotonization. See Freytag (2013). Idea:

- Relax the monotonicity constraints of the FRmono scheme a bit.

Improvements of reconstruction schemes

- There are lots of variants of 1st-order reconstruction schemes around.
- Interpolating between schemes according to appropriate criteria can be used.
- PPM: non-linear criteria can help to decide if, e.g., contact discontinuities should be sharpened further.
- WENO schemes can have a high spatial order.
- WENO schemes are often complemented by high-order Runge-Kutta steps.
- Alternative: use reconstruction/interpolation with standard high-order polynomials + stabilization with clever non-linear hyperviscosity.
- Subcell resolution can resolve the position of discontinuities within cells.
- Spectral methods use all grid points as stencil and achieve *very* high order – for low-Mach-number flows.

At some point only a finer grid helps:

- More grid points
- Non-equidistant grid
- Locally refined (hierarchical) grid
- Adaptively locally-refined grid (AMR: “Adaptive Mesh Refinement”)

Table of contents

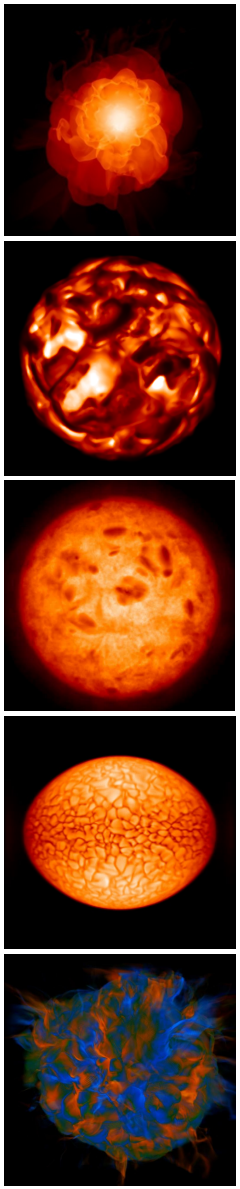

Viscous and inviscid Burgers Equation

Viscous Burgers Equation:

$$\frac{\partial v}{\partial t} + \frac{\partial \frac{1}{2} v^2}{\partial x} = \epsilon \frac{\partial^2 v}{\partial x^2} \tag{163}$$

Inviscid Burgers Equation in conservation form (with flux $\frac{1}{2} v^2$)

$$\frac{\partial v}{\partial t} + \frac{\partial \frac{1}{2} v^2}{\partial x} = 0 \ , \tag{164}$$

quasi-linear form

$$\frac{\partial v}{\partial t} + v \frac{\partial v}{\partial x} = 0 \ , \tag{165}$$

and integral form

$$\int_{x_0}^{x_1} \left[v(x, t_1) - v(x, t_0) \right] dx + \int_{t_0}^{t_1} \left[\frac{1}{2} v^2(x_1, t) - \frac{1}{2} v^2(x_0, t) \right] dt = 0 \tag{166}$$

- It resembles the linear advection equation (66).
- However, it is non-linear with $v(x, t)$ instead of $v = \text{const}$.
- It describes the transport of v with velocity v (momentum equation, sort of).

Solution along characteristic curves

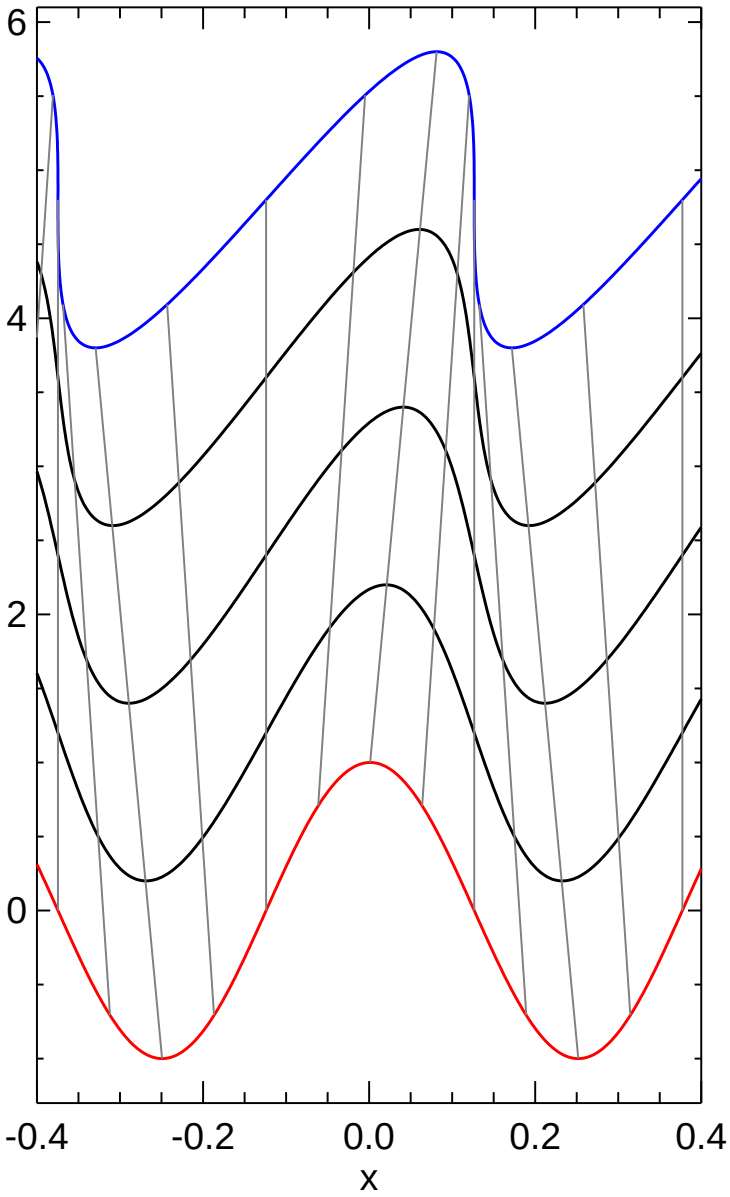

Characteristics already discussed for a quasi-linear PDE (Page 35).

Velocity v is not globally constant anymore. However, it is constant along each characteristic

$$c(t) = v(x_0)\ t + x_0 \quad . \tag{167}$$

$\Leftarrow$ That allows a graphical solution by using characteristics...
... at least, until the waves break, i.e., the characteristics "collide" in compression regions.

Smooth expansion regions are not problematic.

Compression waves and shocks

A compression wave with

$$\frac{\partial v}{\partial x} < 0 \tag{168}$$

steepens with time and characteristic curves can cross: multiple-valued solution?

- The viscous Burgers Equation (163) is a parabolic PDE and has a unique solution for all times $t > 0$.
- Vanishing viscosity: We look for a solution of the inviscid Burgers Equation that is a solution of the viscous Burgers Equation in the limit $\epsilon \to 0$.
- Instead of a multiple-valued solution we get a discontinuity where the characteristics end.
- Discontinuities (shocks) are unavoidable for $\frac{\partial v}{\partial x} < 0$.
- Characteristics run into a shock from both sides.
- Discontinuities should be allowed in the initial conditions.
- We need to find weak solutions (see Page 51).

Shock speed I

Jump across shock:

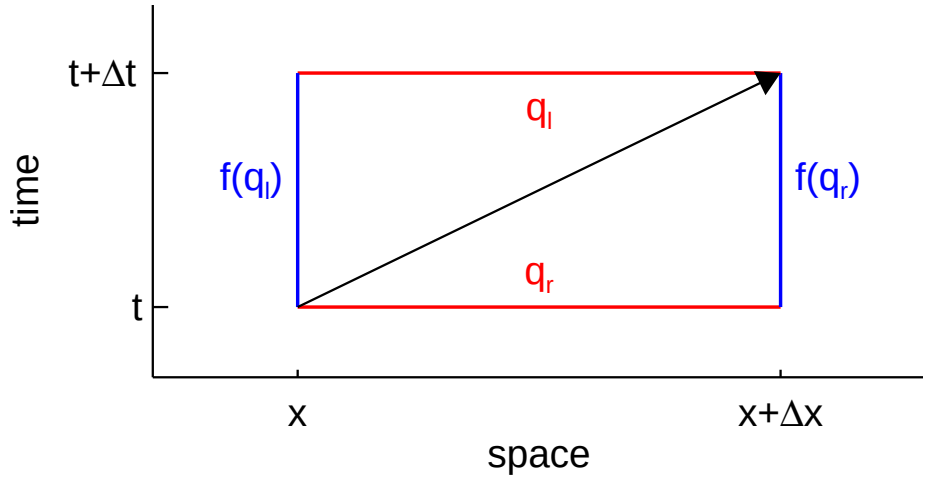

A shock with speed s travels over an infinitesimal time Δt an infinitesimal distance

$$\Delta x = s\,\Delta t \ . \tag{169}$$

Integration of the PDE

$$\frac{\partial q}{\partial t} + \frac{\partial f(q)}{\partial x} = 0 \ , \tag{170}$$

over Δt and Δx results in

$$\int_x^{x+\Delta x} [q(x, t+\Delta t) - q(x,t)]\, dx + \int_t^{t+\Delta t} [f(q(x+\Delta x, t)) - f(q(x,t))]\, dt = 0 \tag{171}$$

Shock speed II

During this time Δt the states q_l, q_r and fluxes $f(q_\mathrm{l})$, $f(q_\mathrm{r})$ on the left and right of the shock do not change (much) and we get

$$\Delta x\, q_\mathrm{l} - \Delta x\, q_\mathrm{r} + \Delta t\, f(q_\mathrm{r}) - \Delta t\, f(q_\mathrm{l}) = O\left(\Delta t^2\right) \quad . \tag{172}$$

For $\Delta x = s\,\Delta t$ and $\Delta t \to 0$ we get the Rankine-Hugoniot jump condition

$$s\,(q_\mathrm{r} - q_\mathrm{l}) = f(q_\mathrm{r}) - f(q_\mathrm{l}) \tag{173}$$

which gives for the shock speed in general

$$s = \frac{f(q_\mathrm{r}) - f(q_\mathrm{l})}{q_\mathrm{r} - q_\mathrm{l}} \tag{174}$$

and for Burgers' equation

$$s = \frac{\frac{1}{2}v_\mathrm{r}^2 - \frac{1}{2}v_\mathrm{l}^2}{v_\mathrm{r} - v_\mathrm{l}} = \frac{1}{2}\left(v_\mathrm{r} + v_\mathrm{l}\right) \quad . \tag{175}$$

Expansion waves

Smooth regions with

$$\frac{\partial v}{\partial x} > 0 \tag{176}$$

produce a rarefaction wave or expansion wave.

- What about steps with $v_{\text{left}} < v_{\text{right}}$?
- Expansion shock with characteristics running out of it is weak solution.
- But: any small but non-zero viscosity would smooth the step and cause a rarefaction wave (or rarefaction fan).
- Only solutions that fulfill an entropy condition are allowed.

Lax entropy condition: For a convex scalar conservation law, a discontinuity propagating with speed s satisfies the Lax entropy condition if

$$v_{\text{left}} > s > v_{\text{right}} \ . \tag{177}$$

- Therefore: expansion shocks are not allowed.
- An entropy condition destroys time-reversibility.

Similarity solutions I

The quasi-linear PDE

$$\frac{\partial q}{\partial t} + \frac{\mathrm{d}f}{\mathrm{d}q}\frac{\partial q}{\partial x} = 0 \tag{178}$$

for the Riemann problem

$$q(x,0) = \begin{cases} q_\mathrm{l} & \text{if } x < 0 \\ q_\mathrm{r} & \text{if } x > 0 \end{cases} \tag{179}$$

has similarity solutions of the form

$$q(x,t) = \tilde{q}\left(\frac{x}{t}\right) \quad . \tag{180}$$

Similarity solutions II

Inserting this ansatz (180) into Eq. (178) gives for $t > 0$

$$-\frac{x}{t^2}\,\tilde{q}' + \frac{\mathrm{d}f}{\mathrm{d}q}\,\frac{1}{t}\,\tilde{q}' = 0 \tag{181}$$

with the solutions

$$\tilde{q}'\left(\frac{x}{t}\right) = 0 \;\Rightarrow\; \tilde{q}\left(\frac{x}{t}\right) = \text{const} \tag{182}$$

or

$$\tilde{q}'\left(\frac{x}{t}\right) \neq 0 \;\Rightarrow\; \frac{\mathrm{d}f}{\mathrm{d}q}\left(\tilde{q}\left(\frac{x}{t}\right)\right) = \frac{x}{t} \tag{183}$$

which for Burgers' equation gives

$$v = \frac{x}{t}\ . \tag{184}$$

This solution (184) describes the state within a rarefaction fan whereas Eq. (182) applies everywhere else (outside of rarefaction waves and shocks).

Classification of Riemann problems

Different Riemann problems for Burgers' equation:

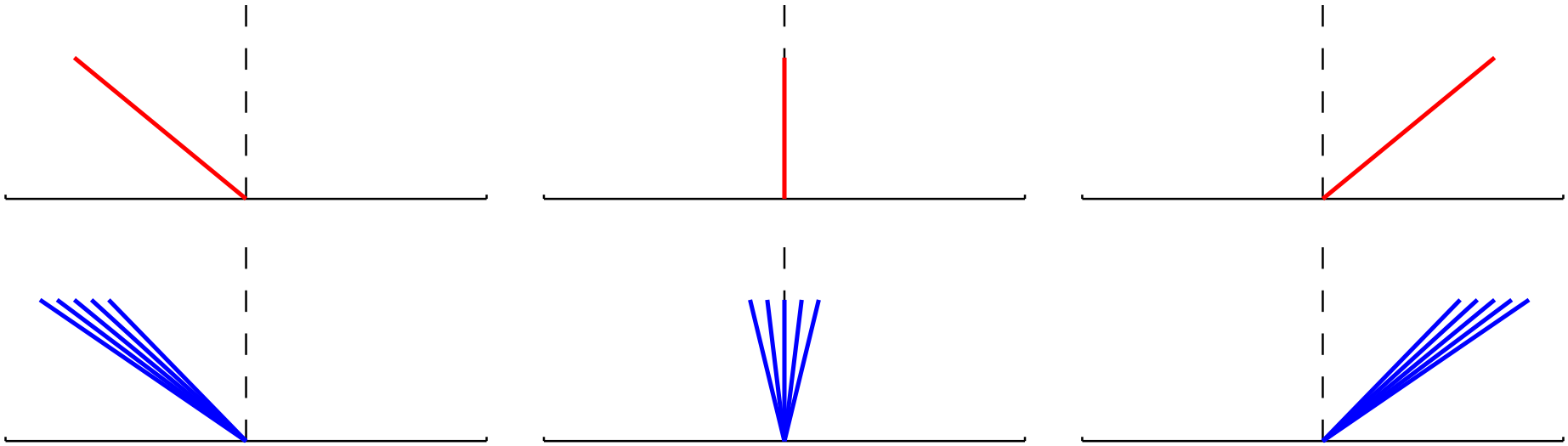

- A Riemann problem consists of a step at $x = 0$ in q with constant states q_l and q_r on the left and right side, see Eq. (179).
- The figure shows different types of solutions with a shock (top) and a rarefaction wave (bottom).
- Except for the transonic rarefaction wave the flux across the boundary (dashed line) is either $f(q_\mathrm{l})$ or $f(q_\mathrm{r})$.

Velocity at cell boundary

- With the velocity possibly varying from cell to cell one needs to define an appropriate value at the cell boundary.

A logical choice is the shock speed from Eq. (174) which results in

$$v_{i+\frac{1}{2}} = \begin{cases} \frac{f\left(q_{i+1}^n\right) - f\left(q_i^n\right)}{q_{i+1}^n - q_i^n} & \text{if } q_{i+1}^n \neq q_i^n \\ \frac{\mathrm{d}f}{\mathrm{d}q}\left(q_i^n\right) & \text{if } q_{i+1}^n = q_i^n \end{cases} \tag{185}$$

or for Burgers' equation from Eq. (175) simply

$$v_{i+\frac{1}{2}} = \frac{1}{2}\left(v_i^n + v_{i+1}^n\right) \quad . \tag{186}$$

Flux-splitting

Both signs of the velocity are now possible.
Flux-splitting allows the use of schemes written for one sign of the velocity, still guaranteeing proper upwinding,

$$f(q) = f^+(q) + f^-(q) \tag{187}$$

with

$$\frac{\mathrm{d}f^+}{\mathrm{d}q} \geq 0 \ , \quad \frac{\mathrm{d}f^-}{\mathrm{d}q} \leq 0 \ . \tag{188}$$

E.g.: extension of FTBS scheme to Courant-Isaacson-Rees scheme (CIR, now stable for both signs of v):

$$f^n_{i+\frac{1}{2}} = \begin{cases} f(\rho^n_i) & \text{if } v_{i+\frac{1}{2}} > 0 \\ f(\rho^n_{i+1}) & \text{if } v_{i+\frac{1}{2}} \leq 0 \end{cases} \tag{189}$$

CIR for Burgers' equation:

$$f^n_{i+\frac{1}{2}} = \begin{cases} \frac{1}{2}\left(v^n_i\right)^2 & \text{if } v_{i+\frac{1}{2}} > 0 \\ \frac{1}{2}\left(v^n_{i+1}\right)^2 & \text{if } v_{i+\frac{1}{2}} \leq 0 \end{cases} \tag{190}$$

Example: small-amplitude wave

Small-amplitude wave: linear behavior (left), shock wave (right):

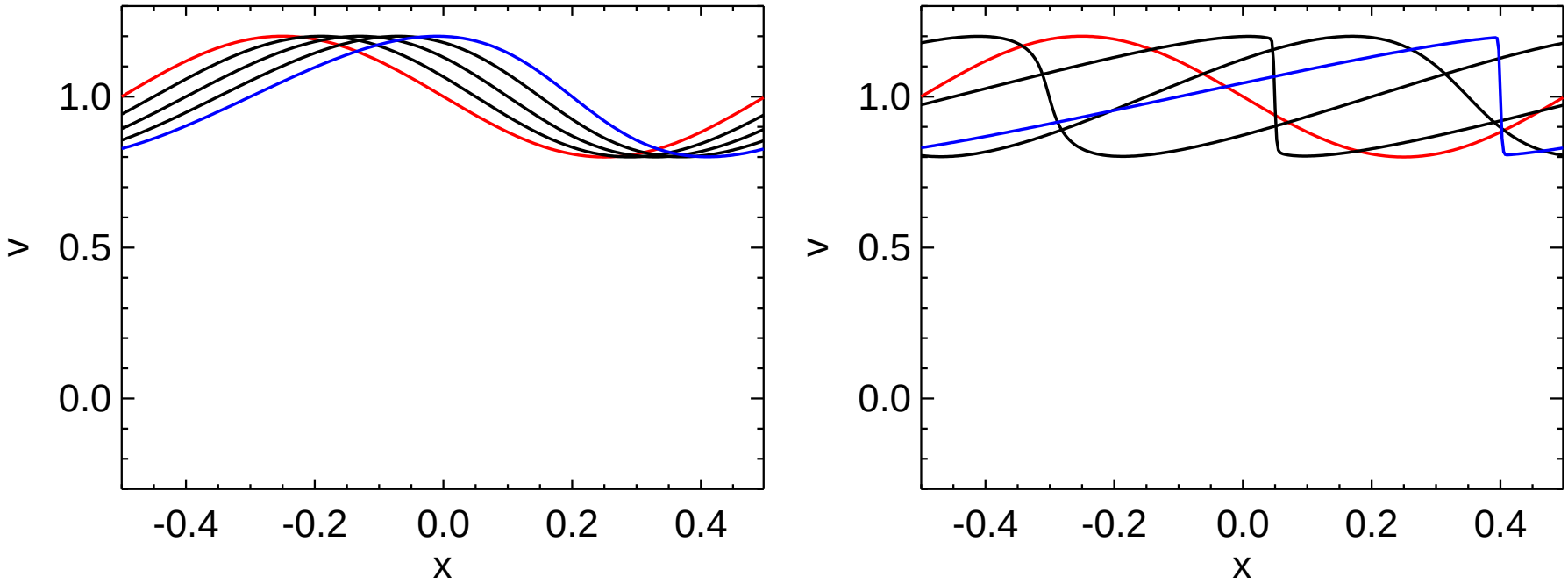

Even a small-amplitude wave that initially behaves like a linear wave (left panel) turns later into a shock wave (right panel).

Example: Gaussian and conservativity

Non-conservative scheme (left), conservative scheme (right):

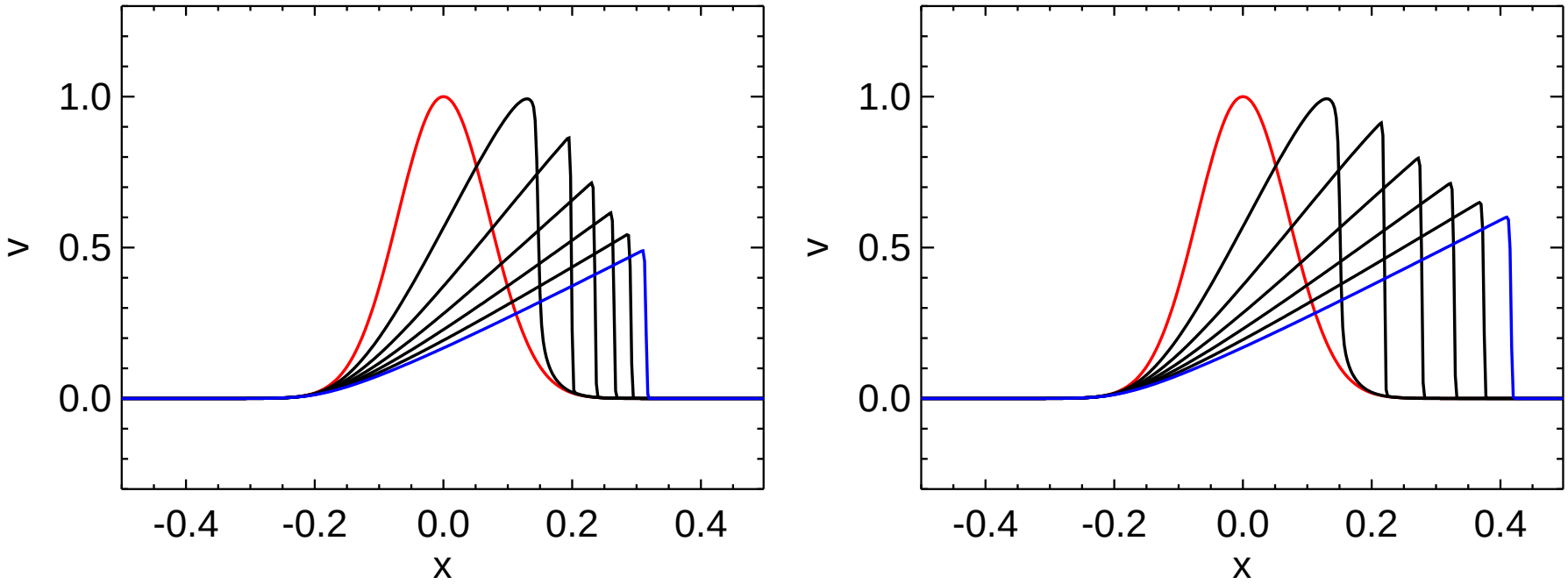

Burgers' equation allows also the non-conservative discretization using upwind values

$$v_i^{n+1} = v_i^n - \frac{\Delta t}{\Delta x} v_i^n \left(v_i^n - v_{i-1}^n \right) \tag{191}$$

which results in the time-evolution in the left panel.
The right panel shows the result with the conservative scheme (190).

Lax-Wendroff theorem

Remarks:

- The initial evolution of the schemes (Page 112) is rather similar.
- However, with the non-conservative scheme, the shock moves with the wrong speed and the non-conservation of the area under v is obvious.
- Remember: the derivation of the Rankine-Hugoniot jump condition on Page 104 used the conservation of q across the shock to derive the shock speed.

Lax-Wendroff theorem:
If the numerical solution of a conservative scheme converges, it converges towards a weak solution.

- Note: an alternative to shock capturing where the scheme itself is able to handle discontinuities is shock tracking where the positions of shocks are explicitly followed to allow a different numerical treatment in smooth regions and near discontinuities.

Example: step-function and conservativity

Non-conservative scheme (left), conservative scheme (right):

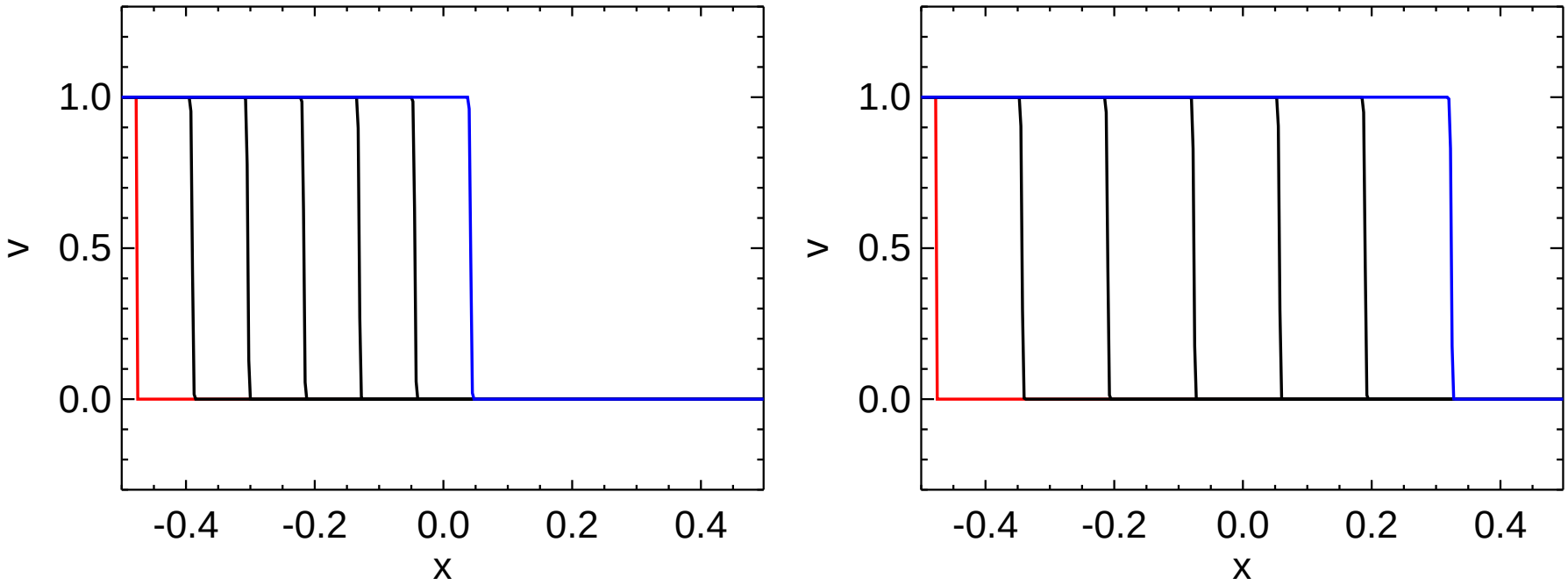

The figure displays the outcome for a test with an initial step-function (a Riemann problem) for the non-conservative scheme (191) and the conservative scheme (190).

- Clearly, the non-conservative scheme fails again to get the shock speed right.
- The wrong solution is not indicated by any helpful wiggles or numerical artifacts.

Example: expansion shock and rarefaction fan

Expansion shock (left) and – correct – rarefaction fan (right):

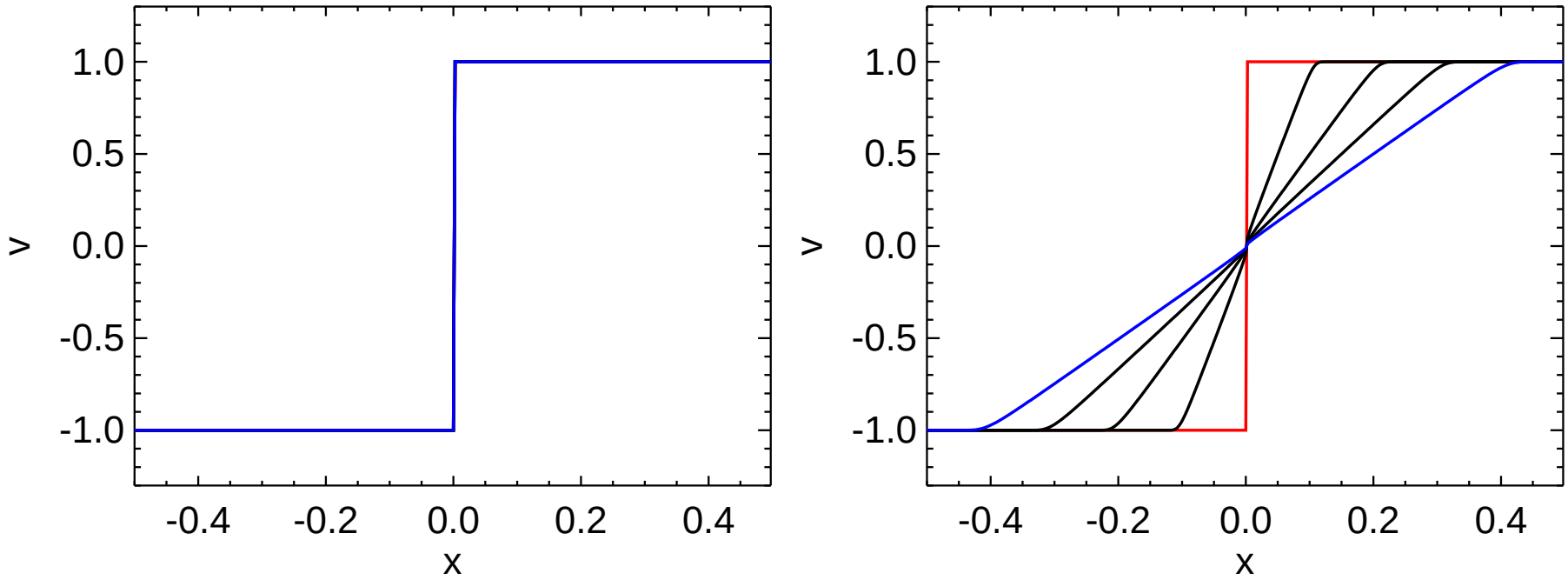

The Riemann problem in the figure should result in a rarefaction fan (right panel).

- Instead, the CIR scheme from Eq. (190) produces a stationary expansion shock that violates the entropy condition (177).
- The solution by the CIR scheme is stationary because its flux ($f = \frac{1}{2}$) is the same everywhere, even if the velocity ($v = \pm 1$) changes sign.

Entropy production by artificial viscosity

A possibly way to prevent the violation of the entropy condition (177) is to produce entropy with an extra (artificial) diffusion term added to the CIR flux (190) according to

$$f^n_{i+\frac{1}{2}} = f^n_{i+\frac{1}{2}}(\text{CIR}) - \epsilon \left(v^n_{i+1} - v^n_i\right) \quad . \tag{192}$$

However, now the parameter ϵ has to be tuned to be large enough to give the correct weak solution while not smearing it more than necessary.

The viscosity parameter ϵ could be replaced e.g. by the function

$$\epsilon = \epsilon' \left(v^n_{i+1} - v^n_i\right)^2 \tag{193}$$

to confine the extra viscosity to regions where the gradient is really large.

One way of stabilizing a numerical scheme is to modify and/or enhance the natural viscosity in the Navier-Stokes Equations (see Eq. 24).

Entropy fix

Observations:

- For most Riemann problems (Page 108), the CIR scheme (190) actually produces initially the exact result.
- Only for a transonic rarefaction wave (as in the last example on Page 115) it differs.
- Godunov's idea: Solve a Riemann problem ($\Rightarrow$ Riemann solver) at every cell boundary and derive the corresponding flux over the boundary.
- For Burgers' equation, the flux through the stagnation point ($v = 0$) in a transonic rarefaction wave is $f = \frac{1}{2}v^2 = 0$.

$\Rightarrow$ Extend the CIR scheme to get a Godunov-type scheme by defining

$$f^n_{i+\frac{1}{2}} = \begin{cases} \frac{1}{2}\left(v^n_i\right)^2 & \text{if } v_{i+\frac{1}{2}} > 0 \text{ and } v_i \geq 0 \\ \frac{1}{2}\left(v^n_{i+1}\right)^2 & \text{if } v_{i+\frac{1}{2}} \leq 0 \text{ and } v_{i+1} \leq 0 \\ 0 & \text{if } v_i < 0 < v_{i+1} \end{cases} . \tag{194}$$

The additional branch is an entropy fix to the CIR scheme.

Concepts from the linear world

Remarks:

- Consistency: the same
- Conservativity: the same (now even more important)
- Stability
  - Linear stability: not directly applicable (linearization possible?)
  - Total variation diminishing (TVD): applicable
  - Alternative: base scheme on concepts that work in the linear case and perform lots of tests for the non-linear PDE
- Accuracy: slope-limiter schemes need adaption

Transformation of shock speed formula

We can rewrite the velocity at a cell boundary based on the shock speed (Eq. (174) and Eq. (185), entropy fix ignored),

$$v_{i+\frac{1}{2}} = \frac{f(q^n_{i+1}) - f(q^n_i)}{q^n_{i+1} - q^n_i} \tag{195}$$

$$= \frac{f(q^n_{i+1}) - \frac{f(q^n_i)+f(q^n_{i+1})}{2}}{q^n_{i+1} - \frac{q^n_i+q^n_{i+1}}{2}} = \frac{f(q^n_i) - \frac{f(q^n_i)+f(q^n_{i+1})}{2}}{q^n_i - \frac{q^n_i+q^n_{i+1}}{2}} \tag{196}$$

$$= \frac{f\left(q^n_{i_{\mathrm{up}\,i+\frac{1}{2}}}\right) - \frac{f(q^n_i)+f(q^n_{i+1})}{2}}{q^n_{i_{\mathrm{up}\,i+\frac{1}{2}}} - \frac{q^n_i+q^n_{i+1}}{2}}, \tag{197}$$

with the upwind index

$$i_{\mathrm{up}\,i+\frac{1}{2}} := \begin{cases} i & \text{if } v_{i+\frac{1}{2}} > 0 \\ i+1 & \text{if } v_{i+\frac{1}{2}} \leq 0 \end{cases}. \tag{198}$$

Second-order extension of flux formula

Resolving Eq. (197) for the upwind flux that we need as flux (189) for the CIR scheme gives

$$f^n_{i+\frac{1}{2}} = f\left(q^n_{i_{\mathrm{up}}\,i+\frac{1}{2}}\right) = \underbrace{\frac{f(q^n_i)+f(q^n_{i+1})}{2}}_{\text{flux average}} + \underbrace{v_{i+\frac{1}{2}}\left(q^n_{i_{\mathrm{up}}\,i+\frac{1}{2}} - \frac{q^n_i+q^n_{i+1}}{2}\right)}_{\text{linear(ized) advection}} . \tag{199}$$

Remember: This is exactly the simple upwind (CIR) flux.
However, the second term looks like linear advection and suggests to apply a higher-order (eg. slope-limiter) scheme to the localized advection problem for

$$q'_j = q_j - \frac{q_i+q_{i+1}}{2} \quad \text{for } j = i-1,\ i,\ i+1,\ i+2\ . \tag{200}$$

Table of contents

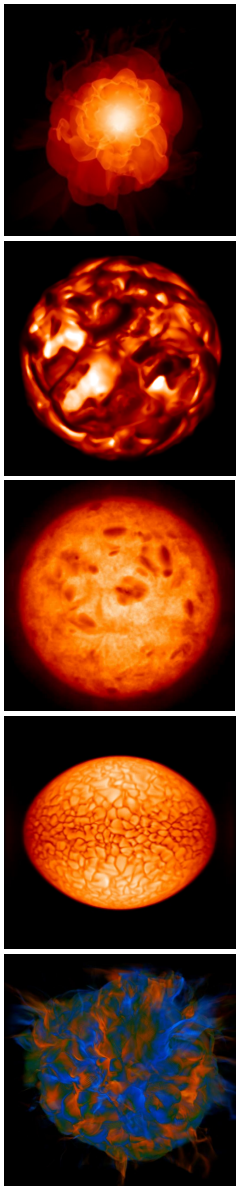

A coupled non-linear system

- The 1D hydrodynamics equations (43) are a non-linear system of 3 coupled equations.
- There is a little bit from the linear advection equation:
  - Derivation of the characteristic form (51).
  - Linear advection as special case (see Page 33).
- There is a little bit from Burgers' equation:
  - Shocks can arise from smooth initial conditions.
  - Discontinuities in the initial conditions can produce rarefaction waves.
  - We need to look for weak solutions (that satisfy an entropy condition).
- Characteristics are not necessarily straight lines.
- The domain of dependence is not only a single point but an interval. However, it is bounded. Therefore explicit methods (with limited full numerical domain of dependence) are often adequate.

Positivity of density

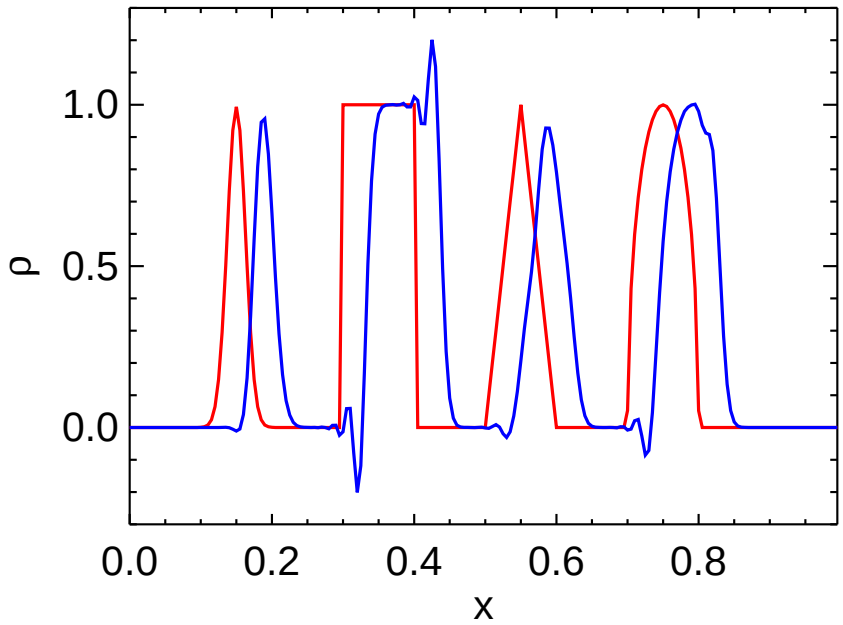

To compute the velocity from momentum and density via

$$v = \frac{\rho v}{\rho} \tag{201}$$

requires

$$\rho > 0 \ . \tag{202}$$

An overshoot of the density to non-positive values is now (usually) disastrous.

Positivity of pressure

The pressure $P(e_{\mathrm{i}}, \rho)$ depends on the conserved quantities via

$$P(\rho, \ \rho v, \ \rho e_{\mathrm{ik}}) = P\left(\frac{\rho e_{\mathrm{ik}}}{\rho} - \frac{(\rho v)^2}{2\rho^2}, \ \rho\right) \ . \tag{203}$$

An overshoot in velocity may lead to negative pressure (or an attempt to access values beyond the limits of a tabulated equation of state).

- This restriction is so severe that in some cases the conservation of total energy might be given up in favor of a (non-conservative) formulation where the positivity of the internal energy is guaranteed.
- The total variation of e.g. density, pressure,... of the true solution can increase $\rightarrow$ *TV* stability arguments no longer hold (in the same way as in the linear case).

Where is upwind?

Bringing the Euler Equations into characteristic form resulted in waves with different velocities (Page 29),

$$v - c, \quad v, \quad v + c \ . \tag{204}$$

Which one should be used to determine the upwind direction?

The Riemann problem

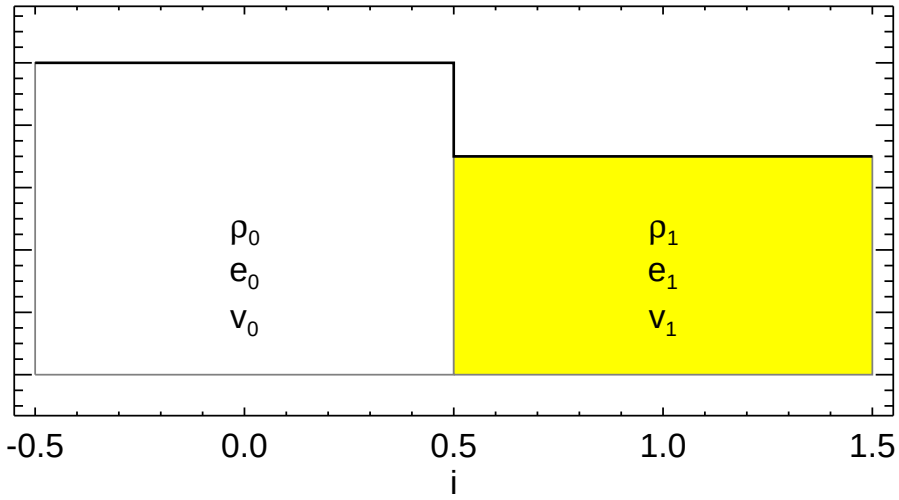

The state on each side is described by 3 values giving rise to 3 wave families.

Each wave family can cause a discontinuity:

- Sound waves can cause shocks or rarefaction waves.
- The material flow (entropy wave) can have a contact discontinuity.

The solution of Riemann problem (for a convex – simple – EOS) can comprise:

- 0 or 1 contact discontinuities,
- 0, 1, or 2 shocks,
- 0, 1, or 2 rarefaction waves; not more than 2 (shocks + rarefaction waves).

Rankine-Hugoniot conditions

The Rankine-Hugoniot jump conditions (see Page 104) for the 1D Euler Equations (43), describing a shock with speed s become

$$s\left(\rho_{\mathrm{r}}-\rho_{\mathrm{l}}\right) = \rho v_{\mathrm{r}}-\rho v_{\mathrm{l}} \tag{205}$$

$$s\left(\rho v_{\mathrm{r}}-\rho v_{\mathrm{l}}\right) = \left(\rho vv+P\right)_{\mathrm{r}}-\left(\rho vv+P\right)_{\mathrm{l}} \tag{206}$$

$$s\left(\rho e_{\mathrm{ik}_{\mathrm{r}}}-\rho e_{\mathrm{ik}_{\mathrm{l}}}\right) = \left(\left[\rho e_{\mathrm{ik}}+P\right]\ v\right)_{\mathrm{r}}-\left(\left[\rho e_{\mathrm{ik}}+P\right]\ v\right)_{\mathrm{l}} \tag{207}$$

They can only be fulfilled for certain combinations of q_{l} and q_{r}.
An arbitrary Riemann problem typically causes more than one jump.

Example: Sod shock tube

Sod shock tube: analytical (lines) and numerical (circles) solution: Velocity, mass flux, pressure, density, internal energy, entropy:

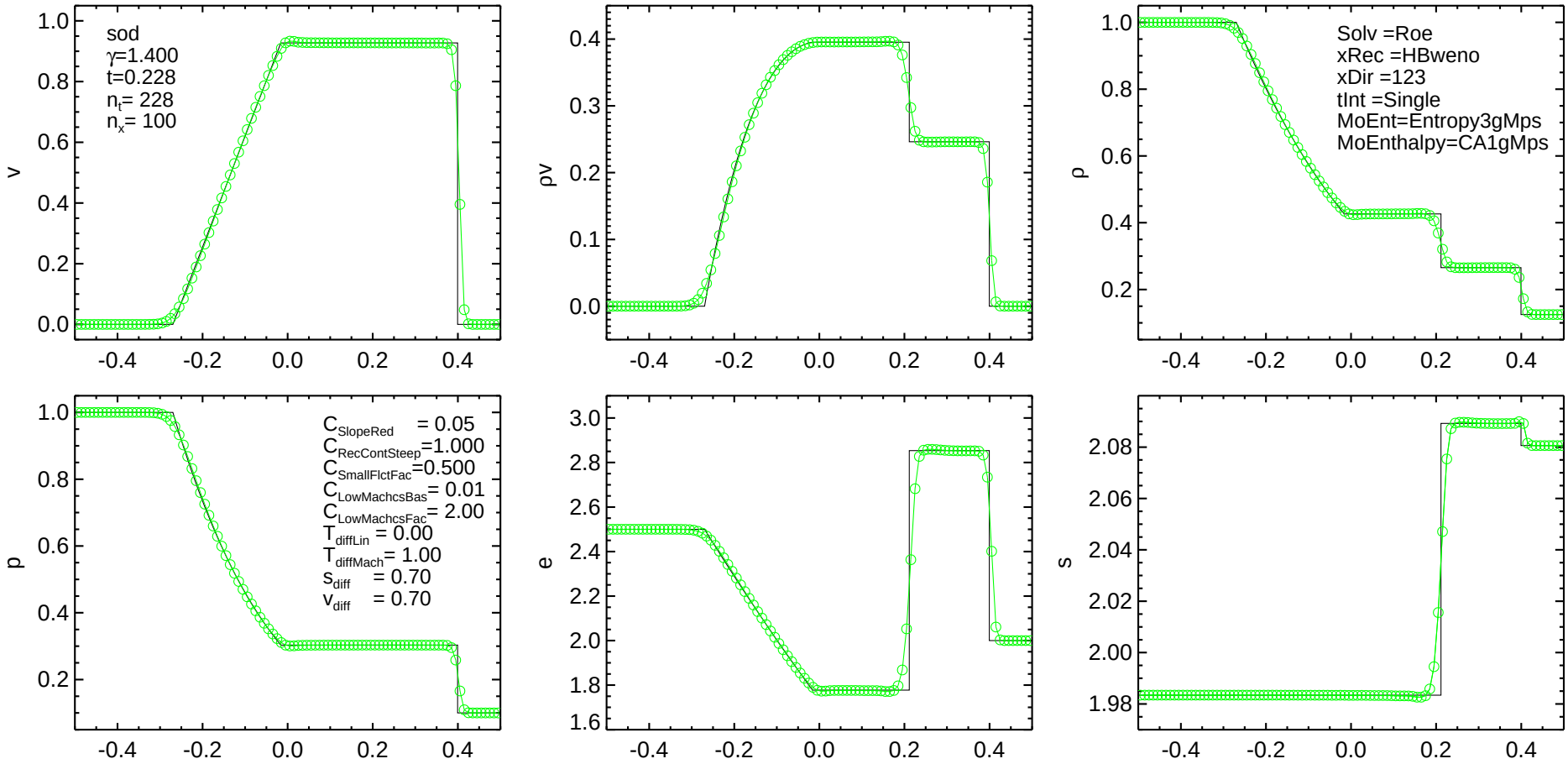

The Sod shock tube is a Riemann problem with:
$(\rho, P, v)_{\mathrm{l}} = (1, 1, 0)$, $(\rho, P, v)_{\mathrm{r}} = (1/8, 1/10, 0)$.

Jumps in the solution of the Sod shock tube problem

The similarity solution of the Sod shock tube problem contains

- a rarefaction fan opening to the left,
- a contact discontinuity travelling slowly to the right,
- a shock wave moving fast to the right.

For the all individual waves, the upwind direction is clear.
Only in the (possible) case of a transonic rarefaction wave “upwind” is not obvious.
However, here an entropy fix has to be applied, anyway.

Godunov-type schemes

Godunov's idea: solve a separate Riemann problem at each cell boundary:

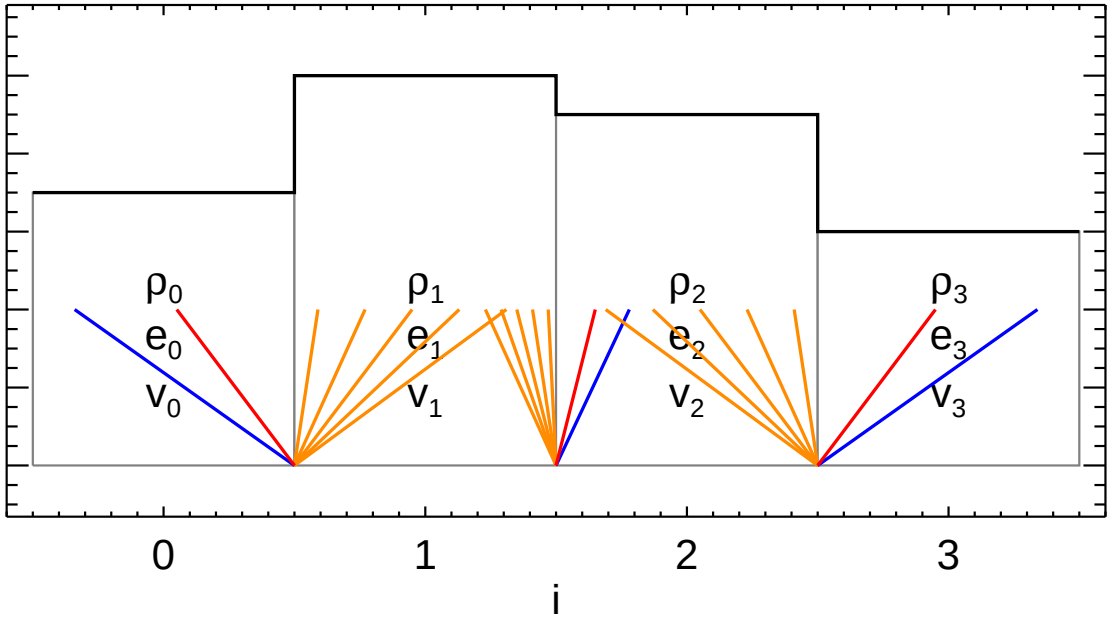

RSA: three steps:

- Reconstruct $\rho(x)$, $\rho\boldsymbol{v}(x)$, $\rho e_{\mathrm{ik}}(x)$ from ρ_i, $\rho\boldsymbol{v}_i$, ρe_{ik_i} (constant values within cell).
- Solve the Riemann problems for Δt (and compute fluxes across cell boundaries).
- Average $\rho(x)$, $\rho\boldsymbol{v}(x)$, $\rho e_{\mathrm{ik}}(x)$ to get ρ_i, $\rho\boldsymbol{v}_i$, ρe_{ik_i} (apply the conservative update formula).

The concept is very useful, but the scheme is too diffusive in its original form.

Riemann solvers and higher-order schemes

Combination of Godunov's concept (local solution of fully non-linear Riemann solvers) with high-order reconstruction (solution averaging):

- Godunov (1959): Exact Riemann solver (with constant reconstruction)
- Van Leer (1979): MUSCL (Monotone Upwind Schemes for Scalar Conservation Laws): linear reconstruction: approximation of piecewise-linear Riemann problems by piecewise-constant Riemann problems including slope-limiter, solution of the Lagrange equations, Eulerian remapping.
- Colella & Woodward (1984): PPM (Piecewise Parabolic Method): piecewise parabolic reconstruction via primitive functions, contact steepening.

Godunov-type schemes are conceptionally appealing.
The improved high-resolution methods give excellent results.

- However, they are relatively complex and require a lot of operations per grid cell.
- Approximate (linearized) Riemann solvers may serve as well in splitting the flow into waves with different characteristic velocities and upwind directions.

Linearized flux

A linearized Riemann solver uses a linearization of the vector flux $\boldsymbol{F}$ in Eq. (44) around reference value $\boldsymbol{q}_{\rm ref}$ to bring it into a form similar to the scalar Eq. (199),

$$\boldsymbol{F} = \boldsymbol{F}(\boldsymbol{q}_{\rm ref}) + \frac{\partial \boldsymbol{F}}{\partial \boldsymbol{q}}(\boldsymbol{q}_{\rm ref})\ (\boldsymbol{q} - \boldsymbol{q}_{\rm ref}) + O\Big((\boldsymbol{q} - \boldsymbol{q}_{\rm ref})^2\Big) \quad . \tag{208}$$

Dropping the 2nd-order term and choosing $x_{\rm ref} = x_{i+\frac{1}{2}}$ we get

$$\boldsymbol{q}_{\rm ref} = \boldsymbol{q}_{i+\frac{1}{2}} \sim \frac{1}{2}\left(\boldsymbol{q}_i + \boldsymbol{q}_{i+1}\right) \quad , \tag{209}$$

$$\boldsymbol{F}(\boldsymbol{q}_{\rm ref}) \sim \frac{1}{2}\left(\boldsymbol{F}(\boldsymbol{q}_i) + \boldsymbol{F}(\boldsymbol{q}_{i+1})\right) \quad . \tag{210}$$

We remember from Page 28 that for the Jacobian

$$\bar{\bar{\rm A}}_{i+\frac{1}{2}} := \frac{\partial \boldsymbol{F}}{\partial \boldsymbol{q}}(\boldsymbol{q}_{\rm ref}) \tag{211}$$

there is a matrix $\bar{\bar{\rm Q}}_{i+\frac{1}{2}}$ that brings it into diagonal form

$$\bar{\bar{\Lambda}}_{i+\frac{1}{2}} = \bar{\bar{\rm Q}}^{-1}_{i+\frac{1}{2}}\ \bar{\bar{\rm A}}_{i+\frac{1}{2}}\ \bar{\bar{\rm Q}}_{i+\frac{1}{2}} \quad , \quad \bar{\bar{\rm A}}_{i+\frac{1}{2}} = \bar{\bar{\rm Q}}_{i+\frac{1}{2}}\ \bar{\bar{\Lambda}}_{i+\frac{1}{2}}\ \bar{\bar{\rm Q}}^{-1}_{i+\frac{1}{2}} \quad . \tag{212}$$

Linearized Riemann solver

The linearized flux vector becomes

$$\boldsymbol{F}_{i+\frac{1}{2}} = \underbrace{\frac{\boldsymbol{F}(\boldsymbol{q}_i) + \boldsymbol{F}(\boldsymbol{q}_{i+1})}{2}}_{\text{centered (naive) fluxes}} + \underbrace{\underbrace{\underbrace{\bar{\bar{\mathrm{Q}}}_{i+\frac{1}{2}}}_{\text{fluxes of characteristic waves}} \underbrace{\bar{\bar{\Lambda}}_{i+\frac{1}{2}}}_{\text{fluxes of characteristic waves}} \underbrace{\left[\bar{\bar{\mathrm{Q}}}^{-1}_{i+\frac{1}{2}} \underbrace{\left(\boldsymbol{q} - \frac{\boldsymbol{q}_i + \boldsymbol{q}_{i+1}}{2}\right)}_{\text{original fluctuations}}\right]}_{\text{fluctuations of characteristic waves}}}_{\text{flux corrections of original quantities}} \tag{213}$$

Note: $\bar{\bar{\Lambda}}_{i+\frac{1}{2}}$ is a diagonal matrix with the characteristic velocities on the diagonal.

Note: The fluxes of the characteristic waves are the result of a localized linear advection problem. A higher-order correction term (with slope-limiter) could be applied.

Examples of schemes

Roe (1981):

- Scheme (essentially) as above.
- With clever choice of matrix A, so that the approximate Riemann solver becomes exact for simple waves (only one shock or only one contact discontinuity).
- Needs entropy fix.
- The fluctuations are taken from the primitive rather than the conservative variables.

HLLE (1983, 1988):

- Uses only the two waves with largest and smallest characteristic velocity.
- The region in between is approximated by a single state.
- The scheme is simple, more robust but also more dissipative than Roe's scheme.

Example: Sod shock tube with Roe solver, constant reconstruction

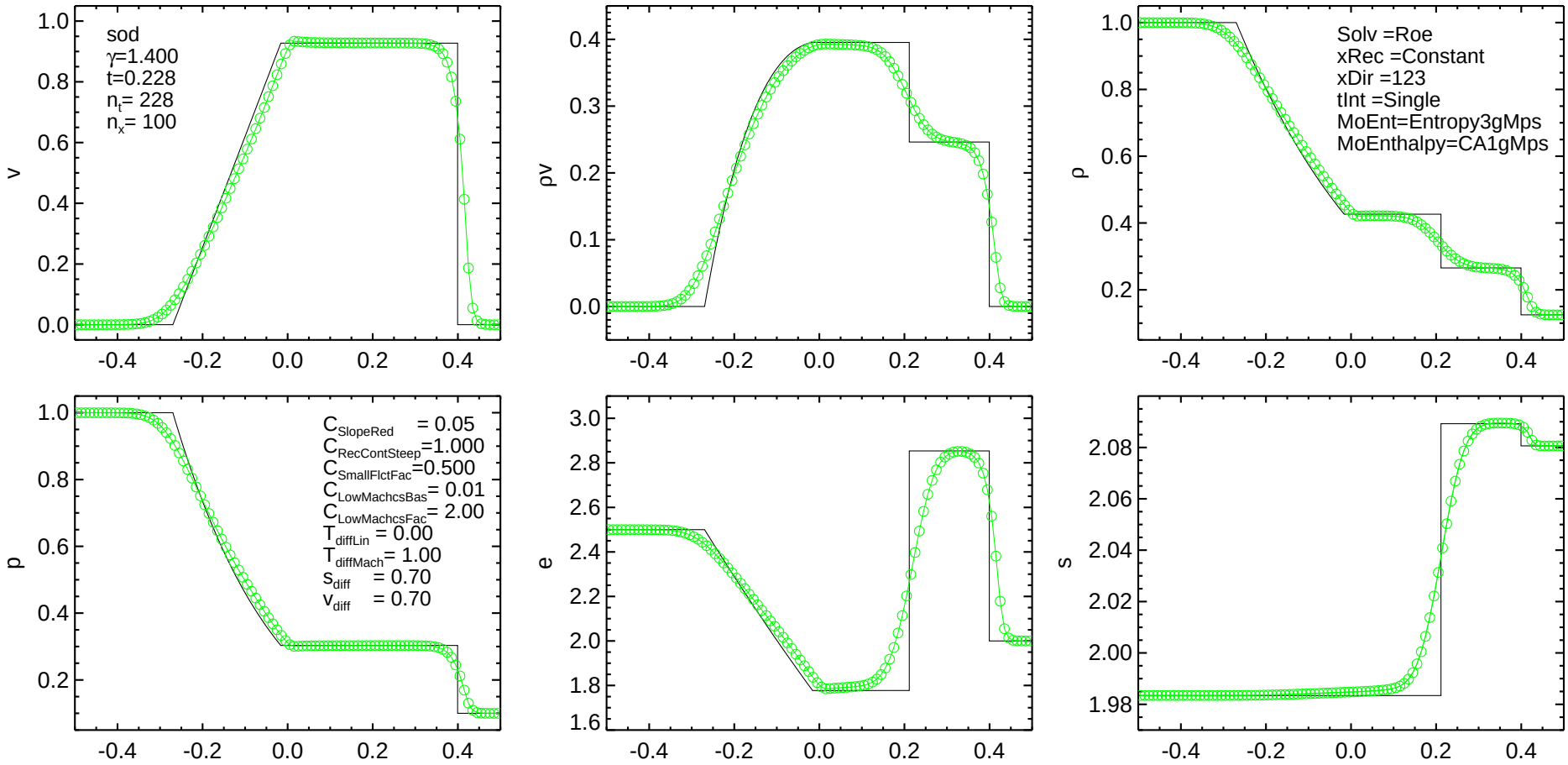

Numerical solution of the Sod shock tube problem with constant reconstruction.

Example: Sod shock tube with Roe solver, Minmod slope limiter

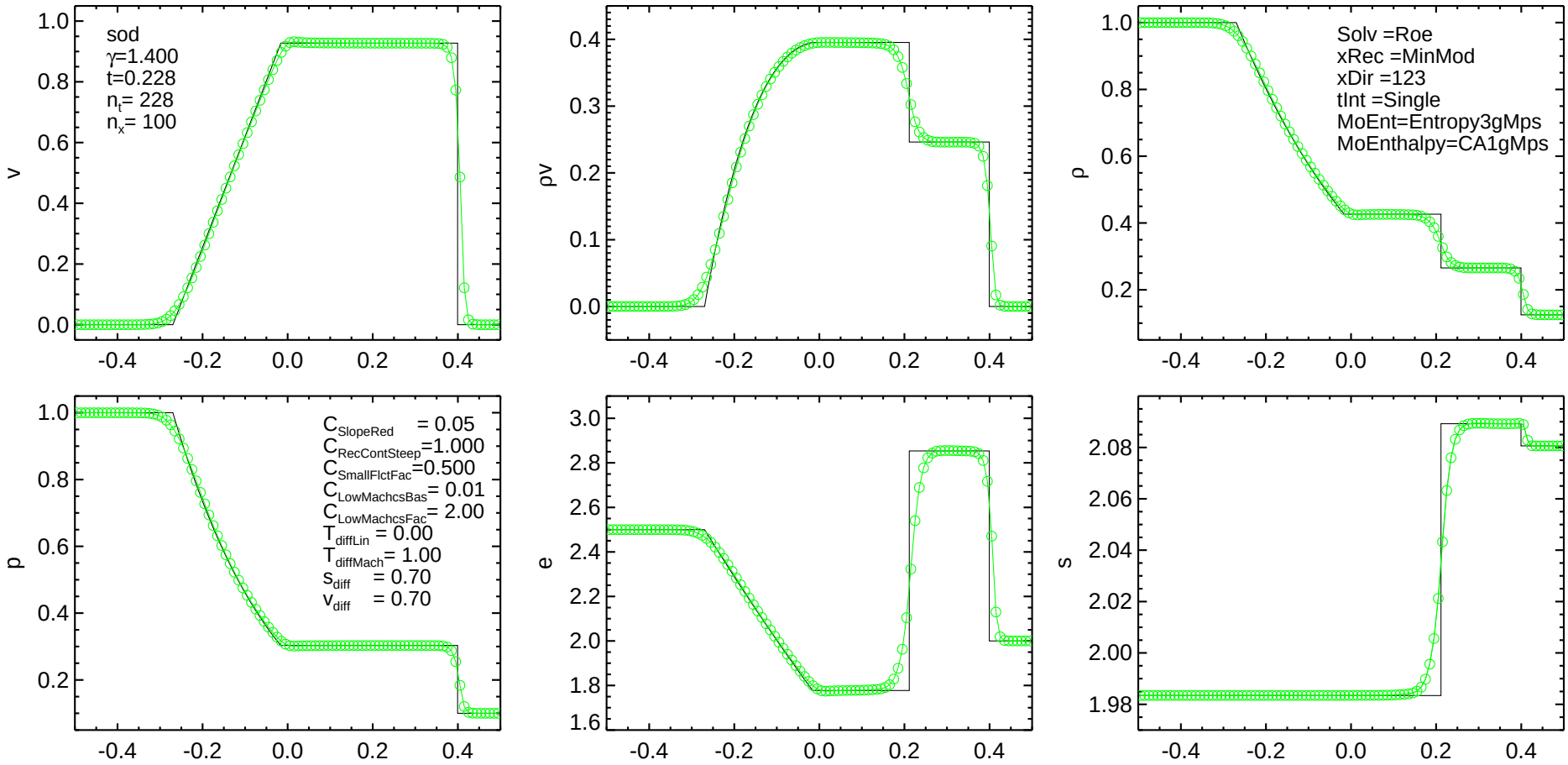

Numerical solution of the Sod shock tube problem with PL reconstruction and Minmod slope-limiter.

Example: Sod shock tube with Roe solver, vanLeer slope limiter

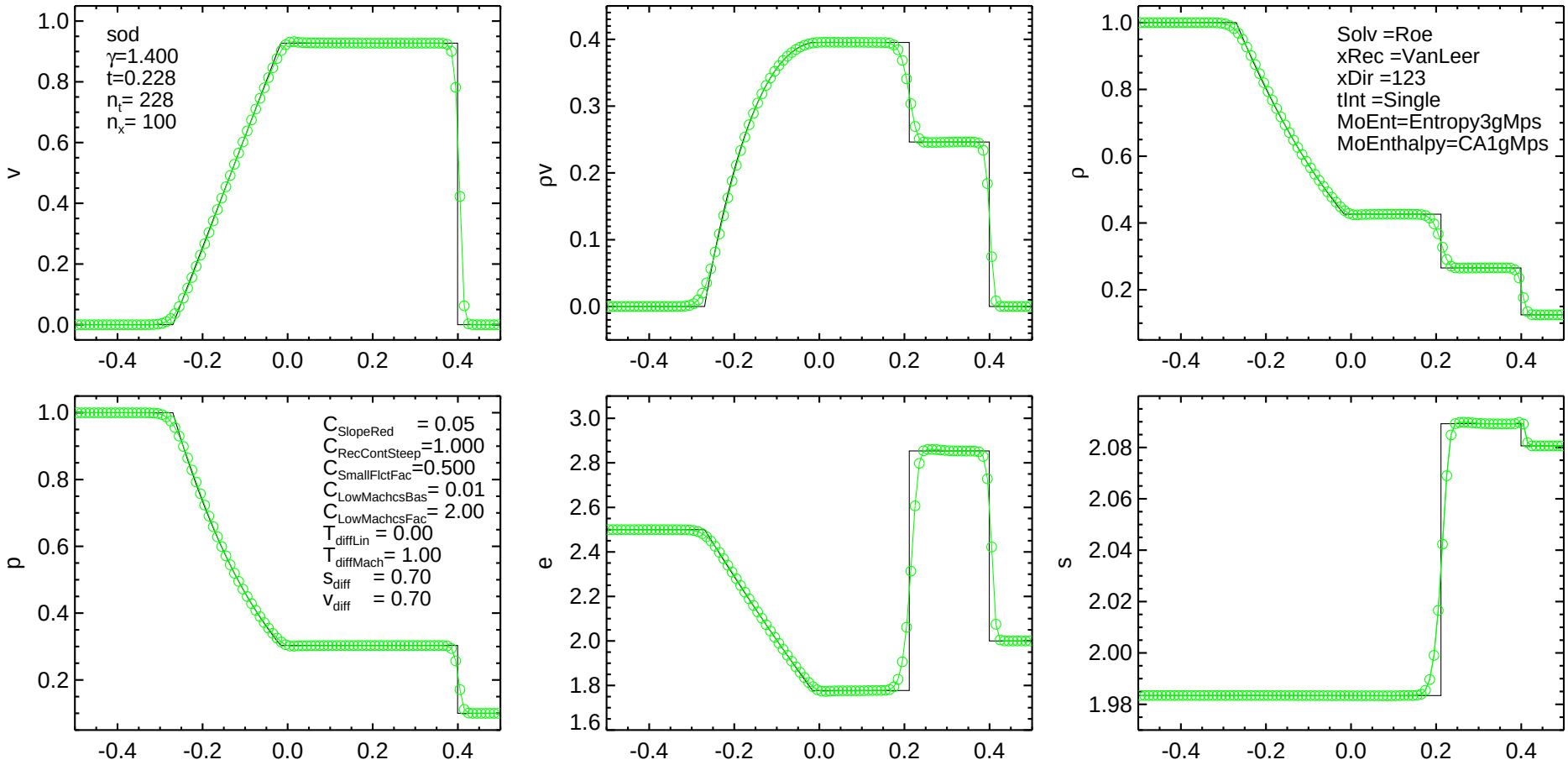

Numerical solution of the Sod shock tube problem with PL reconstruction and vanLeer slope-limiter.

Example: Sod shock tube with Roe solver, Superbee slope limiter

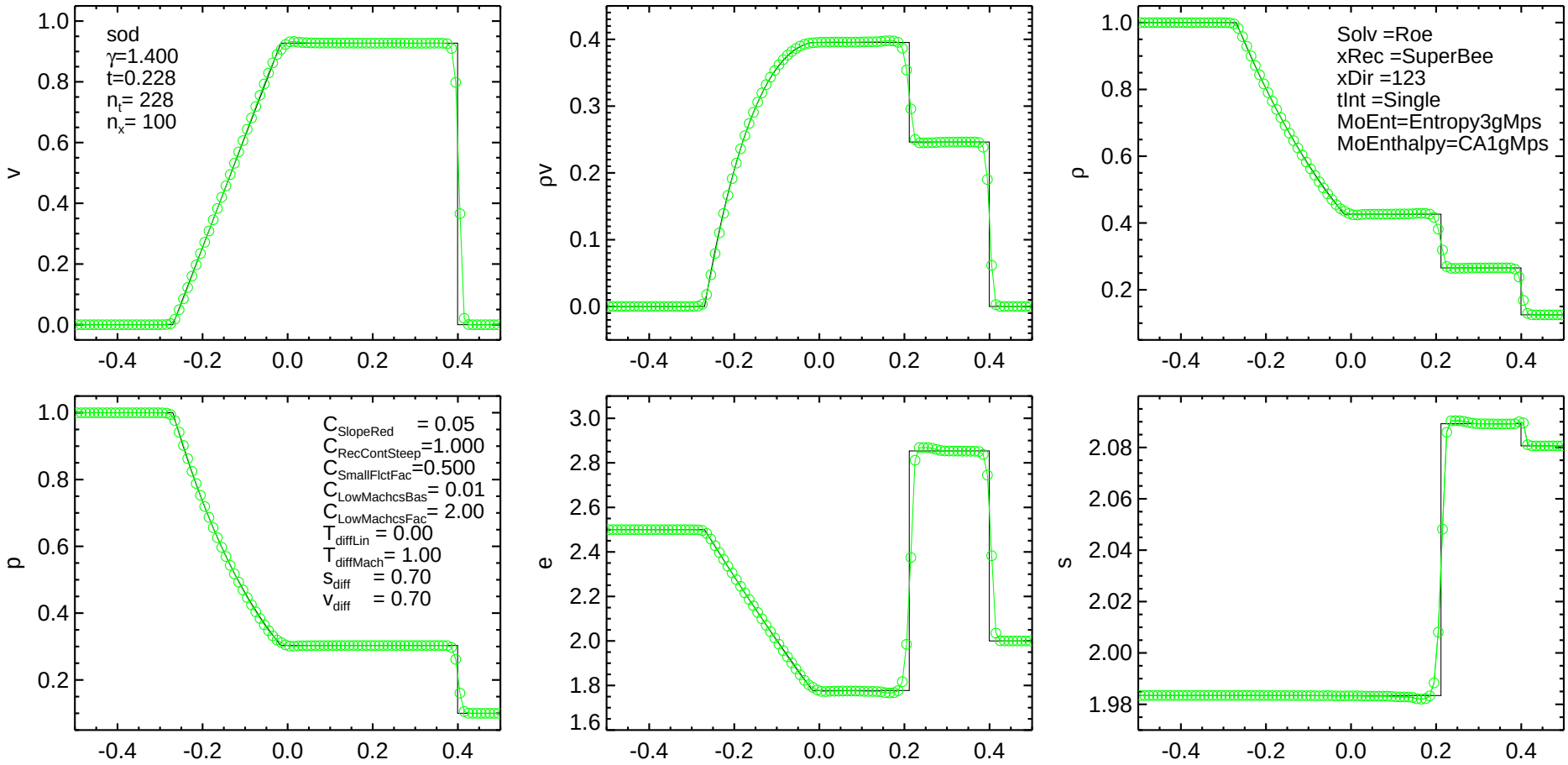

Numerical solution of the Sod shock tube problem with PL reconstruction and Superbee slope-limiter.

Example: Sod shock tube with Roe solver, PP reconstruction

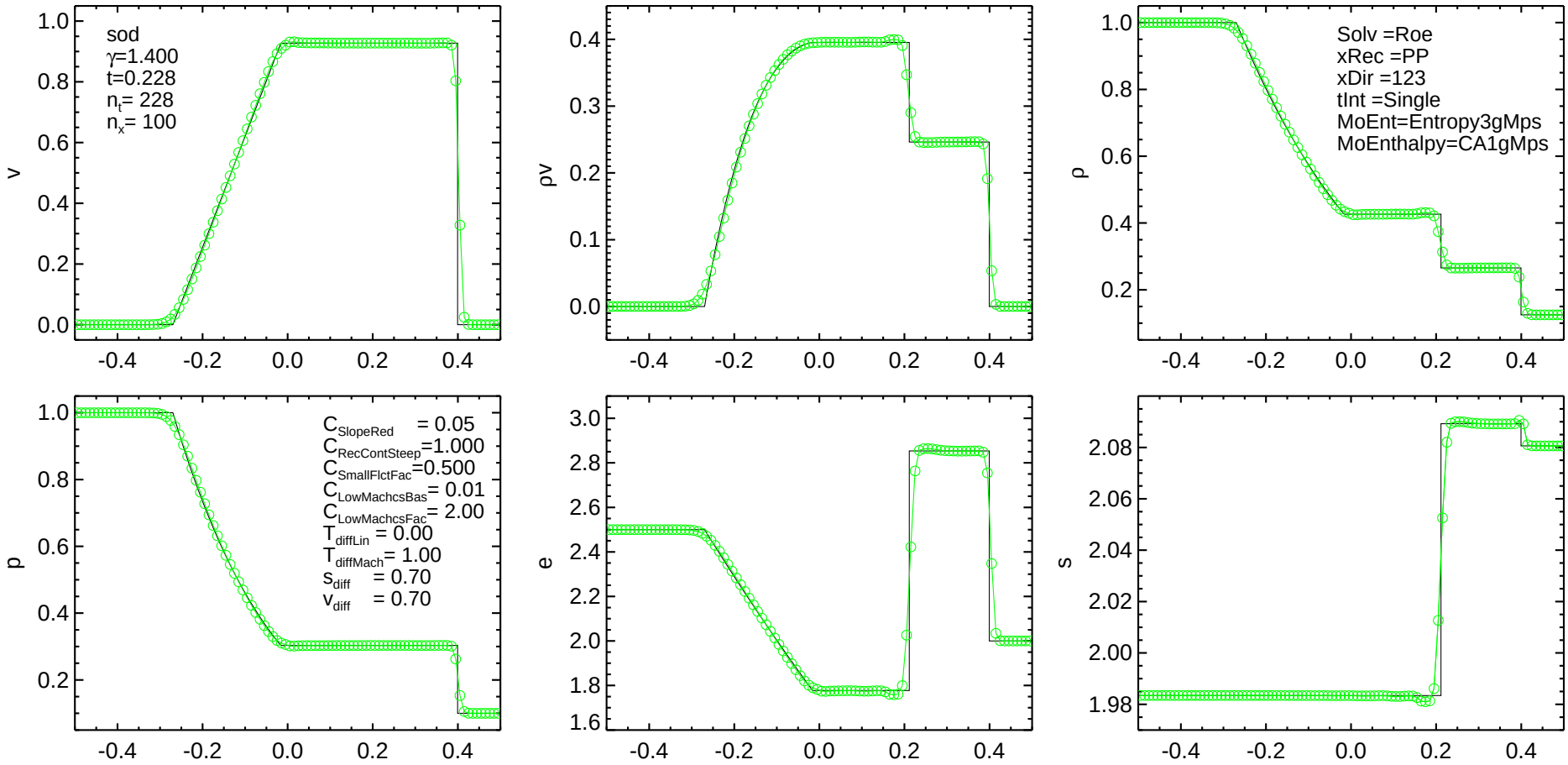

Numerical solution of the Sod shock tube problem with PP reconstruction.

Example: Sod shock tube with Roe solver, WENO reconstruction

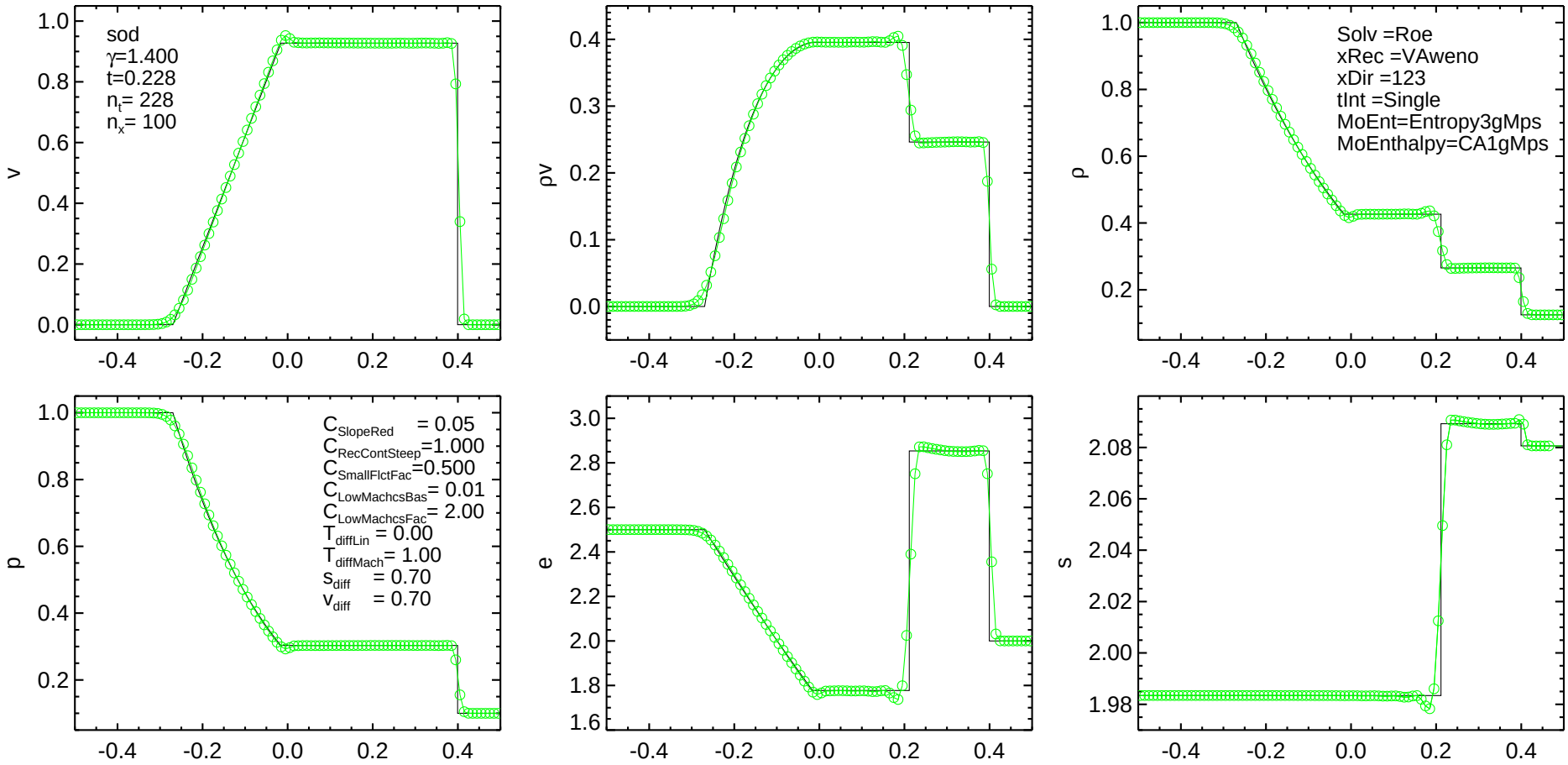

Numerical solution of the Sod shock tube problem with WENO reconstruction based on parabolas.

Example: Sod shock tube with Roe solver, HBweno reconstruction

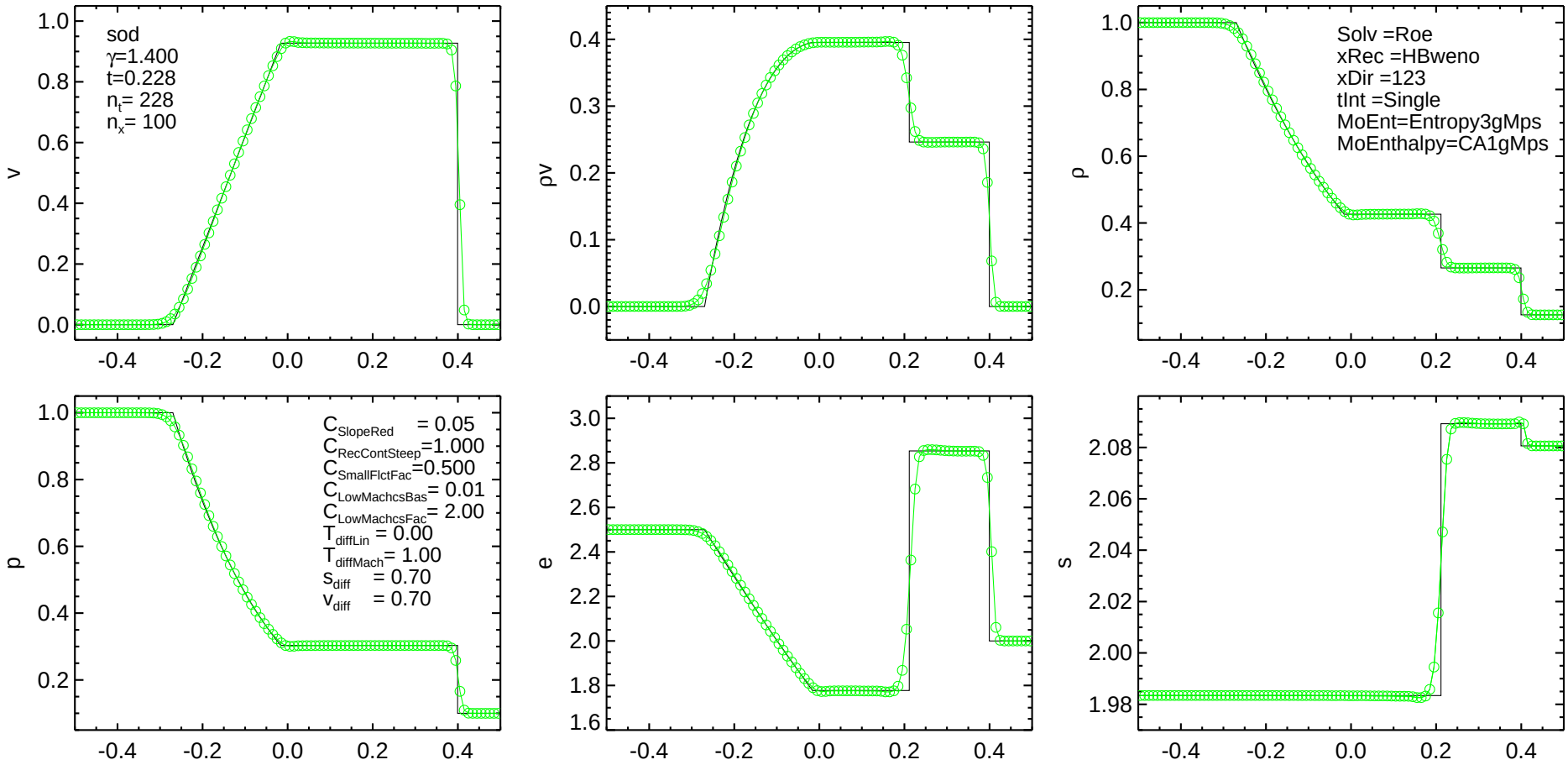

Numerical solution of the Sod shock tube problem with HBweno reconstruction.

Example: Sod shock tube with Roe solver, FRmono reconstruction

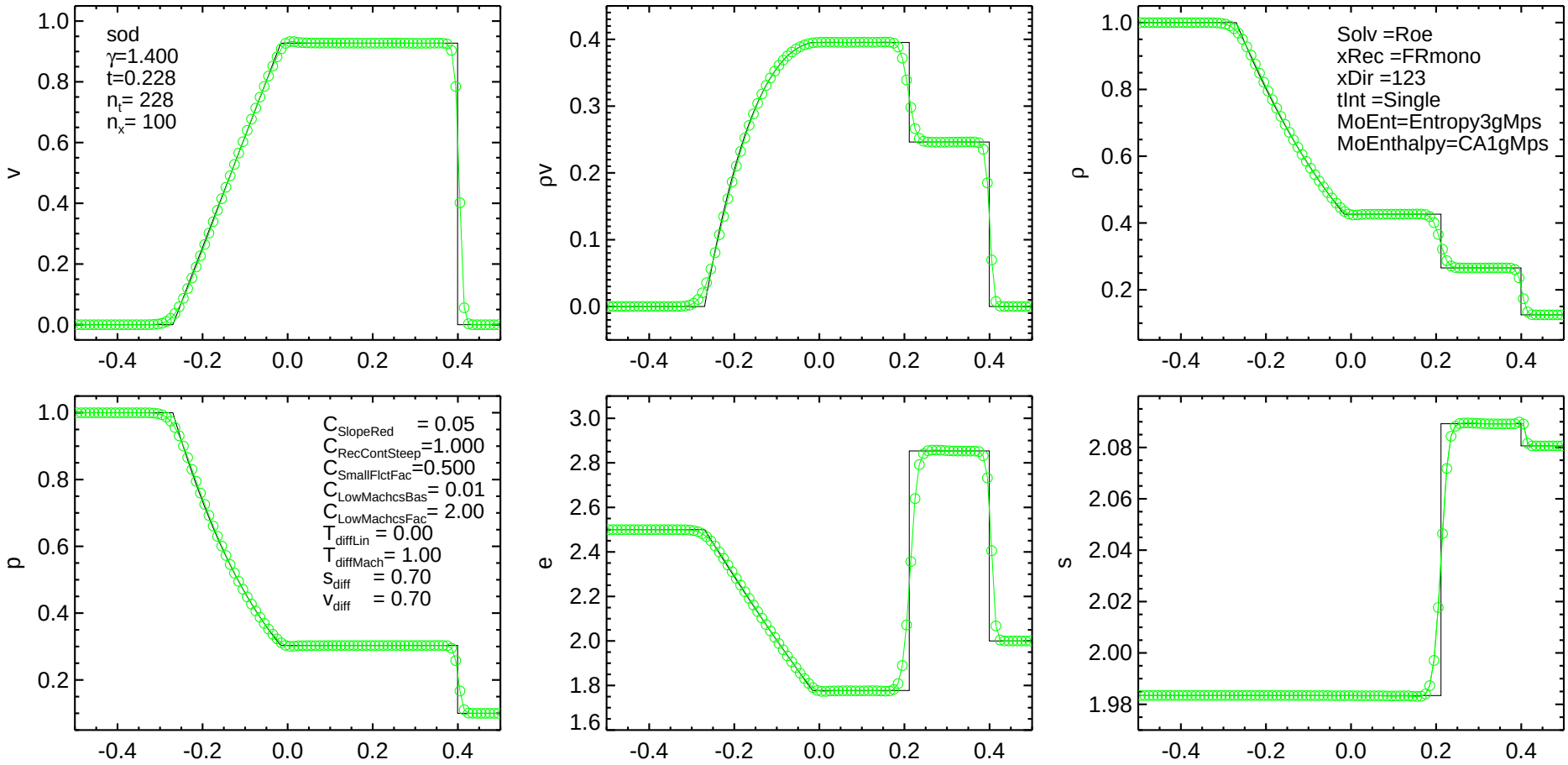

Numerical solution of the Sod shock tube problem with FRmono reconstruction.

Alternatives

(Approximate) Riemann solvers are a way to account for upwinding and shock capturing in a conceptionally elegant manner.
However, they are somewhat involved and there other (simpler? more clever? older? newer?) concepts around, which make use of

- central schemes (to avoid the upwind-direction-finding problem)
  + Runge-Kutta steps
- artificial viscosity: von Neumann-Richtmyer viscosity, hyperviscosity
- operator-splitting of advection and pressure terms

If shocks are unlikely to occur (due to low Mach numbers or large viscosity) other schemes are to be preferred, e.g.:

- Spectral methods (used, e.g., to model stellar interiors)
- Finite-element methods (used for many engineering applications)

Table of contents

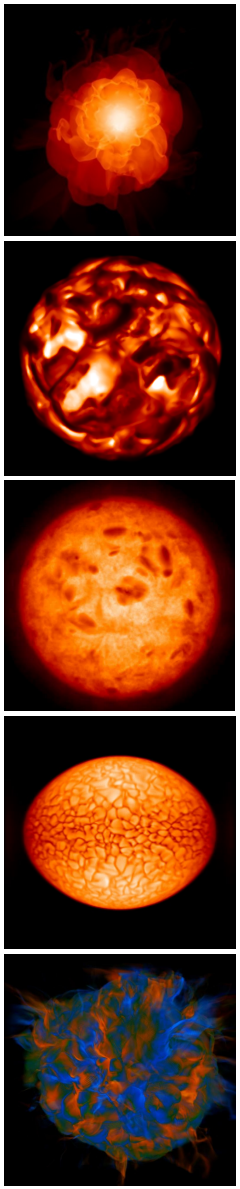

Operator adding versus splitting

Let the time evolution of q be determined by two operators A and B according to

$$\frac{\mathrm{d}q}{\mathrm{d}t} = A(q) + B(q) \ . \tag{214}$$

Suppose there are separate numerical schemes available that allow to compute the individual updates

$$q_A^{n+1} = q^n + \Delta t\, A(q^n) \ , \quad q_B^{n+1} = q^n + \Delta t\, B(q^n) \ . \tag{215}$$

Now, the two schemes could be combined in two ways, e.g.,
by unsplit operator adding

$$q_{A+B}^{n+1} = q^n + \Delta t\, A(q^n) + \Delta t\, B(q^n) \tag{216}$$

or by Godunov operator splitting

$$\begin{aligned} q_A^{n,*} &= q^n + \Delta t\, A(q^n) \\ q_{A+B}^{n+1} &= q_A^{n,*} + \Delta t\, B(q_A^{n,*}) \ . \end{aligned} \tag{217}$$

The results are generally not the same. Both methods have advantages/drawbacks.

Godunov versus Strang operator splitting

The Godunov operator splitting from Eq. (217), where all operators are applied cyclically and with the same time step, might be improved in some cases by Strang operator splitting

$$\begin{aligned} q^{n,*}_{A/2} &= q^n + \frac{\Delta t}{2} A(q^n) \\ q^{n,**}_{A/2+B} &= q^{n,*}_{A/2} + \Delta t\, B(q^{n,*}_{A/2}) \\ q^{n+1}_{A+B} &= q^{n,**}_{A/2+B} + \frac{\Delta t}{2} A(q^{n,**}_{A/2+B}) \ . \end{aligned} \tag{218}$$

Steady-state solutions

Suppose both operators A and B are zero,

$$A = B = 0 \tag{219}$$

resulting in individually stationary solutions (e.g., hydrostatic and radiative equilibrium),

$$q_A^{n+1} = q^n \ , \quad q_B^{n+1} = q^n \ , \tag{220}$$

which gives for both operator combination methods

$$q_{A+B}^{n+1} = q^n \ . \tag{221}$$

Steady-state solutions with operator adding or splitting

However, if the individual operators are non-zero but cancel each other,

$$B = -A \neq 0 \tag{222}$$

the adding of the operator gives equilibrium Eq. (221), while operator splitting gives

$$\begin{aligned} q_A^{n,*} &= q^n + \Delta t\, A(q^n) \\ q_{A+-A}^{n+1} &= q_A^{n,*} - \Delta t\, A(q_A^{n,*}) \ . \end{aligned} \tag{223}$$

This is not necessarily a stationary solution. Here, operator adding is superior. Examples are

- (Nearly) hydrostatic stratification: pressure gradient and gravity
- Multi-dimensional (nearly) incompressible flow: fluxes in different directions

Linear stability of operator adding or splitting

If both operators A and B are linear with amplification factors indicating stability

$$V_A \leq 1 \ , \quad V_B \leq 1 \tag{224}$$

then the amplification factor of the scheme combined by operator splitting is

$$V_{A+B} = V_A \, V_B \leq 1 \tag{225}$$

implying stability of the combined scheme.

- The adding of the operators requires a re-analysis of the combined scheme. It might be stable or not, even if Eq. (224) applies.
- The individual analysis of a non-linear hydrodynamics and a complex non-local radiation transport scheme is difficult enough.
- It is convenient to have a combination method, that – at least in some simple cases – guarantees the stability of the combination

Here, operator splitting is superior.

Going multi-dimensional: directional splitting

Directional splitting or dimensional splitting is simply the technique to apply operator splitting to the spatial derivatives in the Euler Equations:

$$\frac{\partial}{\partial t}\boldsymbol{q} + \frac{\partial}{\partial x}\boldsymbol{F}_x(\boldsymbol{q}) + \frac{\partial}{\partial y}\boldsymbol{F}_y(\boldsymbol{q}) = \boldsymbol{0} \tag{226}$$

becomes (with i and j the spatial indices in x and y direction, respectively)

$$\begin{aligned} q^{n,*}_{X;i,j} &= q^n_{i,j} - \frac{\Delta t}{\Delta x}\left(f_{X;i+\frac{1}{2},j}(q^n_{\cdot,j}) - f_{X;i-\frac{1}{2},j}(q^n_{\cdot,j})\right) \\ q^{n+1}_{X+Y;i,j} &= q^{n,*}_{X,i,j} - \frac{\Delta t}{\Delta y}\left(f_{Y;i,j+\frac{1}{2}}\left(q^{n,*}_{X;i,\cdot}\right) - f_{Y;i,j+\frac{1}{2}}\left(q^{n,*}_{X;i,\cdot}\right)\right) \quad . \end{aligned} \tag{227}$$

- Directional splitting works very well in many cases and allows the application of powerful algorithms developed for 1D problems.
- However, there are cases when a small amount of additional multi-dimensional tensor viscosity is necessary to damp spurious oscillations (even with PPM scheme).

Going multi-dimensional: CTU scheme

Colella's (1990) "Corner-Transport-Upwind" scheme:

$$
\begin{aligned}
q^{n+\frac{1}{2}}_{X;i,j} &= q^n_{i,j} - \frac{\Delta t}{2\Delta x}\left(f_{X;i+\frac{1}{2},j}(q^n_{\cdot,j}) - f_{X;i-\frac{1}{2},j}(q^n_{\cdot,j})\right) \\
q^{n+\frac{1}{2}}_{Y;i,j} &= q^n_{i,j} - \frac{\Delta t}{2\Delta y}\left(f_{Y;i,j+\frac{1}{2}}(q^n_{i,\cdot}) - f_{Y;i,j-\frac{1}{2}}(q^n_{i,\cdot})\right) \\
q^{n+1}_{X+Y;i,j} &= q^n_{i,j} - \frac{\Delta t}{\Delta x}\left(f_{X;i+\frac{1}{2},j}\left(q^{n+\frac{1}{2}}_{Y;\cdot,j}\right) - f_{X;i+\frac{1}{2},j}\left(q^{n+\frac{1}{2}}_{Y;\cdot,j}\right)\right) \\
&\quad - \frac{\Delta t}{\Delta y}\left(f_{Y;i,j+\frac{1}{2}}\left(q^{n+\frac{1}{2}}_{X;i,\cdot}\right) - f_{Y;i,j+\frac{1}{2}}\left(q^{n+\frac{1}{2}}_{X;i,\cdot}\right)\right) \quad . \qquad (228)
\end{aligned}
$$

- Intend: combine the advantages of directional-splitting and unsplit methods.
- Used when the numerical 1D already contain terms $O(\Delta t)$.
  Otherwise: use a Runge-Kutta method.

Runge-Kutta methods to achieve high order in time

Let the time evolution of q be determined by the operator A (possibly containing spatial derivatives) according to

$$\frac{\mathrm{d}q}{\mathrm{d}t} = A(q) \ . \tag{229}$$

Building on the first-order-in-time Euler scheme

$$q_A^{n+1} = q^n + \Delta t\, A(q^n) \tag{230}$$

we can construct higher-order Runge-Kutta methods by employing intermediate steps. E.g., a second-order scheme (Heun's method):

$$\begin{aligned} q^{n,*} &= q^n + \Delta t\, A(q^n) \\ q^{n,**} &= q^{n,*} + \Delta t\, A(q^{n,*}) \\ q^{n+1} &= \frac{1}{2} q^n + \frac{1}{2} q^{n,**} \end{aligned} \tag{231}$$

or another second-order scheme (midpoint method):

$$\begin{aligned} q^{n,*} &= q^n + \frac{1}{2}\Delta t\, A(q^n) \\ q^{n+1} &= q^n + \Delta t\, A(q^{n,*}) \ . \end{aligned} \tag{232}$$

Coupling of hydrodynamics and radiation transport

- If possible one would try to avoid constructing a merged hydrodynamics plus radiation transport scheme.
- Instead one constructs and tests a hydrodynamics and a radiation transport scheme separately.
- The coupling can be done via operator splitting or adding.

Often radiation transport requires small time steps to achieve stability.
These can be handled by

- sub-steps for the radiation transport (many small radiation steps per large hydrodynamics step),
- an implicit treatment of the radiation transport (while the hydrodynamics operator is still explicit).

Stability requirements

Stability requirements on radiation transport operator:

1. Stability of integration along ray (to avoid problems like on Page 37)
2. Stability of (accelerated) Λ iteration
3. Stability of time update

Note: Requirement 1 does not occur if e.g. diffusion approximation is used.
Note: Requirement 2 does not occur if the source function is independent of intensity (LTE).
Note: Requirement 3 is always there.

Approximations

Different approximations for the radiation transport are used during and after a simulation:

Simplified treatment of radiative energy transfer during the simulation:

- Ignoring radiation
- Isothermal flow (no energy transport equation)
- Local cooling (in the optically thin)
- Diffusion approximation (in the optically thick)
- Non-local radiation transport along rays, but LTE and grey opacities
- Non-local radiation transport along rays, but LTE and binned opacities (ODFs)

More sophisticated a-posteriori radiation transport for spectrum synthesis:

- Detailed opacities
- Detailed line broadening and Doppler shifts
- Possibly scattering, polarization
- Possibly effects of magnetic fields onto line formation

Non-Cartesian and/or refined grids

Possible numerical grid improvement techniques:

- Eulerian $\rightarrow$ Lagrangian
- Equidistant $\rightarrow$ non-equidistant
- Structured $\rightarrow$ unstructured
- One $\rightarrow$ many hierarchical
- Fixed in time $\rightarrow$ adaptive
- Grid $\rightarrow$ no grid: SPH

Optimization strategies

All modern computers can calculate (within the processor) much faster than they can access external memory.
Techniques to improve the performance of algorithms have to take this into account (simplified crash course):

- Efficient use of registers: Lots of operations with the same scalars are good.
- Cache optimization: Lots of operations with the same vectors are good.
- Vectorization (on dedicated vector machines, PCs, or “graphics cards”: GPGPUs): “Smooth” access to arrays and simple operations are good.
- Parallelization: Local access to array regions is good.

Hydrodynamics and parallelization:

- A bounded numerical domain of dependence allows straightforward domain decomposition and distribution over different machines.

Radiation transport and parallelization:

- Non-local radiation transport (integration along rays) requires more communication between processors and limits the performance on parallel computers.

Table of contents

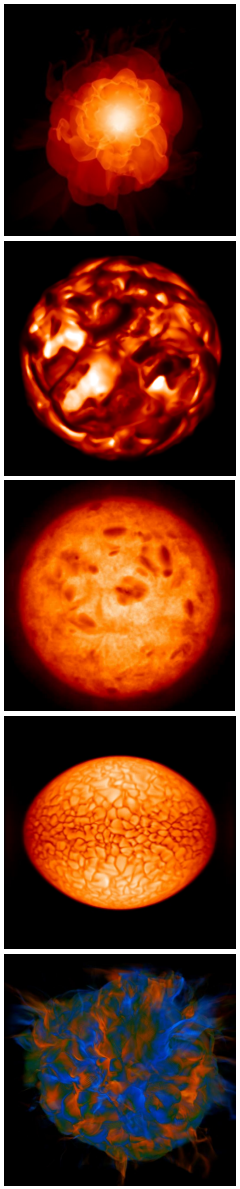

Symbols and descriptions of quantities

symbol	quantity
Δt	discrete time step
Δx	grid size
e_{i}	internal energy density (per mass unit)
e_{ik}	total (internal + kinetic) energy
e_{ikg}	total (internal + kinetic + potential) energy
e_{ikb}	total (internal + kinetic + magnetic) energy
I_ν	frequency-dependent intensity
$\hat{\boldsymbol{n}}$	normal vector of length unity
ν	frequency
P	pressure
ρ	mass density
ρe_{i}	internal energy density (per volume)
$\bar{\bar{\mathrm{I}}}$	unity tensor
$\boldsymbol{v}$	velocity vector

Vector notation: scalar s, vector $\boldsymbol{v}$, and second-rank tensor $\overline{\overline{\mathsf{T}}}$

vector operation	description
$s\,s \rightarrow s$	product of scalars
$s\,\boldsymbol{v} \rightarrow \boldsymbol{v}$	scalar times vector gives vector
$\boldsymbol{v}\,s \rightarrow \boldsymbol{v}$	
$s\,\overline{\overline{\mathsf{T}}} \rightarrow \overline{\overline{\mathsf{T}}}$	scalar times tensor gives tensor
$\overline{\overline{\mathsf{T}}}\,s \rightarrow \overline{\overline{\mathsf{T}}}$	
$\boldsymbol{v}\cdot\boldsymbol{v} \rightarrow s$	scalar product of vectors gives scalar
$\boldsymbol{v}:\boldsymbol{v} \rightarrow \overline{\overline{\mathsf{T}}}$	tensor product of vectors gives tensor
$\overline{\overline{\mathsf{T}}}\,\boldsymbol{v} \rightarrow \boldsymbol{v}$	tensor times vector gives vector
$\boldsymbol{v}\cdot\overline{\overline{\mathsf{T}}} \rightarrow \boldsymbol{v}^{\mathrm{T}}$	"scalar product" of vector and tensor gives "transposed" vector
$\overline{\overline{\mathsf{T}}}\,\overline{\overline{\mathsf{T}}} \rightarrow \overline{\overline{\mathsf{T}}}$	tensor product ("matrix multiplication")
$\boldsymbol{v}\,\boldsymbol{v} \rightarrow ???$	

Table of contents

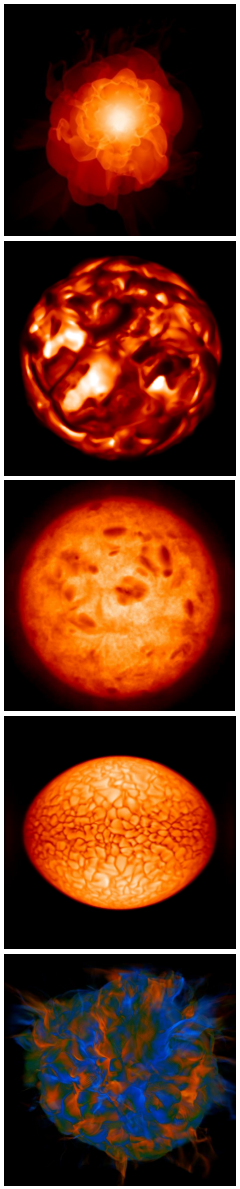

Lecture Notes closely related to the current one

- Bernd Freytag: “Numerical Hydrodynamics (Uppsala Lecture Notes 2005)”
- Susanne Höfner: “Numerical Hydrodynamics (Uppsala Lecture Notes 2012)”
- Rony Keppens: “Computational magneto-fluid dynamics”
- Claus-Dieter Munz: “Numerical Gasdynamic”

Lecture Notes with additional topics

- Axel Brandenburg: “Computational aspects of astrophysical MHD and turbulence”
- Leon van Dommelen: “Partial Differential Equations”
- Cole Miller: “Theoretical Astrophysics”
- M. Manzini: “Numerical methods for 1D compressible flows, an interactive book”
- Kip Thorne: “Applications of Classical Physics”

Books

- Ferziger, J.H., Peric, M. 2001, ”Computational Methods for Fluid Dynamics”, Springer-Verlag, ISBN: 3540420746
- Laney, C.B. 1998, ”Computational Gasdynamics”, Cambridge University Press, ISBN: 0521625580
- LeVeque, R.J. 2002, ”Finite Volume Methods for Hyperbolic Problems”, Cambridge University Press, ISBN: 0521009243
- LeVeque, R.J., Steiner, O., Gautschy, A. 1997, ”Computational Methods for Astrophysical Fluid Flow (Saas-Fee Advanced Course. . . Lecture Notes)”, Springer-Verlag, ISBN: 3540644482
- Tannehill, J.C., Anderson, D.A., Pletcher, R.H. 1984/1997, “Computational Fluid Mechanics and Heat Transfer”, Taylor and Francis, ISBN: 1-56032-046-X

Articles

- Phillip Colella, Paul R. Woodward 1984, “The Piecewise Parabolic Method (PPM) for Gas-Dynamical-Simulations”, JCompPhys 54, 174-201
- Phillip Colella 1990, “Multidimensional Upwind Methods for Hyperbolic Conservation Laws”, JCompPhys 87, 171-200
- S.K. Godunov 1959, “A Difference Scheme for Numerical Computation of Discontinuous Solutions of Hydrodynamics Equations”, Math. Sbornik 47, 271-306
- Guang-Shan Jiang, Chi-Wang Shu 1996, “Efficient Implementation of Weighted ENO Schemes”, JCompPhys 126, 202-228, see CiteSeer
- Bram van Leer 1979, “Towards the Ultimate Conservative Difference Scheme. V. A Second-Order Sequel to Godunov’s Method”, JCompPhys 32, 101-136
- P.L. Roe 1981, “Approximate Riemann Solvers, Parameter Vectors, and Difference Schemes”, JCompPhys 43, 357-372

Hydrodynamics codes

- ANTARES
- ASH code
- BiFrost
- CLAWPACK
- CO5BOLD
- FLASH
- Pencil Code
- MURaM
- PPM
- Stagger Code
- VAC
- VH-1
- ZEUS